ROLE OF MiRNAs REGULATING THE EMT/MET PROCESSES IN COLORECTAL CANCER-DERIVED INDUCED PLURIPOTENT CANCER CELLS (CRC-iPCs)

By

CHENG HAN PING

A dissertation submitted to the Department of Pre-Clinical Science,

Faculty of Medicine and Health Sciences,

Universiti Tunku Abdul Rahman,

in partial fulfilment of the requirements for the degree of

Master of Medical Science

January 2019

ABSTRACT

ROLE OF MiRNAs REGULATING THE EMT/MET PROCESSES IN COLORECTAL CANCER-DERIVED INDUCED PLURIPOTENT CANCER CELLS (CRC-iPCs)

Cheng Han Ping

Exogenous introduction of pluripotency factors may be used to reprogramme cancer cells for use in the development of cancer disease models. MicroRNAs (miRNAs) are negative regulators of gene expression important for cellular reprogramming and cancer metastasis through various mechanisms, including the epithelial-to-mesenchymal transition (EMT) and mesenchymal-to-epithelial transition (MET) processes. However, studies on the roles of miRNAs in regulating the EMT/MET processes in induced pluripotent cancer (iPC) cells are lacking. By using CRC derived iPC cell lines, differential expression of miRNAs related to the early stage of CRC initiation and progression could be identified. Four iPC clones previously generated in our laboratory from two colorectal cancer (CRC) cell lines by retroviral transduction of the Yamanaka factors were subjected to genome-wide miRNA profiling and bioinformatics interrogation. The CRC-iPCs shared similarities in the miRNA profiles of both cancer and pluripotent embryonic stem cells, but did not express some known reprogramming miRNAs, suggesting incomplete reprogramming. The hundred-and-two differentially-expressed miRNAs

identified were predicted to regulate the EMT/MET processes through the PI3K-Akt and TGF-β signalling pathways. The EMT genes, SMAD family member 4 (SMAD4) and Snail (SNAI1), and the MET genes, E-cadherin (CDH1) and occludin (OCLN), are all targeted by the down-regulated miR-362-5p/-3p, as validated in luciferase assays. On western blot analysis, contradictory EMT/MET protein expression was observed in the CRC-iPC clones, suggesting an epithelial/mesenchymal (E/M) hybrid phenotype possibly elicited by partial reprogramming. The EMT/MET gene expression was generally reversible in post-iPCs, indicating the epigenetic regulation. Overexpression of miR-362-5p/-3p mimics down-regulated both EMT and MET proteins, except SNAI1, consistent with an E/M hybrid phenotype. On the contrary, inhibition of miR-362-3p/-5p, as were down-regulated in CRC-iPCs, enhanced MET, which facilitates the early stage of reprogramming. Overexpression of miR-362-3p/-5p significantly enhanced cell migration and invasion. Taken together, partial reprogramming of CRC-iPCs might have elicited an E/M hybrid phenotype. Schemes are also presented to show the interplay between miR-362-5p/-3p and signalling in regulating cellular migration, invasion and CRC reprogramming via targeting EMT/MET genes.

ACKNOWLEDGEMENTS

The completion of this study would not have been possible without the guidance and support provided by many persons that I have met along the journey of life.

Foremost, I would like to express my deepest gratitude to my co-supervisor, Senior Professor Dr. Choo Kong Bung, for his selfless guidance, encouragement and advices in sharing his knowledge and expertise with me throughout the study. I would also like to extend my appreciation to my supervisor, Dr. Ong Hooi Tin, for her kind support and advices on this work. Moreover, I wish to express my sincere gratitude to my co-supervisor, Professor Dr. Chiou Shih-Hwa (National Yang-Ming University, Taiwan), and Professor Dr. Huang Chiu-Jung (Chinese Culture University, Taiwan) for their generous support, valuable feedback and discussion on the issues faced in completing the project.

I would also like to thank Universiti Tunku Abdul Rahman, Faculty of Medicine and Health Sciences, as well as the Institute of Pharmacology of National Yang-Ming University for providing the facilities, laboratory instruments and great study environment to the convenience of students. This work is financially funded by UTARRF research grant (no. 6200/CC5).

A special thank you to my fellow laboratory mates in UTAR Postgraduate Laboratory, Nguyen Phan Nguyen Nhi, Michele Hiew Sook Yuin, Tai Lihui, Vimalan Rengganatan and Looi Hong Keat for their encouragements, guidance and supports that have inspired me throughout the study. I would also like to acknowledge my laboratory colleagues and classmates in Taiwan who have extended their kindness and technical guidance to me during my study in Taiwan. Last but not least, I am deeply indebted to my family for their unconditional support and encouragement that have motivated me to pursue my study.

APPROVAL SHEET

This dissertation entitled **"ROLE OF MiRNAs REGULATING THE EMT/MET PROCESSES IN COLORECTAL CANCER-DERIVED INDUCED PLURIPOTENT CANCER CELLS (CRC-iPCs)"** was prepared by CHENG HAN PING and submitted as partial fulfilment of the requirements for the degree of Master of Medical Science at Universiti Tunku Abdul Rahman.

Approved by:

_____

(Dr. Ong Hooi Tin) Date: ……

Assistant Professor/Supervisor

Department of Pre-clinical Sciences

Faculty of Medicine and Health Sciences

Universiti Tunku Abdul Rahman

_____

(Senior Prof. Dr. Choo Kong Bung) Date: ……

Senior Professor/Co-supervisor

Department of Pre-clinical Science

Faculty of Medicine and Health Sciences

Universiti Tunku Abdul Rahman

FACULTY OF MEDICINE AND HEALTH SCIENCES

UNIVERSITY TUNKU ABDUL RAHMAN

Date: _____

SUBMISSION OF THESIS

It is hereby certified that **Cheng Han Ping** (ID no: **16UMM04901**) has completed this final year project entitled "**ROLE OF MiRNAs REGULATING THE EMT/MET PROCESSES IN COLORECTAL CANCER-DERIVED INDUCED PLURIPOTENT CANCER CELLS (CRC-iPCs)**" under the supervision of Dr. Ong Hooi Tin (Supervisor) from the Department of Pre-clinical Sciences, Faculty of Medicine and Health Sciences, and Senior Prof. Dr. Choo Kong Bung (Co-Supervisor) from the Department of Pre-clinical Sciences, Faculty of Medicine and Health Sciences and Prof. Dr. Chiou Shih-Hwa (Co-Supervisor) from the Department and Institute of Pharmacology, College of Medicine, National Yang-Ming University.

I understand that University will upload softcopy of my thesis in pdf format into UTAR Institutional Repository, which may be made accessible to UTAR community and public.

Yours truly,

_____

(Cheng Han Ping)

DECLARATION

I CHENG HAN PING hereby declare that the thesis is based on my original work except for quotations and citations which have been duly acknowledged. I also declare that it has not been previously or concurrently submitted for any other degree at UTAR or other institutions.

_____

CHENG HAN PING

Date: _____

TABLE OF CONTENTS

LIST OF TABLES

LIST OF FIGURES

LIST OF ABBREVIATIONS

3'UTR	3' untranslated region
APC	Adenomatous polyposis coli
APS	Ammonium persulfate
ASCs	Adipose-derived stem cells
Bcl-2	B-cell lymphoma 2
BMP	Bone morphogenetic protein
BSA	Bovine serum albumin
C19MC	Chromosome 19 miRNA cluster
CDH1	E-cadherin
CDKN1A/p21	Cyclin dependent kinase inhibitor 1A
cDNA	Complementary DNA
CDS	Coding sequence
CML	Chronic myeloid leukaemia
c-MYC	V-myc avian myelocytomatosis viral oncogene homolog
CO2	Carbon dioxide
CRC	Colorectal cancer
CRC-iPCs	Colorectal cancer-derived induced pluripotent cancer cells
CSCs	Cancer stem cells
CTCs	Circulating tumour cells
DAVID	Database for Annotation, Visualization, and Integrated
ddH_2O	Double distilled water
DEPC	Diethylpyrocarbonate
DGCR8	DiGeorge syndrome Critical Region gene 8
DMEM	Dulbecco's Modified Eagle Medium
DMEM/F12	Dulbecco's Modified Eagle Eedium/Ham F-12
DMSO	Dimethyl sulfoxide
dNTP	Deoxynucleotide

EDTA	Ethylenediaminetetraacetic acid
E/M	Epithelial/mesenchymal hybrid
EMT	Epithelial-to-mesenchymal transition
ESCs	Embryonic stem cells
ESCC-miRNA	ESC-specific cell cycle-regulating miRNA
FAP	Familial adenomatous polyposis and
FBS	Fetal bovine serum
FC	Fold change
FDR	False Discovery Rate
GEO	Gene Expression Omnibus
GFP	Green fluorescence protein
GO	Gene ontology
GSK3	Glycogen synthase kinase-3 beta
GSKß3	Glycogen synthase kinase beta 3
HGNC	HUGO Gene Nomenclature Committee
HIF1α	Hypoxia-inducible factor 1 alpha
HNPCC	Hereditary nonpolyposis colorectal cancer
HRP	Horseradish peroxidase
IKK	I kappa B kinase
iPC	Induced pluripotent cancer
iPSCs	Induced pluripotent stem cells
KEGG	Kyoto Encyclopedia of Genes and Genomes
KLF4	Kruppel-like factor 4
KRAS	Kirsten rat sarcoma 2 viral oncogene homolog
LB	Luria-Bertani broth
MEFs	Mouse embryonic fibroblasts
MEM	Minimum Essential Medium
MET	Mesenchymal-to-epithelial transition
miRNAs	MicroRNAs
MMP9	Matrix metallopeptidase 9
MMR	Mismatch repair genes
mRNA	Messenger ribonucleic acid
MSC	Mesenchymal stem cells

$NaHCO_3$	Sodium bicarbonate
NANOG	Nanog homeobox
NC	Negative control
NF-κB	Nuclear factor kappa B
nt	Nucleotide
OCLN	Occludin
OCT4	Pou class 5 homeobox 1
OSKM	OCT4, SOX2, KLF4, and c-MYC
P (Corr)	Corrected p value
p16Ink4a	Cyclin dependent kinase inhibitor 2A
p53	Tumour protein p53
PanIN	Pancreatic intraepithelial neoplasia
PBS	Phosphate buffered saline
PCR	Polymerase chain reaction
PDAC	Pancreatic ductal adenocarcinoma cells
PDCD4	Programmed cell death 4
PI	Propidium iodide
PI3K-Akt	Phosphatidylinositol 3-kinase-Protein Kinase B
Post-iPC	Post-induced pluripotent cancer cell
pre-miRNA	precursor miRNA
pri-miRNA	primary miRNA
PTEN	Phosphatase and tensin homolog
PVDF	Polyvinylidene fluoride
qRT-PCR	Quantitative reverse transcription polymerase chain
Rac1	Rac family small GTPase 1
RBL2	RB transcriptional corepressor like 2
RhoA	Ras homolog gene family, member A
RISC	RNA-induced silencing complex
RNA	Ribonucleic acid
rpm	Resolution per minute
RPM1 1640	Roswell Park Memorial Institute 1640 medium
RT	Reverse transcription
SDS	Sodium dodecyl sulphate

SDS-PAGE	SDS-polyacrylamide gel electrophoresis
SEM	Standard error of mean
SLUG	Snail Family Transcriptional Repressor 2
SMAD4	SMAD family member 4
SNAI1	Snail homolog 1
snRNA U6	Small nuclear RNA U6
SOX2	Sry (sex determining region y)-box 2
STAT3	Signal transducer and activator of transcription 3
STAT3	Signal transducer and activator of transcription 3
TEMED	Tetramethylethylenediamine
TGFBR2	Transforming growth factor-β receptor type II
TGFβ	Transforming growth factor beta
TS	Trophoblast stem cells
UC	Untransfected control
VEGF	Vascular endothelial growth factor
VIM	Vimentin
ZEB1/2	Zinc finger E-box binding homeobox 1/2
β-catenin	Beta-catenin
ΔΔCt	Delta delta ct

CHAPTER 1

INTRODUCTION

Colorectal cancer (CRC) is the third most common malignancy in Asia with the highest incidence observed amongst the Chinese (Veettil et al., 2017). More than 95% of colorectal cancer first arises as benign adenomatous polyps, which gradually accumulate both genetic mutations and epigenetic alterations, turning more dysplastic and eventually leading to the development of colorectal carcinoma and becoming metastatic in advanced stages (DeRosa et al., 2015). Metastasis remains a major cause of CRC mortality as most patients with distant metastasis usually show a poor 5-year survival rate of less than10% (Haggar and Boushey, 2009). Epithelial-to-mesenchymal transition (EMT) and the reversed process, mesenchymal-to-epithelial transition (MET), have been reported to play a crucial role in mediating tumour metastasis (Vu and Datta, 2017).

EMT is the conversion of cells from non-motile polarised layers of epithelial cells into motile and invasive mesenchymal cells. Previous reports have indicated the sequential EMT-MET activation is required for completion of the metastatic cascade (Tsai and Yang, 2013). In addition, besides the increased migratory properties, EMT activation also facilitates cancer progression through the acquisition of stem cell-like feature in cancer stem cells (CSCs), which further contributes to chemoresistance and CRC recurrence (Liu and Fan, 2015). In contrast, MET is activated during the initial

stage of somatic cell reprogramming. Interestingly, the association of stemness and EMT/MET regulation under different contexts shows that dynamic transition of EMT and MET is critical for cell-fate determination (Li et al., 2014).

MicroRNAs (MiRNAs) are negative regulators of expression of genes that play important roles in cellular reprogramming and cancer metastasis through various mechanisms, including regulation of the EMT and MET processes. Specifically, miR-200 family has emerged as tumour suppressive miRNAs in regulating cancer metastasis through suppression of EMT (Gregory et al., 2008) and cancer stem cell (CSC) properties (Shimono et al., 2009). Moreover, miR-302 promotes the reprogramming process by inhibiting TGF-ß and BMP signalling (Subramanyam et al., 2011), resulting in MET activation. Hence, it is important to understand the underlying mechanism between miRNA and EMT/MET interaction in cancer progression and the reprogramming process.

Tumourigenesis is progressive multi-step event that may take years for normal tissues to become tumours. The study of tumourigenesis has long been hampered by the lack of suitable study models for investigating mechanisms involved in the different steps of tumourigenesis. Since most of the tumour cell lines and animal xenografts are derived from primary tumour of advanced stages, early events of oncogenic transformation cannot be recapitulated. One

possible approach to overcome such limitations, transcription factors such as the Yamanaka factors Oct4, Sox2, Klf4 and c-Myc (OSKM) (Takahashi and Yamanaka, 2006; Takahashi et al., 2007), and other reprogramming factors, may be used to reprogramme cancer cells into induced pluripotent cancer cells (iPCs). Subsequently, the pluripotent iPCs may be differentiated into early organoids for use as disease study models to dissect early events in tumourigenesis. Such iPC models may also serve as platforms for biomarker discovery and drug screening (Câmara et al., 2016).

Moreover, iPCs have been reported to show less aggressive cancer phenotype and increased sensitivity to chemotherapeutic drugs (Miyoshi et al., 2010; Zhang et al., 2013). The reduced tumourigenicity may be attributed to the epigenetic remodelling of both oncogenes and tumour suppressor genes (Zhang et al., 2013; Miyazaki et al., 2015). Notably, the induction of the MET state and down-regulation of EMT-related genes by the reprogramming factors have also been postulated to contribute to the attenuation of cancer malignancies (Takaishi et al., 2016).

Clones of CRC-derived induced pluripotent cancer (CRC-iPCs) have previously been generated in our laboratory and subjected to miRNA profiling (Hiew et al, 2018). MiRNAs that are differentially expressed in the CRC-iPCs are predicted to play a role in the CRC reprogramming process. In this thesis, I further examine the involvement of the differentially expressed miRNAs in the

CRC-iPC clones in the EMT/MET processes. Using the down-regulated miR-362, this thesis also aimed to present experimental evidences that miR-362 directly regulated EMT and MET proteins.

Problem statements

Models to study early events of tumourigenesis are lacking; cancer cell reprogramming may provide such study models. However, reprogramming of cancer cells faces many obstacles due to genetic and epigenetic alterations (Izgi et al., 2017). Furthermore, most published studies have focused on the roles of EMT/MET in the reprogramming of somatic cells (Li et al., 2010; Samavarchi-Tehrani et al., 2010; Anokye-Danso et al., 2011; W.Wang et al., 2011), but not in cancers, particularly in exploring the regulatory roles of miRNAs in EMT/MET process underlying the cancer reprogramming. Hence, this study aimed to elucidate the regulatory network by which miRNAs mediating EMT/MET-related target genes in cancer cell reprogramming and possibly in cancer metastasis.

Hypothesis of study

In this study, colorectal cancer cell reprogramming was hypothesised to induce changes in miRNA expression profiles and signalling pathways that lead to alterations of the EMT and MET processes by targeting one or more EMT/MET genes to regulate cancer-cell reprogramming and mobility.

Research Objectives:

The main objective of my thesis was to elucidate the role of miRNAs in regulating the EMT and MET processes in relation to cancer-cell reprogramming and cell motility.

The specific objectives of this study were:

1. To identify and validate differentially expressed miRNAs in CRC-iPCs by genome-wide miRNA profiling.
2. To identify target genes of the differentially expressed miRNA and to predict functional roles and pathways by bioinformatics analysis.
3. To validate targeting of selected miRNA(s) and the effects on expression of EMT and MET target gene(s).
4. To elucidate the biological and functional effects of the miRNAs on the EMT/MET characteristics of cell migration and cell invasion.

CHAPTER 2

LITRETURE REVIEW

2.1 Colorectal Cancer (CRC)

Colorectal cancer is the third most common malignancy that diagnosed globally with estimated rate of 608,700 mortalities per year in both genders (Ferlay et al., 2010). Colon cancer usually begins as a benign growth known as adenomatous polyps which evolves into malignant carcinoma due to mutational loss of tumour suppressor genes and acquisition of oncogenes, resulting in uncontrolled cell proliferation, self-renewal and eventually lead to distant metastasis (DeRosa et al., 2015).

2.1.1 Risk Factors of Colorectal Cancer

The increasing CRC incidences in Asian countries have been associated with sedentary lifestyle, westernised dietary intake, tobacco smoking and alcohol consumption (Raskov et al., 2014). Notably, Chinese populations, living in South East Asia have higher incidences of CRC, compared to other ethnics (Veettil et al., 2017). Similar pattern of ethnic influence has also been observed in Japan and Korea, implying the etiological role of genetic predispositions in CRC development (Pourhoseingholi, 2012).

The prevalence of CRC also increases with aging, with about 80% of CRC diagnosed in patients over fifty years old (Granados-Romero et al., 2017). Moreover, fibre-deficient and high fat diets coupled with lack of physical activities may progressively lead to obesity, thereby increasing the risk of acquiring CRC (Haggar and Boushey, 2009). Carcinogenic by-products from smoking and alcohol consumption facilitate early development of adenomatous polyps (Raskov et al., 2014). In addition to external environmental factors, inherited genetic mutations are accountable for less than 10% of all the recorded CRC cases. The two most common CRC hereditary diseases are familial adenomatous polyposis (FAP) and hereditary nonpolyposis colorectal cancer (HNPCC) (Brosens et al., 2015; DeRosa et al., 2015). Mutations to germline adenomatous polyposis coli (APC) gene in FAP and multiple DNA mismatch repair genes (MMR) in HNPCC contribute to higher CRC risk (DeRosa et al., 2015). Routine screening is effective in detecting early symptoms of CRC to prevent onset of the disease.

2.1.2 Molecular Basis of Colorectal Cancer

CRC begins with chromosomal instability that leads to sequential inactivation of the tumour suppressor gene APC, followed by activation of the oncogene KRAS and subsequently causes loss-of-function of another tumour suppressor gene, TP53 (Tariq and Ghias, 2016).

The loss of APC protein disrupts the formation of protein complex with glycogen synthase kinase (GSK)-3β, resulting in accumulation of β-catenin oncoprotein that activate the Wnt signalling pathway (Najdi et al., 2011; Colussi et al., 2013). Activation of the Wnt signalling leads to increased cell proliferation (MacDonald et al., 2009). Moreover, aberrant activation of K-ras oncogene causes dysregulation in signal transduction that drives the cell cycle progression and transition of adenoma to carcinoma (Al-Sohaily et al., 2012). Inactivation of TP53 also enables neoplastic cell to escape cell-cycle arrest and p53-mediated apoptosis. Hence, loss of TP53 promotes transition of adenomas to invasive carcinomas (Li et al., 2015).

Epithelial-to-mesenchymal transition (EMT) plays a critical role in promoting CRC metastasis at advanced stage. Besides the increased invasiveness, EMT also induces expression of stem-cell specific genes and therefore promotes sustained proliferation and self-renewal ability (Cao et al., 2015). EMT-induced signalling pathways include transforming growth factor-β (TGF-β), Wnt, and phosphoinositide 3-kinase (PI3K-AKT) pathway. Genetic mutations in TGF-β receptors (TGFBR2) and Smad proteins have been implicated for approximately 50% of all CRC incidences (Bellam and Pasche, 2010). Loss-of-function of SMAD4 has been correlated with increased levels of β-catenin (Freeman et al., 2012) and STAT3 (Zhao et al., 2008) which further induce EMT process by activating the transcription of ZEB1 to up-regulate matrix metalloprotease MMP9 (Xiong et al., 2012). In addition, loss of PTEN, a negative regulator of PI3K/AKT signalling, is often associated with

CRC progression (Molinari and Frattini, 2014). Phosphorylated AKT regulates EMT by elevating the expression of EMT transcription factors, SNAI1 and SLUG (Suman et al., 2014). Moreover, the downstream effectors of PI3K/AKT signalling, mTORC1 and mTORC2 also promote EMT and metastasis of CRC via RhoA and Rac1 signalling (Gulhati et al., 2011).

Surgical removal of tumours still remains the best approach to improve patient survival rates. However, more than 50% of all CRC patients show distant metastasis at the time of diagnosis or relapse after intended treatment, which is the major cause of CRC-associated death (Calon et al., 2012). Low 5-year survival rate of less than 10% is correlated to metastatic CRC (Brenner et al., 2014). Therefore, better understanding of genetic mutations and molecular pathways underlying the regulation of CRC progression and metastasis is imperative in the development of effective therapeutic treatments for CRC patients.

2.1.3 Current Models of CRC and limitations

The low success rate of drug development, with only 5% of candidate drugs are approved for clinical use in Phase I /II clinical trials, is partly due to the use of preclinical models that poorly recapitulate the disease progression (Kola and Landis, 2004).

Conventional 2D monolayer cell models are easy to handle and inexpensive but harbour numerous disadvantages due to the lack of cellular heterogeneity and cell-to-matrix interactions as well as failure to model the activation of the immune systems during tumourigenesis process (Garnett and McDermott, 2014).

In vivo mouse model established by transplanting CRC cell line into immune-deficient mouse is also widely used for the preclinical testing of drug compounds. The subcutaneous xenograft models are useful for rapid drug target screening in large numbers because the transplanted cell lines are easily accessible for genetic manipulation prior to transplantation and tumour growth can be observed within two weeks (McIntyre et al., 2015). However, the inoculated homogenous cell population may not reflect heterogeneity in tumour (Golovko et al., 2015). Furthermore, the functional role of immune system in tumourigenesis cannot be studied in immune-deficient mice (Golovko et al., 2015). Alternatively, these problems can be circumvented with the use of patient-derived xenografts (PDX) which enables preservation of original tumour heterogeneity, vascularity and interaction between tumour and stromal cells (Katsiampoura et al., 2017).

A major disadvantage of subcutaneous and PDX transplantation is the natural difference between the microenvironment of the subcutaneous space from that of the colon (McIntyre et al., 2015). Therefore, orthotropic models

have been developed whereby CRC cells are directly inoculated into the wall of the colon or caecum to overcome the problems posed by tumour growth in artificial environment (Evans et al., 2016). The orthotropic mouse model also allows metastasis studies in advanced CRC as they closely mimic the local tumour invasion, vascular spread and distant metastasis to secondary organs (Evans et al., 2016). In addition, metastatic models are also established to facilitate studies of the metastatic process as well as testing of novel drug compounds. Tumour cells are inoculated into the spleen, portal vein or liver parenchyma of mice to mimic liver metastases, whereas tail vein injection is used to model lung metastases (Szabo et al., 2015). Many CRC models have been developed to facilitate drug discovery. However, most of the tumour cell lines and xenografts are derived from primary tumour of advanced stage. In such cell lines, early events of oncogenic transformation cannot be recapitulated.

2.2 Induced Pluripotency in Cancers

2.2.1 Induced Pluripotent Cancer Cells (iPCs)

Since the early successes in reprogramming of normal somatic cells, recent studies have centred on the development of iPSCs derived from malignant cells; the cancer-derived cells are known as induced pluripotent cancer cells (iPCs) (Izgi et al., 2017). These iPCs were capable of differentiating into three germ layers *in vitro* and form teratoma, indicating the presence of pluripotency (S.Lin et al., 2008; Miyoshi et al., 2010). However,

they are different from iPSCs due to the expression of oncogenes and abnormal karyotypes (Carette et al., 2010; Miyoshi et al., 2010).

The generation of iPCs facilitates the recapitulation of early disease. Thus, may serve as a suitable platform to explore the mechanisms of tumour initiation and progression *in vitro* (Zhu et al., 2018). Moreover, the iPCs can be differentiated into cancer cell progenitors for novel drug screening and biomarker discovery, particularly in the early stages of the disease (Izgi et al., 2017). The reprogrammed cancer cells may also provide alternative way to generate large population of cancer stem cells (CSCs) for studying biological properties that contribute to tumour recurrence (Zhu et al., 2018).

However, unlike somatic cells, cancer cell reprogramming has faced numerous obstacles. In somatic cells, reprogramming process complies with a continuous stochastic model, in which all cells are transduced at equal probability into a pluripotent state (Yamanaka, 2009). However, the presence of cancer-specific genetic mutations, chromosomal rearrangements and accumulation of DNA damage, has hindered the success in resetting the cancer-associated epigenome to that close to an embryonic stem cell-like state (Ramos-Mejia et al., 2012; Izgi et al., 2017). Therefore, successful cancer cell reprogramming is currently limited to certain cancer cell types. Moreover, the issue of low reprogramming efficiency has been commonly encountered in cancer cell reprogramming. Various methods have been proposed to augment

the reprogramming efficiency. The introduction of Hypoxia-inducible factor 1 alpha (HIF1α) has been shown to accelerate the induction of iPCs from the lung carcinoma cell line, suggesting the involvement of hypoxia in regulation of pluripotency (Mathieu et al., 2011). In line with that, hypoxia has been reported to activate the expression of stemness genes, such as Oct4, Klf4, c-MYC (OKM) and NANOG, as well as stem cell-associated miRNAs to promote the self-renewal ability (Mohyeldin et al., 2010; Mathieu et al., 2011). Furthermore, inhibition of p53 expression may promote induction of pluripotent state through repression of mir-34 family which functions in the suppression of pluripotency genes (Lin et al., 2012).

Despite the challenges faced, iPCs have been generated from various cancer types including melanoma (Bernhardt et al., 2017), gastrointestinal (Miyoshi et al., 2010), chronic myeloid leukaemia (CML) (Carette et al., 2010; Kumano et al., 2012), sarcoma (Zhang et al., 2013), osteosarcoma (Choong et al., 2014) , pancreatic ductal adenocarcinoma (Kim et al., 2013) and glioblastoma (Stricker and Pollard, 2014). These reprogrammed cancer cells exhibit pluripotent state with an altered differentiation programme that leads to the loss of tumourigenicity (Miyoshi et al., 2010; Zhang et al., 2013).

Although reprogramming efficiency was further enhanced through combinational treatment with small molecules, transcription factors, and signalling pathway regulators, the mechanisms by which differentiated cells

lose their somatic epigenetics and acquire pluripotency remains to be elucidated.

.

2.2.2 Application of iPCs in Disease Modelling

As mentioned in section 2.1.3, currently available CRC models uses tumour cell lines or xenografts derived from advanced-stage tumour. This limitation can be overcome with the application of iPC technology which enables the recapitulation of cancer phenotype (Izgi et al., 2017). To date, a few studies managed to elucidate disease progression using the iPC derived from malignant cancers (Carette et al., 2010; Kumano et al., 2012; Kim et al., 2013).

iPC cells were reported to exhibit reduced cancer phenotype and increased chemosensitivity (Miyoshi et al., 2010). iPC clones derived from gastrointestinal cancers showed higher levels of the tumour suppressor genes p16Ink4a and p53 (Miyoshi et al., 2010). Upon re-differentiation into post-iPCs, these differentiated cells did not form any secondary tumour when injected into immune-deficient mice compared to parental tumour cells, suggesting diminished tumourigenicity. This observation is concurrent with the activation of tumour suppressor genes (Miyoshi et al., 2010). In a separate study, CML-derived iPCs was found to be imatinib-resistant (Carette et al., 2010). However, re-differentiation of CML-derived iPCs to haematopoetic

cells recapitulated disease phenotype and the differentiated cell become susceptible to imatinib again, exemplifying the acquisition of cancer phenotype during hematopoietic differentiation (Kumano et al., 2012). In a similar study, reprogrammed pancreatic ductal adenocarcinoma cells (PDAC) injected into immune-deficient mice evolve into pancreatic intraepithelial neoplasia (PanIN) precursors that exhibits invasive phenotype (Kim et al., 2013). The PanIN-like cells were shown to secrete putative biomarkers of early-stage pancreatic cancer (Kim et al., 2013).

Previous studies have shown that iPCs may serve as a disease model to gain new insights on cancer development. The reversible phenotypic nature conferred by cancer cell reprogramming is crucial to elucidate the molecular network underlying cancer initiation and progression to fuel the development of targeted therapeutic treatments as alternative to currently available regimen (Ramos-Mejia et al., 2012).

2.3 Epithelial-to-Mesenchymal Transition (EMT) and Mesenchymal-to-Epithelial Transition (MET)

Epithelial-to-mesenchymal transition (EMT) and the reversed process Mesenchymal-to-epithelial transition (MET) have been known to play critical role in multiple cell-fate conversions including embryonic development

(Thiery et al., 2009), tumour progression (Tsai and Yang, 2013) and somatic cell reprogramming (Li et al., 2010; J.Chen et al., 2012). EMT involves phenotypic conversion of non-motile and polarised layers of epithelial cells into motile and invasive mesenchymal cells (Figure 2.1) (Kalluri and Weinberg, 2009; Craene and Berx, 2013). In contrast, MET reverts EMT phenotypes where mesenchymal cells are converted back to differentiated epithelial cells for maintenance of tissue stability and structure (Lamouille et al., 2014). Under normal physiological condition, EMT plays critical role in developmental morphogenesis and gastrulation while MET enables the cells to differentiate into specialised lineages (Thiery et al., 2009). In adults, EMT program is activated during wound healing for regenerative purpose upon exposure to inflammatory cytokines and under hypoxia condition (Chapman, 2011).

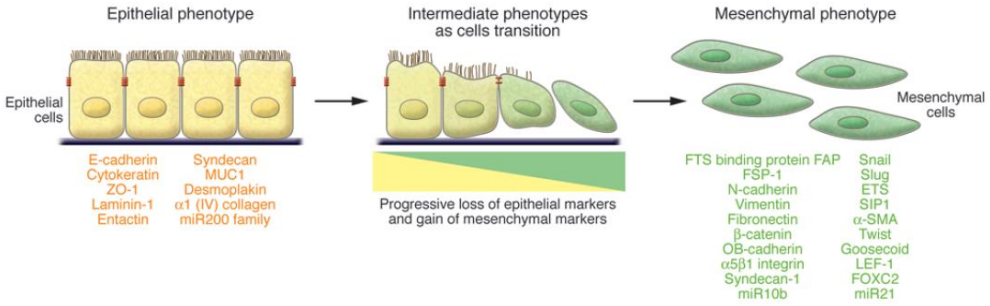

Figure 2.1 Morphological changes involved in EMT regulation. Adapted from Kalluri and Weinberg, 2009. Cellular markers commonly used to distinguish the epithelial and mesenchymal phenotypes are listed. EMT transforms cells from non-motile and polarised epithelial cells into motile and invasive mesenchymal cells. The reverse of this process is known as mesenchymal-to-epithelial transition (MET). Both processes occur in developmental morphogenesis, wound healing and cancer progression.

2.3.1 Molecular Mechanism of EMT/MET Signalling Pathway

Activation of EMT involves a collection of transcriptional and post-translational events that subsequently lead to the acquisition of mesenchymal phenotype (Zheng and Kang, 2014). For example, specific structural proteins such as E-cadherin and Vimentin are transcriptionally altered and serves as primary markers to characterise the EMT and MET status of a cell (Neureiter, 2012). The EMT process is activated in response to extracellular signalling pathways called EMT inducers, including TGF-β, PI3K-AKT, Wnt, and Notch signalling, that subsequently lead to activation of a set of EMT core transcription factors (Craene and Berx, 2013; Lamouille et al., 2014).

The major EMT transcription factors, such as the SNAI1, ZEB and Twist family member proteins work co-ordinately and synergistically to repress the epithelial gene expression as well as to induce the expression of mesenchymal genes, leading to enhanced migratory and invasive abilities (Zhang et al., 2016). For instance, studies have demonstrated that cells overexpressing SNAI1 acquire spindle-shaped morphology and are correlated with increased cell motility and invasiveness *in vitro* (Fan et al., 2012). Such morphological change is caused by transcriptional repression of E-cadherin, followed by the concurrent increase in the expression of mesenchymal markers, such as vimentin and N-cadherin, resulting in alteration of cell polarity and cytoskeletal remodelling. It has been proposed that EMT also facilitates cancer progression by conferring resistance towards apoptosis and generation of stem

cell-like feature besides enhancing mesenchymal migratory properties (Wang and Zhou, 2013).

Moreover, EMT is also regulated at epigenetic levels by modifications such as DNA methylation, histone modification and microRNAs (miRNAs), which collectively contribute to the plasticity underlying EMT/MET processes (Škovierovï et al., 2017). Taken together, the regulation of EMT/MET processes is dynamic, intricate and highly modulated by numerous signalling pathways at epigenetic, transcriptional and post-transcriptional levels during cellular transition. Therefore, a better understanding of the molecular mechanisms that are involved in EMT/MET regulation may lead to the development of new therapeutic approaches.

2.3.2 Roles of EMT and MET in Cancer Development and Metastasis

Acquisition of invasive phenotype is associated with EMT whereby tumour cells become motile and capable to migrate from the primary tumour site (Figure 2.2) (Thiery, 2002). EMT initiates the degradation of extracellular matrix (ECM) and basement membrane, liberating the migratory cells (Tsai and Yang, 2013). Breach of basement membrane is followed by intravasation, a process of which tumour cells crosses the endothelial lamina and enter the systemic vascular circulation for dissemination. At the new distant site, MET is reactivated for the establishment of cell-to-cell contacts that promotes cell

proliferation and secondary tumour formation (Tsai and Yang, 2013). Reversion to MET is necessary as cancer cells with EMT phenotype are limited in proliferation capacity (Brabletz, 2012). This is consistent with the finding that showed EMT-related transcription factors Snail and ZEB2 cause growth arrest by inhibiting cyclin D activity (Mejlvang et al., 2007). Separate studies have demonstrated that EMT mediates only the early stages of metastasis including invasion, intravasation and dissemination (Ocaña et al., 2012; Tsai et al., 2012). However, the loss of EMT transcription factor is observed at the later stage of cancer metastasis (Ocaña et al., 2012; Tsai et al., 2012). For instance, Twist1 was upregulated in the primary skin tumour during local invasion and dissemination whereas it was found to be downregulated during re-differentiation of the tumour (Tsai et al., 2012).

Surprisingly, there is increasing number of evidence showing that cancer cells may activate EMT to different extents, leading to acquisition of the epithelial/mesenchymal (E/M) hybrid or partial EMT state, where both epithelial and mesenchymal markers are co-expresssed (Jolly, 2015). In fact, in the context of cancer progression, circulating tumour cells (CTCs) surviving in bloodstream display E/M hybrid phenotype which is associated with the gain of resistance to anoikis as well as favouring extravasation (Aceto et al., 2014; Joosse et al., 2015). Moreover, cancer cells with E/M hybrid phenotype exhibit cell cluster migration due to retention of epithelial characteristics concurrent with enhanced extracellular matrix attachment from acquisition of mesenchymal characteristics (Jolly, 2015). Moreover, the hybrid E/M states are

also associated with cancer stem cell functions and confer higher tumour-initiating potential (Hou et al., 2012).

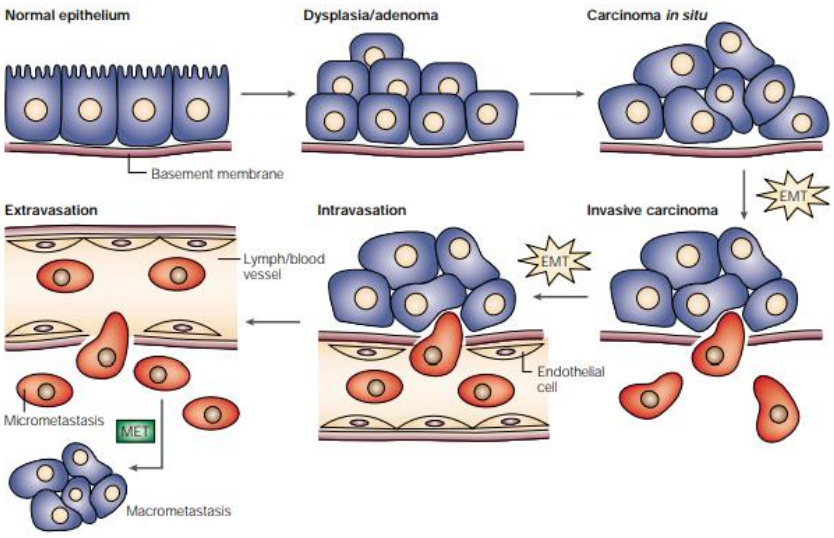

Figure 2.2 Regulation of EMT and the reversed process, MET in cancer metastasis. Adapted from Thiery, 2002. The initial stage of cancer metastasis involves activation of EMT with the loss of polarity in epithelial cells, resulting in detachment from the basement membrane and invasion across the endothelial lamina. Progression from the invasive cancer stage to metastatic cancer also involves the activation of EMT that enables cancer cells to be distributed in blood circulation and facilitates extravasation into secondary site, where MET is reactivated for the formation micro- and macro-metastases to facilitate colonization of secondary organ.

2.3.3 Roles of EMT and MET in Somatic and Cancer Cells Reprogramming

The first induced pluripotent stem cells (iPSCs) were established from mouse and human fibroblast through the ectopic introduction of four different transcription factors known as Oct4, Sox2, Klf4, and c-Myc, or collectively known as OSKM factors (Takahashi and Yamanaka, 2006; Takahashi et al., 2007).

Increasing number of evidence has shown that activation of MET is crucial during the early phase of reprogramming (Li et al., 2010; Hawkins et al., 2014). Experimentally, both the Oct4 and Sox2 were reported to inhibit the expression of Snail (Li et al., 2010). c-Myc was involved in blocking the TGF-ß1 and TGF-ß receptor 2 (TGF-ßRII), whereas Klf4 induced MET by upregulating E-cadherin (Li et al., 2010). In addition, induction of EMT by overexpressing TGF-ß in the early stage of reprogramming prevented MET, resulting in blockage of reprogramming process (Maherali andHochedlinger, 2009). In brief, any process that favours MET and inhibits EMT may enhance the reprogramming efficiency (Hawkins et al., 2014). It was reported that SMAD 7, an inhibitor of EMT, targeted TGF-B signaling pathway and replaced Sox2 in the reprogramming process (Li et al., 2010). Another study demonstrated that bone morphogenetic protein (BMP) improved reprogramming by inducing MET in the absence of Klf4 (Chen et al., 2011). All these studies have proposed a link between MET and reprogramming.

A separate study found that knockdown of EMT transcription factor, Snail, reduces reprogramming efficiency of somatic cells (Unternaehrer et al., 2014). Further investigation revealed that Snail bind to Let-7 promoter and suppresses let-7 miRNAs expression. Let-7 miRNAs compromises efficiency in the early reprogramming (Unternaehrer et al., 2014), highlighting that Snail is required to keep let-7 miRNA in check for initiation of reprogramming. Moreover, sequential introduction of reprogramming factors, along with early treatment of TGF-ß or Slug overexpression, was reported to induce early EMT response which increased reprogramming efficiency of iPSCs (Liu et al., 2013), suggesting that EMT may play a role in reprogramming process.

Taken together, EMT and MET processes are regulated in a context-dependent manner, in which EMT/MET transition is different between somatic and cancer cells. Hence, the use of CRC-iPC may serve as a platform to identify the molecular mechanism that involves in the regulation of EMT/MET processes during CRC reprogramming and cancer progression

2.4 MicroRNAs (miRNAs)

MiRNAs are short, non-coding RNAs (20-21 nucleotides in length) that regulate gene expression post transcriptionally by binding at the 3' untranslated region (3'UTR) of target mRNA (Bartel, 2009). Interactions between miRNA and mRNA are usually restricted to the ~6 to 8-nt seed sequence near the 5' terminal end. The base pairing between miRNA and mRNA may lead to mRNA degradation and translation suppression, depending on the degree of complementarity (Bartel, 2009). The seed sequence of a specific miRNA is highly conserved among species which facilitate regulation of various biological processes including development, cell differentiation, proliferation and apoptosis (Tétreault and DeGuire, 2013). Moreover, miRNAs are encoded as polycistronic transcripts, suggesting that members of the same miRNA family may evolve simultaneously, thus allowing the same members to recognize and target the same set of mRNAs (Wang et al., 2016). Dysregulated miRNA expression is associated with disease development such as cancers (Andrés-León et al., 2017).

2.4.1 Biogenesis and Function of miRNAs

The synthesis of miRNAs is a tightly-controlled multistep process that begins with miRNA transcription in the nucleus followed by processing of mature miRNA in the cytoplasm, where the mature miRNAs function as gene

regulators (Figure 2.3) (Tétreault and DeGuire, 2013). The miRNAs can be categorized as intronic or intergenic based on their genomic location (MacFarlane and R. Murphy, 2010). Intronic miRNAs are encoded within the introns of protein-coding transcripts, and are transcribed along with primary transcript from the same promoter (Kim and Kim, 2007; Ramalingam et al., 2014). On the contrary, intergenic miRNAs coding are frequently distributed between protein-coding genes, and are regulated by independent transcriptional promoters (Lee et al., 2004).

MiRNA is first transcribed as long primary miRNA (pri-miRNA) transcripts by RNA polymerase II (Lee et al., 2004). Next, the pri-miRNA is then cleaved by a microprocessor complex, composed of RNase III enzyme Drosha and RNA binding protein DiGeorge syndrome Critical Region gene 8 (DGCR8), into precursor miRNA (pre-miRNA) with a hairpin-loop structure (Lee et al., 2003; Gregory et al., 2004). The resultant pre-miRNA is exported out of nucleus into cytoplasm by Exportin5/Ran-GTP complex (Lund et al., 2004) before it is further processed by another enzyme, Dicer, into mature miRNA: miRNA* duplex (Hutvágner et al., 2001). One of the strand, the miRNA strand, of the duplex functions as guiding strand and is incorporated into the Argonaute-containing RNA-induced silencing complex (RISC) (Maniataki and Mourelatos, 2005). The RISC-miRNA assembly recognises and interacts with the 3'-UTR of the target mRNA via complementary base-pairing with miRNA seed sequence. Perfect base-pairing leads to mRNA degradation. In circumstances where the base-pairing is only partially complement,

translational suppression of mRNA occurs (Mallanna and Rizzino, 2010). The remaining strand, usually designated as miRNA* or passenger strand, is released and degraded elsewhere (Winter et al., 2009).

In some cases, both the guiding and passenger strands of a pre-miRNA survive the processing process. Both mature miRNAs, excised from the 5'- and 3'- arms, are designated as the -5p and -3p species, respectively (Choo et al., 2014). Both the -5p and -3p miRNA species have been reported to be functional and target different mRNAs due to different seed sequence (Griffiths-Jones et al., 2006). The nomenclature of miRNA-5p and -3p is currently applied according to the arm which the miRNA is derived from.

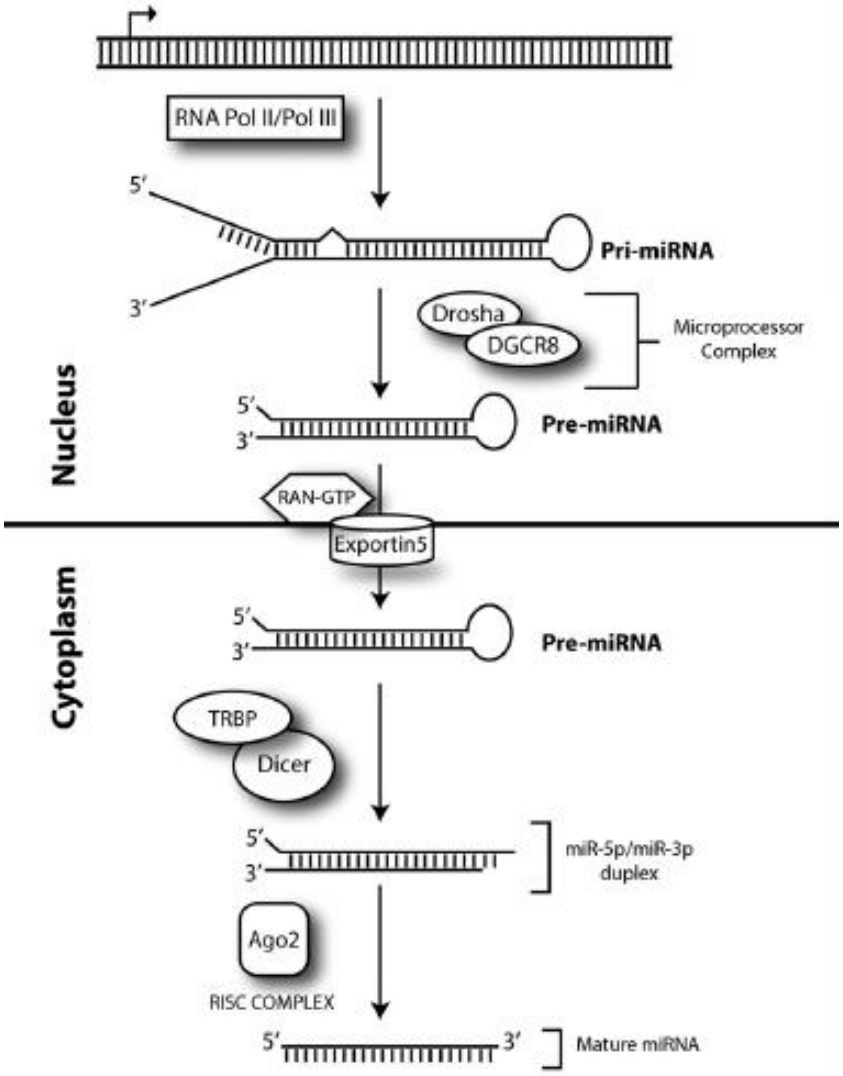

Figure 2.3 Biogenesis process of microRNAs. Adapted from Tétreault and DeGuire, 2013. Synthesis of miRNA is a multistep pathway, which starts in the nucleus with the transcription of miRNA followed by the maturation of the miRNA in the cytoplasm.

2.4.2 Roles of miRNAs in Pluripotency Maintenance and Self-Renewal

MiRNAs play an important role in the regulation of pluripotency, self-renewal and differentiation process in embryonic stem cells (ESCs) (Lüningschrör et al., 2013). It has been noted that specific miRNAs, particularly members from the miR-290, miR-302 and miR-17-92 families, are specifically upregulated in ESCs, but are absent in terminally differentiated cells (Marson et al., 2008). This specific subset of miRNAs is identified as ESC-cell cycle (ESCC)-regulating miRNAs. The effect of these miRNAs in the regulation of ESCs self-renewal was investigated using miRNA-deficient models with defects in miRNA processing complex (Wang et al., 2008; Y.Wang et al., 2013). Results showed a markedly delayed cell-cycle progression in Dicer- and Dgcr8-deficient murine ESCs, supporting the importance of ESCC-miRNAs in regulating cellular pluripotency (Wang et al., 2008; Y.Wang et al., 2013).

Core ESC transcription factors such as OCT4, SOX2 and NANOG have been reported to bind and activate promoters of several ESCC miRNAs, including miR-290-295, miR-302/367 and miR-92 (Marson et al., 2008), establishing a relationship between these miRNA clusters to pluripotency-regulation pathways. These ESCC-miRNAs have been shown to reinforce the pluripotent identity of ESCs by inhibiting expression of the developmental genes such as RB transcriptional corepressor like 2 (RBL2) and CDKN1A/p21, which in turns upregulate the pluripotency-associated genes, such as OCT4,

SOX2, LIN28 and NANOG, and forms a positive feedback loop (Lin et al., 2011; Anokye-Danso et al., 2012). In addition, the high expression of ESCC miRNAs has also been reported to upregulate LIN28, which directly suppresses miRNA let-7 maturation, thereby maintaining the self-renewal state of ESCs (Shyh-Chang and Daley, 2013).

In contrast, as the ESC differentiation occurs, the expression of ESCC-miRNAs is down-regulated whereas pro-differentiation miRNAs, such as let-7, miR-134, miR-296 and miR-470 are upregulated (Melton et al., 2010; Lüningschrör et al., 2013). These pro-differentiation miRNAs can be categorised into two groups depending on their distinctive functions in promoting differentiation. The first group consists of miRNAs that indirectly suppress the self-renewal state of pluripotent ESCs by inhibiting the transcription of OCT4, SOX2 and NANOG, such as miR-134, miR-296 and miR-145 (Y.M.-S.Tay et al., 2008; Y.Tay et al., 2008). The second group of miRNAs mainly functions to stabilise the differentiated state, including let-7 family which inhibits c-MYC and the downstream targets of the ESC pluripotency transcription factors (Melton et al., 2010). During differentiation, LIN28 expression is down-regulated as the expression of the OCT4, SOX2, NANOG and ESCC-miRNAs is suppressed (Thornton and Gregory, 2012). In the absence of LIN28, let-7 expression is not suppressed and resulting in suppression of genes that function in maintaining self-renewal ability (Thornton and Gregory, 2012).

In brief, synergistic interplay between ESC core transcription factors and ESCC-miRNAs may help to sustain the pluripotent identity through simultaneous repression of lineage-differentiation programme and activation of pluripotent programme.

2.4.2.1 MiRNA-Mediated Reprogramming of Somatic and Cancer cells

Since the importance of miRNAs in pluripotency regulation is well established, miRNA-mediated reprogramming has been applied in the generation of iPSCs and iPCs (S. L.Lin et al., 2008; Subramanyam et al., 2011). Studies have shown the ESCC-regulating miRNAs enhance iPSC reprogramming efficiency. Overexpression of mir-290 family members in combination with only three pluripotency factors, Oct4, Sox2, and Klf4, in mouse embryonic fibroblasts (MEFs) raises the reprogramming efficiency by about 10 folds showing that miRNAs are capable of replacing the oncogenic c-MYC (Judson et al., 2009). The replacement of c-MYC by mir-290s in reprogramming suggests that c-MYC could be a transcriptional regulator governing promoters of miR-290 cluster (Judson et al., 2009). Moreover, other groups have reported the use of miRNA groups to reprogramme human fibroblast cells in the absence of OSKM factors, including miR-302-367 (Anokye-Danso et al., 2011), miR-200c, miR-302 and miR-369 (Miyoshi et al., 2011).

Similarly, miRNAs have also been employed in cancer cell reprogramming. The first study involve transfecting miR-302 family into human skin cancer cells (Colo) in the absence of OSKM factor (S. L.Lin et al., 2008). In addition, miR-200c, miR-302a-d and miR-369-3p and -5p have also been used to reprogramme hepatocellular carcinoma (Koga et al., 2014) and colorectal cancer cells (Miyazaki et al., 2015).

Mechanistically, miRNAs promote reprogramming by regulating the target genes that are involved in the reprogramming processes, including MET, cell proliferation, inhibition of senescence and apoptosis (Anokye-Danso et al., 2012). The initiation phase of somatic cell reprogramming is characterised by MET which explains the beneficial roles of the miR-200 and miR-302-367 clusters (Samavarchi-Tehrani et al., 2010; Subramanyam et al., 2011). For instance, miR-302 inhibits TGF-ß signalling by down-regulating expression of the transforming growth factor β receptor II (TGFβR2) (Subramanyam et al., 2011) as well as promoting BMP signaling by targeting BMP inhibitors, DAZAP2, SLAIN1, TOB2 (Lipchina et al., 2011), resulting in MET activation. Moreover, over-expression of the miR-200 family has also shown to promote MET by inhibiting the EMT transcription factors, ZEB1/2, via a negative feedback loop (G.Wang et al., 2013).

Furthermore, miRNAs also play an important role in promoting rapid cell cycle progression and proliferation (Wang et al., 2008). For instance, the

miR-302-367 family promotes cellular proliferation by targeting the cell cycle inhibitors, RBL2 and CDK1NA/p21, to overcome the G1/S phase barrier (Tian et al., 2011; Y.Wang et al., 2013). Increased proliferation facilitates reprogramming by remodelling the epigenome through new DNA synthesis, thus removing the epigenetic barriers that repress the pluripotency-regulation network (Wang et al., 2008). Besides, the p53-induced senescence remains as a major barrier in reprogramming cell to full pluripotency (Spike and Wahl, 2011). Therefore, inhibition of p53 level by overexpressing miR-138 promotes reprogramming process (Ye et al., 2012). On the other hand, suppression of miR-34 family, which functions in repression of the pluripotency genes and anti-apoptotic gene, B-cell lymphoma 2 (Bcl-2), also facilitates iPSC formation (Choi et al., 2011).

The use of miRNAs as a tool for reprogramming has offered alternative approaches to circumvent problems associated with the viral-mediated transduction, the use of oncogenic transcription factors and the low reprogramming efficiency (Hu, 2014). However, compared to somatic cells, there are few studies on miRNA expression profile in reprogrammed cancer cells. Little is known about the miRNA-mediated molecular mechanisms in promoting the reprogramming of cancer cells or iPCs. Hence, genome-wide miRNA profiles of reprogrammed cancers may help to provide insights in the miRNA expression pattern in iPCs as well as in elucidating functions of the differentially-expressed miRNAs in promoting pluripotency and reprogramming process.

2.4.3 Roles of miRNAs in Tumourigenesis

MiRNA dysregulation has been implicated in most cancer progression (Mendell and Olson, 2012). Generally, miRNAs have been classified as oncogenic or tumour suppressive, depending on the oncological consequences of the miRNA expression. Oncogenic miRNAs or known as oncomiRs, are overexpressed in cancer and contribute to cancer phenotype by targeting and inhibiting expression of the tumour suppressor genes (Jansson and Lund, 2012). On the contrary, tumour suppressive miRNAs are usually underexpressed which results in up-regulation of oncogenes (Jansson and Lund, 2012). The collective regulatory outcome of both oncogenic and tumour suppressive miRNAs may function to promote or inhibit tumour development by regulating cell proliferation, apoptosis, invasion and metastasis (Jansson and Lund, 2012).

For instance, miR-21 is commonly overexpressed in various types of cancer and involved in targeting numerous tumour suppressor genes, including anti-apoptotic Bcl-2, phosphatase and tensin homolog (PTEN) and programmed cell death 4 (PDCD4) (Feng and Tsao, 2016). Thus, up-regulation of miR-21 contributes to increased proliferation and suppression of apoptosis. In contrast, miR-34a, which is transcriptionally activated by the tumour suppressor gene, p53, is frequently repressed in many cancers and is involved in targeting genes function in regulation of cell proliferation, apoptosis, motility and immune evasion (R.Wang et al., 2013).

Due to the dysregulated expression in cancer development and tissue-specific distribution, miRNAs may serve as potential diagnostic, prognostic, and predictive biomarkers. For example, miR-143 and miR-145 are often down-regulated in colorectal cancers, suggesting that these miRNAs may be used in diagnosis of CRC (Li et al., 2012). The application of miRNAs as CRC biomarkers may serve as a cost-effective and less invasive alternative approach for CRC screening and prediction of therapeutic response as miRNAs can be readily identified in blood sample (Dong et al., 2011; Ren et al., 2015).

MiRNA-orientated therapy usually involves reintroduction of synthetic miRNA mimics to restore the tumour suppressive miRNA expression to normal levels (Baumann and Winkler, 2014)) whereas inhibition of oncomiRs via delivery of antisense onligonucleotides or antagomiRs (Baumann and Winkler, 2014) may be used to restore the function of tumour suppressor genes. Therefore, thorough characterization of miRNAs according to respective oncological role is vital knowledge to develop effective miRNA-oriented therapy. Such comprehensive characterization is feasible by identifying differentially-expressed miRNAs between parental and treated cells. This approach of miRNA characterization is adopted in this study and could present novel miRNA candidates to serve as CRC biomarker for diagnosis and miRNA-based cancer therapy.

2.4.3.1 Roles of MiRNAs in Regulating EMT and MET in Cancer Metastasis

Given the critical roles of miRNAs in cancer initiation and progression, aberrant miRNA expression may modulate the EMT-related signaling networks to drive malignant transformation and encourage tumour invasion and metastasis (Yilmaz and Christofori, 2009). The transformation is featured by molecular and phenotypic changes in cells that trigger transition of immotile epithelial cells to motile invasive mesenchymal cells as evidenced by the down-regulation of epithelial E-cadherin (CDH1) protein (Heerboth et al., 2015).

MiRNAs regulate EMT by inhibiting expression of EMT transcription factors (Figure 2.4) (Chi and Zhou, 2016). The miR-200 family, which consists of miR-200a/b/c, miR-141, and miR-429, is known as EMT regulator in many cancers, including CRC (Korpal et al., 2008; Park et al., 2008; M. L.Chen et al., 2012). Family members of miR-200 were shown to upregulate CDH1 expression by repression of ZEB1 and ZEB2 mRNA translation. Overexpression of miR-200c inhibited cell migration and invasion in various CRC cell lines via direct targeting of ZEB1 (M. L.Chen et al., 2012). Moreover, down-regulation of miR132, miR-192 and miR-335, which directly target ZEB2, is closely correlated to distant metastasis and advanced-stage of CRC (Geng et al., 2014; Z.Sun et al., 2014; Zheng et al., 2014).

In contrast, studies have also reported that ZEB1/2 promotes EMT by repressing the transcription of miR-200 family members by binding to the miR-200 regulatory promoter and form a double-negative feedback loop (Hill et al., 2013). The mutual feedback loop may be important during metastasis process where partial EMT, as characterised by collective cluster migration, is acquired to enable cancer cells to adapt to different microenvironments more efficiently (Lu et al., 2013). Another study has demonstrated that miR-429 reverses TGF-β-induced EMT by inhibiting the expression of Onecut2 in SW620 and SW480 cells (Y.Sun et al., 2014).

MiR-34 family members inhibit CRC metastasis by targeting EMT transcription factor, SNAI1, as well as EMT-induced IL-6R/STAT3 signaling pathway (Rokavec et al., 2014). MiR-29c and miR-29b negatively regulate Wnt/β-catenin and PI3K/AKT pathways, respectively, in CRC to suppress cell migration and invasion (Wang et al., 2014; Zhang et al., 2014). Besides targeting the EMT transcription factors, MiR-29a also directly targets and represses expression of EMT effector, E-cadherin, which mediates the formation of adhesion junction that defines epithelial identity, (Tang et al., 2014). Therefore, the identification of downstream target genes in miRNA-mediated network in EMT may lead to biomarker discovery during cancer progression, which facilitates improvements in CRC screening and therapy.

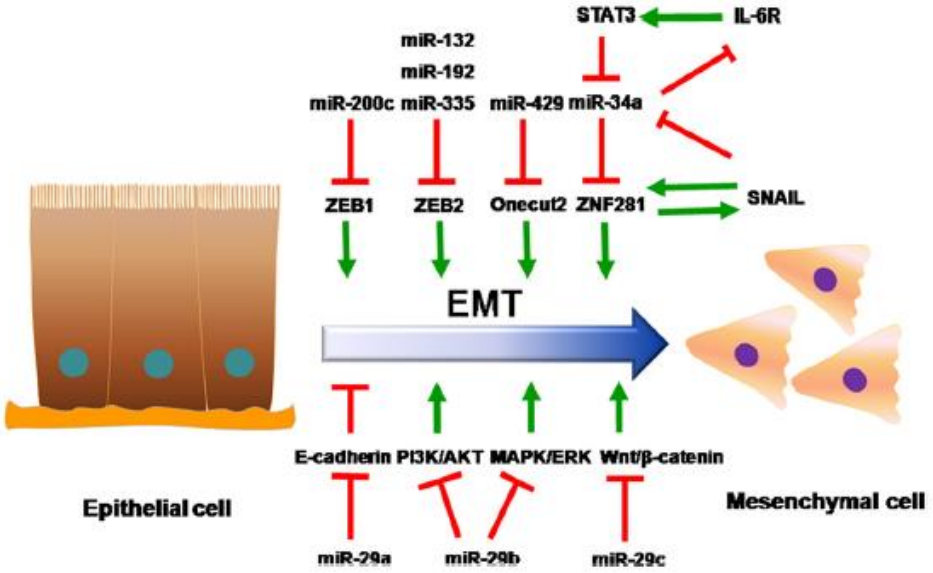

Figure 2.4 MiRNA-mediated regulation of epithelial mesenchymal transition (EMT) in colorectal cancer. Adapted from Chi and Zhou, 2016. Numerous miRNAs, including miR-29a, miR-29b, miR-29-c, miR-200c and miR-34a, are involved in regulation of EMT by targeting and down-regulating EMT-associated transcription factors and signaling pathways in colorectal cancer progression.

CHAPTER 3

MATERIALS AND METHODS

3.1 Cell Culture and Maintenance

3.1.1 Preparation of Cell Culture Media

Basal media including Roswell Park Memorial Institute (RPMI) 1640 medium, Dulbecco's Modified Eagle Medium (DMEM)/high glucose, DMEM/F12 and Minimum Essential Medium (MEM) (Gibco, California, USA) were prepared according to the manufacturer's instruction for different cell lines. RPMI 1640, DMEM/high glucose and MEM powder were dissolved in 900 mL of nuclease-free ddH_2O. Recommended amount of sodium bicarbonate (NaHCO3) (Merck KGaA, Darmstadt, Germany) was measured before added into the medium solution (RPMI 1640: 2.0 g/L; DMEM/high glucose: 3.7 g/L; DMEM/F12, 1.2 g; MEM: 2.2 g/L). Subsequently, pH of the medium was adjusted to pH 7.2 – pH 7.4 before topping up with ddH2O to one litre. The medium was immediately sterilised by passing through a 0.2-µm cellulose acetate filter unit (Techno Plastic Product, Trasadingen, Switzerland) connected to a vacuum pump system (GAST, Michigan, USA). For preparation of the complete culture medium for cancer cell lines, 10% (v/v) fetal bovine serum (FBS) (Gibco) and 1% of 100 U/mL penicillin (Gibco) were added to the basal medium.

3.1.2 Cell Revival from Liquid Nitrogen Frozen Stock

To revive the cancer cell lines, a vial of cryopreserved cells, was retrieved from liquid nitrogen tank and immediately placed in a 37 ℃ water bath until cells were partially thawed. The thawed cells were transferred into a centrifuge tube containing 9 mL pre-warmed complete growth medium and centrifuged at 1,000 rpm for 5 min in a benchtop centrifuge (Allegra® X-15R, Beckman Coulter, California, USA). The supernatant was removed prior to re-suspending the pellet in 1 mL complete culture medium. The cell suspension was subsequently transferred into appropriate culture flask and maintained in the incubator at 37 ℃ with 5% CO_2. The culture medium was discarded on next day and replaced with fresh complete medium.

3.1.3 Cell Culture Maintenance and Sub-culturing

All cell lines were cultured in the appropriate culture media (Table 3.1) and maintained in a 37℃ cell culture incubator with 5% CO_2. Culture medium was changed every two days. Cells were sub-cultured and passaged when the cells reached 70-80% confluency. Old medium was first discarded and the cells were washed once with 1X PBS at pH 7.4 (Amresco, Ohio, USA) to remove traces of serum which could inhibit trypsin activity. One mL of 0.25% trypsin-EDTA solution (Gibco) was added to the cells and then incubated at 37 ^{o}C for 5 -10 mins for cell detachment. Twice the amount of serum-containing culture

Table 3.1 Sources and culture of cell lines used

Cell type	Cell line	Source	Culture medium
Normal somatic cell	293FT	Invitrogen	- DMEM high glucose - 10% FBS
Stem cells	ASC Lonza derived iPSC (MH#1)	A gift of Dr. S. Sugii[1]	- DMEM/F12 (Gibco) - 20% knockout serum replacement (KOSR) - 1% glutamax - 1x NEAA (Gibco) - 0.1% β-mecaptoenthanol3 - 10 ng/ml bFGF4
	MSC (WJ0706)	Cytopeutics Sdn. Bhd[2]	- DMEM/F12 (Gibco) - 10% FBS (Gibco)
Human cancer cells	Placenta choriocarcinoma (JEG-3)	ATCC	- MEM - 10% FBS
	Colorectal cancer (HCT-15 & SK-CO-1)	ATCC	- DMEM high glucose - 10% FBS
	Liver cancer (HepG2)	A Gift of Prof. Y.M. Lim[3]	- DMEM high glucose - 10% FBS
	Breast cancer (MCF-7)	A Gift of Prof. Y.M. Lim[3]	- RPMI 1640 - 10% FBS

[1]Gifts of Dr. S Sugii, Singapore BioImaging Consortium, A*STAR, Singapore; [2]Cytopeutics Sdn. Bhd, Selangor, Malaysia (http://www.cytopeutics.com); [3]Prof. Y.M. Lim, Cancer Research Center, Universiti Tunku Abdul Rahman, Selangor, Malaysia

medium was added to inactivate trypsin activity. The cell suspension was then centrifuged at 1,000 rpm for 5 min. The supernatant was discarded after centrifugation and the pellet was re-suspended in appropriate amount of culture medium.

3.1.4 Cryopreservation of Cell Lines

The cryopreservation mixture was first prepared by adding 900 µL FBS and 100 µL dimethyl sulfoxide (DMSO) (Sigma-Aldrich, Missouri, USA) per vial. Following cell trypsinisation as described in Section 3.1.3 above, the cell pellet was re-suspended in the cryopreservation mixture before aliquoted into sterile cryotubes (Corning, New York, USA). The cryovials were incubated at -80℃ for 24 h. For long-term storage, the cryovials were placed in a liquid nitrogen container (Chart Industries, Ohio, USA) at approximately -180 ℃.

3.2 Establishment of Stable Cell Lines with Selected miRNAs Knockdown

3.2.1 Production of Lentiviral Vectors in 293FT Cells

The day before transfection, 293FT cells were plated at a density of 2.5 x 10^6 cells per dish in 10 mL complete medium as described in Tables 3.1. On the day of transfection, the cells were at 60-70 % confluency. Twenty-four hours post-seeding, the medium was aspirated and replaced with 5 mL of complete medium. Three lentiviral constructs containing miRNA sponges

namely pLKOAS7w.mCherry-CMV d2EGFP-miR362-3p, miR362-5p and CXCR (Control) (National RNAi Core Facility, Academic Sinica, Taiwan) were individually transfected into the packaging cell line 293FT cells by using the TransIT-LT1 transfection reagent diluted (Mirus Bio, Madison, WI, USA).

For each 10-cm dish, 10 µg lentivirus vector construct, 10 µg psPAX2 (second generation lentiviral packaging plasmid) and 1 µg pMD2.G (VSV-G envelope) plasmids were diluted in 100 µL OptiMEM serum-free medium. In another tube, 30 µL of TranslT-LT1 was added to 330 µL of OptiMEM serum-free medium and incubated for 5 min at room temperature. The tubes containing the diluted plasmid mixture and TranslT-LT1 transfection reagent were combined and vortexed. The mixture was subsequently incubated at room temperature for 30 mins. After incubation, the DNA-TranslT-LT1 complexes were added dropwise to the plated 293FT cells, and incubated at 37 ℃, 5% CO_2 in humidified incubator. After 48 and 72 h post-transfection, virus supernatant harvested was filtered through a 0.45-µm pore size PVDF filter (EMD Millipore, Massachusetts, United States) and aliquoted in 1.5 mL micro-centrifuge tubes to be stored at -80℃.

3.2.2 Transduction of Lentiviral Vectors in HCT-15 cells

For establishment of miR-362 knockdown stable cell lines, HCT-15 cells were seeded at a density of 5.0 x 10^5 cells/mL in six-well plates 24 h prior to transduction. On the day of transduction, the cells were at 60-70% confluency. Virus supernatant with lentiviruses carrying miR-362-5p/-3p and control sponges were transduced individually into the HCT-15 cells, supplemented with 8 µg/mL polybrene (EMD Millipore). The cell mixture was centrifuged at 2250 x rpm for 1 h at 37 ℃ to enhance viral transfection. Media were changed with fresh complete media supplemented with 4 µg puromycin 48 h post-transduction. Growth media, supplemented with puromycin, was replaced every two days for selection of transduced cells. The transduced HCT-15 cells were checked for green fluorescence protein (GFP) and Mcherry fluorescence signals. Puromycin-selected HCT-15 cells stably expressing miRNA sponges were expanded and harvested for RNA and protein to check the efficiency of miRNA knockdown and the target gene expression respectively.

3.3 Genome-wide Analysis of miRNA Expression

3.3.1 MiRNA Microarray Analysis and Target Gene Prediction

The miRNA microarray dataset obtained were analysed and normalised using the GeneSpring GX software version 13.0 (Agilent Technologies, California, United States). Comparative analysis between samples was carried out using the t-test (p-values) and the Benjamini-Hochberg False Discovery Rate (FDR) correction (adjusted p-values) to remove false positive miRNAs. The criteria set for selection of differentially-expressed miRNAs was $\log_2$ (fold change) > 2 or < -2 with adjusted p-values < 0.05. Hierarchical clustering was performed to identify and visualise patterns of miRNAs expression between samples. The differentially-expressed miRNAs were used to predict target genes using the microRNA.org (http://microrna.sanger.ac.uk) and TargetScan (http://www.targetscan.org) algorithms.

3.3.2 Gene Ontology and KEGG Pathway Analysis

The predicted target genes of differentially-expressed miRNAs were then analysed using web-based programme Database for Annotation, Visualization, and Integrated (DAVID) (http://david.abcc.ncifcrf.gov/tools.jsp) (Huang et al., 2009a; Huang et al., 2009b) for gene ontology (GO) annotation and KEGG pathway analyses to identify the functional roles and potential pathways. The criterion of analysis for gene-enrichment analysis was EASE

score ≤ 0.05, a modified Fisher Exact P value. $p \leq 0.05$ was regarded as statistically significant for the particular annotation.

3.3.3 Identification of Differentially-Expressed miRNAs Targeting at EMT/MET-Related Genes

EMT/MET-related target genes were predicted by one or more of the databases TargetScan 7.0, miRWalk2.0 and Diana tools (microT-CDS).

3.4 RNA Isolation by TRIZOL

Total RNA was isolated from the samples by using TRIzol reagent (Invitrogen) according to the manufacturer's instructions. Medium was discarded and 1X cold PBS was used to rinse the cell monolayer once. One mL of TRIzol reagent was then added to lyse the cells directly in 10cm-culture dish by scraping with cell scraper. The amount of TRIzol required was calculated according to the area of the culture dish (1 mL per 10 cm^2). The cell lysate was then re-suspended for a few times by passing through a pipette before vortexed thoroughly. Two hundred µL chloroform (Amresco, USA) was added to the homogenate before vortexed vigorously to mix properly and incubated at room temperature for 15 min. To separate the RNA phase from genomic DNA and protein, the homogenate was subsequently centrifuged at 12,000 x g for 15 min at 4 ℃. The colourless upper aqueous phase containing RNA was carefully

pipetted into a new 1.5 mL microcentrifuge tube without disturbing the interphase. Five hundred µL isopropanol (EMD Millipore) was added to precipitate the RNA, followed by incubation at room temperature for 15 min. The mixture was then centrifuged at 12,000 x g for 15 min at 4 ℃ and the supernatant was decanted. The precipitated RNA pellets were washed twice with 1 mL of 75% ethanol (EMD Millipore) by gently inverting the tubes for a few times. The supernatant was removed and the pellet was air-dried for 10 min prior to elution with 30 – 50 µL RNase-free water. The RNA isolated was quantified by NanoPhotometer (Implen, Munich, Germany) to check the purity and concentration of the sample. The ratio of the readings at 260 nm and 280 nm (A260/A280) provides an estimation of RNA purity and should be within the range of 1.8-2.1. A260/A230 ratio of the RNA samples was also measured and should have a minimum value of 2.0, indicating minimum organic contaminations carried over from the RNA isolation. All the isolated RNAs were stored at -80 ℃.

3.4.1 cDNA Synthesis by Reverse Transcription

Total RNA was subjected to reverse transcription by using the SuperScript III Reverse Transcriptase Kit (Invitrogen) according to the manufacturer's guidelines. Approximately one microgram of total RNA, 1 µL of 10 mM dNTP and 100 ng oligo(dT) primer were combined with nuclease-free water to reach a total volume of 13 µL before incubated at 65 ℃ for 5 min to pre-denature the RNA. Subsequently, the reaction mixture containing 4 µL

of 5X First Strand buffer, 1 µL of 0.1 M DTT, 1 µL of RNAse inhibitor and 1 µL of SuperScript III RT enzyme mix was added to the pre-denatured RNA reaction. The reaction tube was incubated at 25 ℃ for 5 min, followed by 50 ℃ for 60 min and lastly at 75 ℃ for 15 min to terminate the reaction.

3.5 Quantification and Validation of the miRNA Expression Levels

3.5.1 MicroRNA (miRNA) Primers for qRT-PCR

For the miRNA validation of microarray data, mature sequences of selected miRNAs were obtained from miRBase ver. 21 (www.mirbase.org) and synthesised for use as specific forward primers; the miRNA primers listed in Table 3.2 were synthesised by First BASE Oligos (Singapore).

3.5.2 Polyadenylated-Reverse Transcription of miRNAs

For miRNA expression analysis, total RNA was first reverse transcribed into cDNA using NCode™ miRNA First-Strand cDNA Synthesis Kit (Invitrogen) according to manufacturer's guidelines. Briefly, 1 µg of total RNA was subjected to polyadenylation tailing at 37 ℃ for 15 min. Following miRNA poly (A) tailing, Superscript III RT/RNaseOUT enzyme mix was

Table 3.2 miRNA primer sequences for qRT-PCR.

miRNA	Accession[1]	Forward primer sequence (5' – 3)
miR-125b-5p	MIMAT0000423	GGTCCCTGAGACCCTAACTTGTGA
miR-150-3p	MIMAT0004610	CTGGTACAGGCCTGGGGGACAG
miR-194-3p	MIMAT0004671	CCAGTGGGGCTGCTGTTATCTG
miR-195-5p	MIMAT0000461	GCGGTAGCAGCACAGAAATATTGGC
miR-199a-5p	MIMAT0000231	GGCCCAGTGTTCAGACTACCTGTTC
miR-199a-3p	MIMAT0000232	GCGACAGTAGTCTGCACATTGGTTA
miR-362-5p	MIMAT0000705	GGAATCCTTGGAACCTAGGTGTGAGT
miR-362-3p	MIMAT0004683	GGCGAACACACCTATTCAAGGATTCA
miR-500-3p	MIMAT0002871	ATGCACCTGGGCAAGGATTCTG
miR-532-3p	MIMAT0004780	CCTCCCACACCCAAGGCTTGCA
U6-F	-	CTC GCT TCG GCA GCA CA
U6-R	-	AAC GCT TCA CGA ATT TGC GT
Universal reverse primer	-	CCA GTG CAG GGT CCG AGG TA

F: forward primer; R: reverse primer

added to the poly (A) tailed RNA to synthesise the first-strand cDNA using Universal RT primer. The specific sequence at the 5' end of the Universal RT primer allows amplification of microRNA cDNAs in real-time SYBR green PCR. The reaction mixture was incubated at 65 ℃ for 5 min, followed by 50 ℃ for 50 min before terminating at 85 ℃ for 5 min in a 96-well Thermal Cycler (Takara, Shiga, Japan).The reagent mixture used was listed in Table 3.3.

3.5.3 MicroRNA Quantification by qRT-PCR

Synthesised miRNA cDNA was quantified with real-time RT-PCR by using SYBR Select master mix reagents (Applied Biosystems, Foster City, California, USA) prepared according to Table 3.4. Amplification was carried out for 40 cycles at 95 ℃ for 15 s and primer annealing at 60 ℃ for 1 min. Experiments were performed in triplicates and were normalised to the data of the small nuclear RNA (snRNA) U6. The miRNA expression in the CRC-iPC cell lines, iHCT 15 and iSK-CO-1, were calculated relative to the parental CRC cell lines, HCT 15 and SK-CO-1, and the differences in fold change were calculated by comparative ΔΔCt method.

Table 3.3 MicroRNA cDNA synthesis mix

Reagent	Volume per reaction
RNA	1 μg
5x miRNA buffer	4 μL
25 mm $MnCI_2$	2 μL
Diluted ATP*	1 μL
Poly (A) Polymerase	1 μL
DEPC water	Top up to 20 μL
Poly (A) RNA	4 μL
Annealing buffer	1 μL
Universal RT primer	3 μL
2x First Strand Buffer	10 μL
Superscript III RT/RNaseOUT	2 μL

*****1 uL of 10 mm ATP was added to 4 uL of 1 mm Tris buffer at pH 8.0

Table 3.4 miRNA qRT-PCR reaction mixture

Reagents	Volume per reaction	Final concentration/amount
2X SYBR Green qPCR SuperMix	10 μL	1X
Forward primer (10 μM)	0.2 μL	100 nM
Universal qPCR primer (10 μM)	0.2 μL	100 nM
cDNA template (10 ng/μL)	1.0 μL	10 ng
DEPC-treated water	8.6 μL	-
Total volume	20 μL	

3.6 Western Blot Analysis of Protein Expression

3.6.1 Buffers and Reagents Preparation

The buffers and reagents used for western blot analysis are as described in Table 3.5.

3.6.2 Preparation of Cell Lysates

1X RIPA Lysis Buffer (Merck) was prepared by adding 100 µL of RIPA and 5 µL of protein inhibitor to 895 µL of ddH_2O. Cells were washed twice with 1X cold PBS, scraped directly from the culture dish and pelleted by centrifugation at 1000 rpm for 5 min at 4 ℃. The cell pellets were lysed in appropriate amount of 1X RIPA Lysis Buffer (Merck) and vortexed gently for one sec. The cell suspension was then incubated on ice for 15 min, followed by centrifugation at 21,300 x g for 20 min at 4 ℃ in a Herarus Fresco 21 refrigerated microfuge (Thermo Scientific). The supernatant was collected into a new microfuge tube without disturbing the cell pellet and stored at -80 ℃.

Table 3.5 Buffers and reagents prepared for western blot analysis

Buffer	Preparation
10% (w/v) sodium dodecyl sulphate (SDS) solution	- 5 g SDS (EMD Millipore) - top up to 50 mL H_2O
10% (w/v) ammonium persulfate (APS)	- 0.1 g APS (EMD Millipore) -add 1 mL H_2O
1.5 M Tris, pH 8.8 (Resolving gel)	- 36.33 g Tris base (Norgen Biotek) - top up to 200 mL H_2O
1.5 M Tris, pH 6.8 (Stacking gel)	- 36.33 g Tris base , pH 6.8 - top up to 200 mL H_2O
6X SDS loading buffer (0.5M Tris pH 6.8, 100% glycerol)	-1.2 mL of Tris base, pH 6.8 -1.2 g SDS - 4.7 mL glycerol (Sigma-Aldrich) - 6 mg Bromophenol blue (Sigma-Aldrich) - 2.1 mL H_2O - 0.93 g DTT (Sigma-Aldrich)
SDS-PAGE 1X running buffer (25 mM Tris, 192 mM glycine, 0.1% SDS)	- 6.04 g Tris base - 28.8 g Glycine (EMD Millipore) - 2 g SDS - top up to 2 L H_2O
10X Tris-buffered saline (TBS) (0.5 M Tris, 1.5 M NaCl) (pH 7.4 ~7.8)	- 14 g Tris base, - 60 g Tris HCl (Sigma-Aldrich) - 87.5 g NaCl - top up to 1 L H_2O
Washing buffer: 1X TBS with 0.1% Tween-20 (TBST)	- 100 mL of 10X TBS - 900 mL H_2O - 1 mL Tween-20 (EMD Millipore)
Blocking buffer: TBST with 5% milk	- 2.5 g non-fat milk powder (Bio Basic Inc.) - 50 mL of 1X TBST
1X Wet transfer buffer (25 mM Tris, 192 mM glycine, 10% methanol)	- 3.03 g Tris base - 14.4 g glycine - 1 L mL H_2O_2 - 200 mL of methanol (EMD Millipore)

3.6.3 Preparation of Standard Curve and Quantification of Protein by Bradford Protein Assay

Protein quantification was carried out using Quick Start Bradford Protein Assay (Bio-Rad, CA, USA). Bovine serum albumin (BSA) stock of 1 mg/mL was prepared by dissolving 0.01 g of BSA powder in 10 mL of ddH2O. Standards containing 2 – 10 mg of BSA were prepared from the stock in a total volume of 1mL. 200 µL of 1X Bradford Dye Reagent (Bio-Rad) was added to each tube, vortexed, followed by measurement of the absorbance at 595 nm in an Infinite M200 PRO Microplate Reader (Tecan). A Standard curve was plotted based on serial concentrations of BSA (Table 3.6 and Figure 3.1). Measurements of all standards and samples were performed in triplicates. The protein concentrations of the sample were calculated from the standard curve.

3.6.4 Separation of Protein by Sodium Dodecyl Sulfate-Polyacrylamide Gel Electrophoresis (SDS-PAGE)

A Mini-PROTEAN Tetra Cell system (Bio-Rad) was used in SDS-polyacrylamide gel electrophoresis (SDS-PAGE). The taller spacer plate (1.5 mm thickness) and a small glass plate were inserted in the casting frame and secured before clamped into the casting stand to form a gel cassette assembly.

Table 3.6 Preparation of standard curve

Protein concentration (mg/mL)	ddH_2O (µL)	BSA (1 mg/mL) (µL)	1X Bradford reagent (µL)
0	800	0	200
2	798	2	200
4	796	4	200
6	794	6	200
8	792	8	200
10	790	10	200

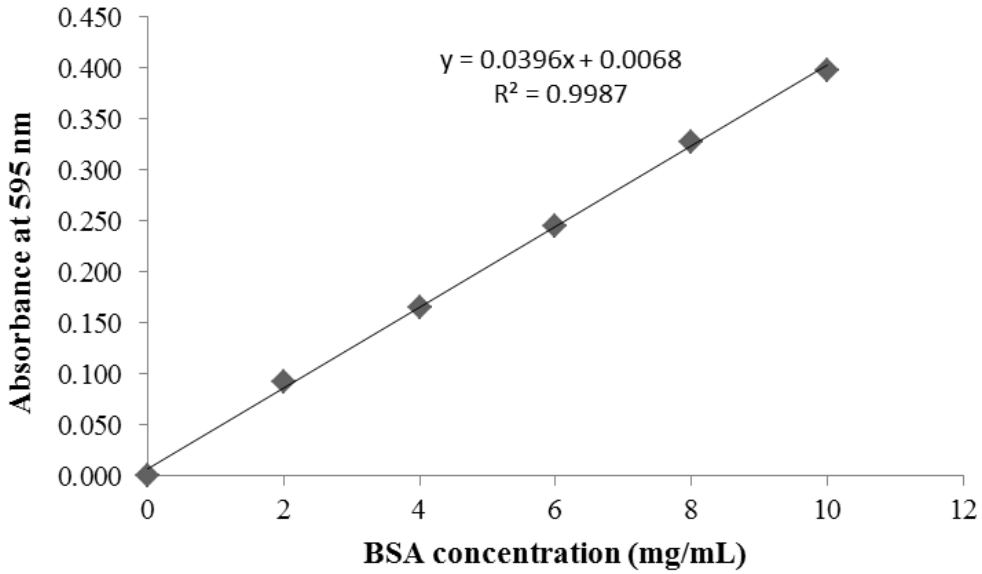

Figure 3.1 Plotting of Standard Curve of BSA. The x-axis represents the different concentrations of BSA whereas the y-axis represents the absorbance at wavelength of 595 nm. A linear plot was derived to calculate for the protein sample concentration.

To prepare 10% resolving gel, 2.5 mL 1.5 M Tris (pH 8.8), 3.3 mL 30% (w/v) bis/acrylamide (Bio-Rad), 100 µL of 10% SDS are added into 4.1 mL distilled water. 10 uL of Tetramethylethylenediamine (TEMED) (Calbiochem, EMD Millipore) and 100 µL of 10% APS were added at the last step to the 10% resolving gel mixture.

All the components were mixed well by gently inverting the mixture a few times before poured into the space between the glass plates clamped on the casting stand. Appropriate amount of 99% ethanol (EMD Millipore) was overlaid on top of the resolving gel to inhibit any bubble formation. After the resolving gel polymerised, the 99% ethanol was drained out. A 5% stacking gel was prepared while waiting for the resolving gel to solidify. One mL 0.5 M Tris (pH 6.8), 0.67 mL 30% (w/v) bis/acrylamide, 40 µL 10% SDS were added to 1.9 mL distilled water. 3.3 µL TEMED and 40 µL 10% APS were subsequently added to the stacking gel solution and mixed by gently inverting the mixture a few times. The stacking gel solution was then pipetted to the top of the polymerised resolving gel. A 10-well 1.5-mm comb was carefully inserted into the stacking gel layer without forming air bubbles.

After the stacking gel polymerised, the gel cassette was removed from the stand and clamped onto an electrode assembly before transferred into the Mini-PROTEAN Tetra Tank. The comb was then removed and the electrode assembly was filled with SDS-PAGE running buffer in the center until full.

The tank was also filled with 1X SDS-PAGE running buffer to the recommended level.

Five volumes of protein lysate at a final amount of 40 µg were mixed with one volume of 6X SDS loading buffer (Table 3.5). The mixture was then topped up with 1x RIPA lysis buffer to 24 µL. The protein mixture was denatured by heating at 95 ℃ for 10 min in a block heater (Stuart Scientific, Staffordshire, UK). Twenty µL of the denatured protein sample and 5 µL PageRuler Prestained Protein Ladder (Thermo Fisher Scientific) were loaded into the wells accordingly. Electrophoresis was performed at a constant voltage of 120 V for approximately 70 min to separate the protein according to the molecular weight.

3.6.5 Wet Transfer of Protein to PVDF Membrane

Amersham Hybond P 0.45 PVDF blotting membrane (GE Healthcare, Little Chalfont, UK) and filter paper (Thermo Scientific) were cut to the dimension of the gel, which was approximately 10 cm x 6 cm. The PVDF membrane was equilibrated in methanol for 10 min and then soaked briefly in 1X wet transfer buffer (Table 3.5).

After the SDS-PAGE electrophoresis run had completed, the gel was carefully removed from the gel cassette and the stacking gel layer was discarded, leaving only the resolving gel layer behind for transfer of the separated proteins by wet transfer using the Mini Trans-Blot Electrophoretic Transfer Cell (Bio-Rad). The transfer sandwich was assembled sequentially according to Figure 3.2 with two sheets of filter paper on the fibre pad, followed by gel on the filter paper, the buffer-pre-equilibrated membrane on the gel, and finally two sheets of filter paper placed on top of the membrane. Air bubbles were removed by gently rolled the sandwich with a roller. The assembly cassette was closed firmly without disturbing the sandwich layer and placed in the module, with the black side of cassette facing the black cathode. The module was placed in the transfer tank and the tank was then filled with transfer buffer to the "blotting" mark. The transfer was performed at a constant voltage of 100 V for 2 h on ice.

After the transfer, the PVDF membrane was removed from the sandwich and stained with RedAlert Stain (Novagen, EMD Millipore) to verify the successful transfer of proteins before western blot analysis. The RedAlert stain was then removed by rocking the membrane in 1X TBST wash buffer.

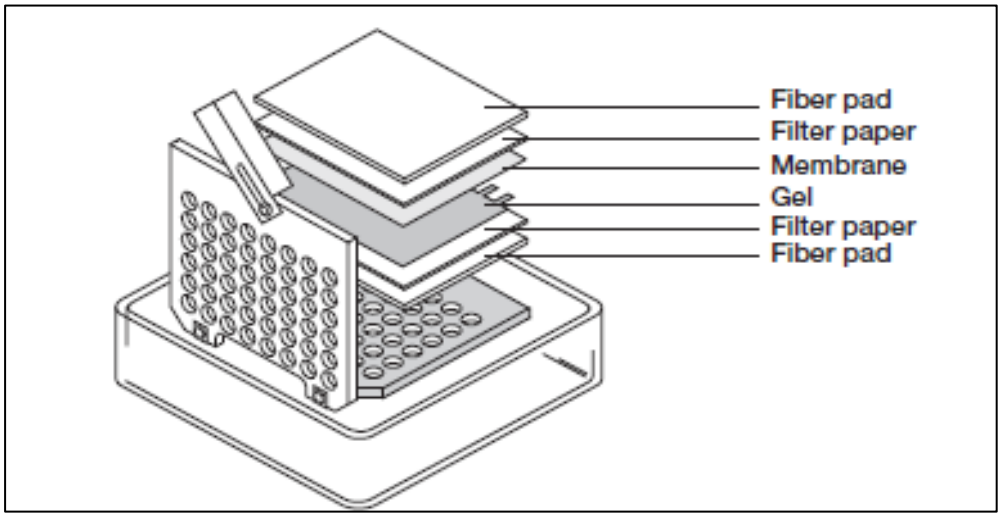

Figure 3.2 Schematic arrangement of transfer sandwich. The transfer sandwich was assembled in a sequential order with two sheets of filter paper on the fibre pad, followed by gel on the filter paper, the membrane on the gel, and finally two sheets of filter paper placed on top of the membrane.

3.6.6 Membrane Blocking

The transferred PVDF membrane was blocked with 5% skim milk to prevent non-specific binding of the antibodies. The membrane was incubated in approximately 10 mL of blocking buffer (Table 3.5) for 1 h at room temperature with gentle shaking.

3.6.7 Primary and Secondary Antibody Staining

After the membrane was blocked using blocking buffer, the membrane was incubated with monoclonal antibodies anti-CDH1 (1:1,000 dilution, Cell Signaling Technology), anti-OCLN (1:500, Merck Millipore), anti-Vimentin (1:1000, Cell Signaling Technology), anti-SNAI1 (1:250, Cell Signaling Technology), anti-SMAD4 (1:1000, Cell Signalling Technology) and anti-GAPDH (1:2000, Cell Signaling Technology) in 5% skim milk overnight at 4 ℃ with gentle agitation. On the next day, the membrane was washed three times with 1X TBST washing buffer for 10 min each. The membrane was then incubated in HRP-conjugated mouse anti-rabbit IgG secondary antibody (1:5000, Cell Signalling Technology) for 1 h at room temperature with gentle agitation. The membrane was washed three times with 1X TBST buffer for 10 min each.

3.6.8 Chemiluminescence Detection

Detection Solution 1 and 2, supplied in the Amersham Enhanced Chemiluminescent Western Blotting Detection Reagent (GE Healthcare), were mixed at a ratio of 1:1 and the mixture was added directly onto the membrane. Chemiluminescent signal emitted from the membrane was captured by the LI-COR C-DiGit chemiluminescence western blot scanner (Li-Cor Biosciences; Lincoln, NE, USA). The band densitometric analysis was then performed by Image Studio™ Lite software (Li-COR Biosciences) to measure the intensity of the protein bands developed in the western blot membrane.

3.6.9 Stripping and Reprobing of Membrane

The bound primary and secondary antibodies on the membrane were stripped by first rinsing the membrane with the wash buffer followed by incubation in 3 mL of Restore Plus Western Blot Stripping Buffer (Thermo Fisher Scientific) for 10 min at room temperature. The membrane was then washed with 1X TBST wash buffer twice for 10 min each before blocking again in the blocking buffer. The stripped membrane was then reprobed using primary and secondary antibodies as described in sections 3.6.6 and 3.6.7.

3.7 Ectopic Expression of miRNAs

3.7.1 Transient Transfection of miRNA Mimics

Hsa-miR-362-5p/-3p MirVana miRNA mimics and negative control #1 (NC) were synthesised by Ambion (Foster City, CA, USA). The synthetic miRNA mimics were transfected into MCF-7 and HCT-15 cells by using Lipofectamine 2000 Reagent (Invitrogen) according to the manufacturer's protocol. The day before transfection, the MCF-7 and HCT-15 cells were seeded at a density of 7.5 x 10^5 cells/well 5.0 x 10^5 cells/well respectively, in a 6-well plate. Twenty-four hours post-seeding, 100 nM synthetic miRNAs diluted in 250 µL OptiMEM medium (Gibco) and 5 µL Lipofectamine 2000 (Invitrogen) diluted in 250 µL OptiMEM medium (Gibco), were incubated for 5 min at room temperature. Both diluted synthetic miRNAs and Lipofectamine 2000 were then mixed and incubated at room temperature for 25 min. Five hundred µL synthetic miRNA-lipofectamine complex was then added to the cells. The plate was rocked gently back and forth for even distribution of the complex before incubated at 37 ℃ for 48 h. At 48 h post-transfection, the cells were trypsinised for further analysis.

3.7.2 Co-transfection of miRNA Mimics and Plasmid Vectors containing 3'UTR Regions of Putative Target Genes

MCF-7 cells were transiently transfected with either the blank luciferase reporter or reporter constructs with the 3'-UTR of predicted target

genes containing the miRNA binding sites. For each reporter construct, transfection was performed in the presence or absence of a NC or miR-362-5p/-3p mimics by using Lipofectamine 2000 Reagent (Invitrogen). The day before transfection, MCF-7 cells were seeded onto 24-well plates at a density of 2.5 x 10^5 cells/mL. At 24 h post-seeding, 20 nM synthetic miRNA mimics and 250 ng/µL plasmids were diluted in 50 µL OptiMEM medium (Gibco) while 1 µL Lipofectamine 2000 (Invitrogen) was diluted in 50 µL OptiMEM medium (Gibco) and incubated for 5 min at room temperature. MiRNA mimic and Lipofectamine reagent mixtures were then combined and incubated at room temperature for 25 min before added dropwise to the cells. Medium was changed to complete RPMI medium after 24 h to optimise cell growth.

3.8 Validation of miRNA Targeted Transcripts by Luciferase Assays

3.8.1 Construction of PmirGLO Plasmids containing 3'UTR of Putative Target Genes

To amplify 3'UTR sequences of EMT/MET target genes carrying the predictive miRNA target sites, primers were designed using NCBI primer blast (Table 3.7). The cDNA was converted using method as described in Section 3.4.1 and were used as template for amplification using SeqAmp DNA Polymerase (Clontech, Palo Alto, CA, USA) according to manufacturer's protocol. The PCR amplification was performed at 94 ℃ for 5 min, followed by 30 cycles of 94 ℃ for 10 sec, 60 ℃ for 30 sec and 72 ℃ for 1 min/kb, and a final extension at 72 ^{o}C for 5 min using a thermocycler (Takara

Table 3.7 Primers with restriction sites used for cloning of luciferase constructs

Primer designation	Sequence (5' > 3')	Product size (bp)
OC1-F	CTG**GAGCTC**AGTACCATCCGCCCAGAAAT	2051
OC1-R	GCA**TCTAGA**AACTGAAGCTAAGGTCCCCG	
OC2-F	CTT**GAGCTC**GCCAAACCTCTGTGAGCATC	2051
OC2-R	CGT**TCTAGA**GCCTTCACGAACTGACTTCC	
CD-F	ATC**GAGCTC**CCCAGCACCTTGCAGATTTTC	1036
CD-R	ATC**TCTAGA**TTCCGCTCTGTCTTTGGCTG	
SM1-F	GCT**GAGCTC**TGTGCCATGTGGGTGAGTTA	341
SM1-R	GAT**TCTAGA**CTTAGCAACCAACCTTGTGCC	
SM2-F	AGT**GAGCTC**GGGACTTCCCCATGGACATT	1998
SM2-R	AGT**CTCGAG**ACCATCAAACCAGGCACAGA	
SM3-F	ATG**CTCGAG**AGTAATGGCTCTGGGTTGGG	939
SM3-R	ATC**TCTAGA**AAAGCTGGCCTCTACCAGGA	
SN-F	GCT**GAGCTC**CCCTCGAGGCTCCCTCTT	810
SN-R	GCA**TCTAGA**TGCTTTATTGAATATCAATAAAC	

Restriction enzyme recognition sites are highlighted in bold in primer sequence where SacI: GAGCTC; XbaI:TCTAGA; XhoI:CTCGAG.

After the amplification process, PCR purification was conducted using NucleoSpin Gel and PCR Clean-up (Macherey-Nagel, Duren, Germany) to remove any primer-dimers, enzymes and dNTPs, before the purified PCR products were subjected to restriction enzymes double digestion. The digested PCR fragments were ligated with linearised pmirGlo plasmid (GenBank accession FJ376737) (Promega, Madison, WI, USA) using T4 DNA Ligase (New England Biolabs Inc., USA). Briefly, the amount of PCR insert required for the ligation was calculated using formula:

$$\text{Amount of PCR insert (ng)} = \frac{vector\ mass\ (ng) x\ size\ of\ insert(kb)}{size\ of\ vector\ (kb)}\ x\ molar\ ratio \frac{insert}{vector}$$

The ligation reaction mixture was prepared by mixing 2 μL of 10X T4 DNA ligase buffer, 1000 ng of vector DNA and appropriate amount of insert DNA in ddH_2O. The T4 DNA ligase enzyme was added last to the reaction and incubated at room temperature for 30 min, followed by 65 ℃ for 10 min to terminate the reaction.

3.8.2 Cloning of PmirGLO Plasmids containing 3'UTR of Putative Target Genes

DH5α competent cells (Invitrogen) were thawed on ice for 10 min. Ligated products were added into the competent cells and mixed gently before incubated on ice for 30 min. Next, the cells were transformed by heat-shock at 42 ℃ for 45 sec in a water bath. The transformed DH5α cells were then

incubated on ice for 2 min before addition of 250 µL SOC recovery medium (Invirogen). The mixture was placed in a shaking incubator at 250 rpm for 1 h at 37 ℃. After the incubation, 50 µL of the transformed cells was spread on a pre-warmed LB (Sigma-Aldrich) agar containing 100µg/mL ampicillin (Amresco). The plates were inverted and incubated overnight at 37 ℃ for 16-18 h.

3.8.3 Culture of Transformed Colonies and Plasmid DNA Extraction

Single colonies were picked from the LB agar plate with pipette tips and inoculated in the pre-warmed LB broth (Sigma-Aldrich) containing 100 µg/mL ampicillin (Amresco) and were incubated overnight at 37 ℃ with shaking at 250 rpm.

Plasmid DNA was purified using GeneJet Plasmid Miniprep Kit (Thermo Fisher Scientific). On the next day, the bacterial culture was first harvested by centrifugation at 6,000 rpm for 10 min in a Sorvall Legend centrifuge X1R machine (Thermo Fisher Scientific). The pelleted bacterial cells were re-suspended in 250 µL re-suspension solution by vortexing until no cell clumps were left behind. To lyse the bacteria cells, 250 µL lysis solution was added and immediately inverted several times until the solution became viscous and clear followed by incubation at room temperature for 3 min. The lysate was subsequently neutralised. Denatured plasmid DNA was reannealed by adding 350 µL neutralisation solution to the lysate and mixed thoroughly

until the lysate turned cloudy. Cell debris and chromosomal DNA were then precipitated by centrifugation at 13,000 rpm for 5 min in a Sigma 1-14 benchtop centrifuge machine (Sartorius Corporation, NY, USA). The resulting supernatant contained the plasmid DNA was loaded onto a purification column provided in the kit and centrifuged at 13,000 rpm for 1 min.

The flow-through was discarded and the column was returned to the same collection tube. Washing was performed twice by adding 500 µL wash solution to the spin column and centrifuged at 13,000 rpm for 1 min. The flow-through was discarded and the column was centrifuged for another 1 min to remove the remaining wash solution. The spin column was then transferred into a new 1.5 mL microcentrifuge tube. Fifty µL elution buffer was added to the centre of the column membrane and incubated for 5 min at room temperature before centrifugation at 13,000 rpm for 5 min to elute the plasmid DNA.

The purified plasmids DNA from different colonies were digested with SacI, XbaI and XhoI restriction enzymes for 1 hour at 37 ℃. The digested plasmids were subsequently run on a 0.8% agarose gel and visualised by exposure to UV light under BioSpectrum Imaging System (Ultra-Violet Products Ltd) to identify the presence of recombinant plasmid constructs (Appendix A). The sequence of recombinant plasmid constructs containing the predictive miRNA binding sites were confirmed by sequencing.

3.8.4 Dual Luciferase Reporter Assays

The Dual-Luciferase Reporter Assay System (Promega, WI, USA) was used to identify miRNA direct targeting. Co-transfection of plasmid constructs and synthetic miRNAs into MCF-7 cells was performed using Lipofectamine 2000 (Invitrogen) as described in Section 3.7.2. At 48 h post-transfection, the culture medium was removed and the cells were rinsed twice with 1X PBS before 100 µL of 1X Passive Lysis Buffer was added to the cells. The cells were then rocked at room temperature for 15 min. Twenty µL cell lysate was then pipetted onto a 96-well plate, followed by 100 µL Luciferase Assay Reagent II to measure the Firefly luciferase activity in an Infinite M200 PRO Microplate Reader (Tecan). After the firefly luminescence was quantified, 100 µL Stop & Glo Reagent was added simultaneously to the same well to measure the Renilla luciferase activity. The luciferase signal was normalised to renilla signal to obtain a ratio for each transfected constructs (Luminescence= Luciferase signal/Renilla signal). Data were calculated as the means ± standard error of the mean (SEM) of three independent experiments.

3.9 Cell Migration and Invasion Assays

3.9.1 Wound Healing Assay

MiR-362-5p/-3p mimics or NC transfected MCF-7 cells were seeded at 3 $\times 10^5$ cells/mL in each of the two chambers of a culture-insert dish (Ibidi, Martinsried, Germany) to create a cell free gap of 500 μm by exclusion. At 24 h post-seeding, the insert was gently removed and the cells were washed once with 1X PBS to wash away cell debris before overlaid with warm complete RPMI medium. Images were taken at a precise localisation before and after 24 h to monitor the closure of the wound area. The percentage of closure of the wound was calculated by performing an 8-bit image analysis and MRI Wound Healing Tool plugin provided by the ImageJ software (NIH). The percentage of wound area after 24 h was calculated in relative to the original area at 0 h for each condition.

3.9.2 Transwell Migration Assay

MiR-362-5p/-3p mimics or NC transfected MCF7 cells were trypsinised and harvested at 48 h post-transfection and resuspended in serum free media. A total of 2.0 x 10^5 cells/mL MCF7 cells were seeded onto the top chamber of 8.0-μm FluoroBlok transwell insert (BD, Franklin Lakes, NJ, USA). Seven hundreds μL RPMI medium supplemented with 10% FBS was used as chemoattractant in the bottom chamber. The cells were incubated overnight at

37 ℃ with 5% CO_2. After 24 h, the medium was aspirated from the top chamber and the cells were washed twice by transferring the insert to a 24-well plate containing 500 µl of 1X PBS, followed by fixing the cells in ice-cold methanol for 1 h at room temperature. The cells were than washed once with 1X PBS before staining with 50 µg/mL of propidium iodide (PI) for 1 h at room temperature in the dark. The number of PI-labelled cells that had migrated to the lower membrane surface was visualised using an inverted fluorescence microscope (Olympus IX71, Taiwan). Five images of randomly selected fields were captured on each filter using the cellSens software for microscopy image analysis (Olympus). Migrating cells were counted with the image J software (NIH).

3.9.3 Transwell Invasion Assay

MiR-362-5p/-3p mimics and NC transfected HCT-15 cells were harvested by trypsinisation 48 h post-transfection and resuspended in serum free media. Geltrex LDEV-Free Reduced Growth Factor Basement Membrane Matrix (Gibco) was thawed at 2℃ to 8℃ overnight and mixed properly before diluting to 7 mg/mL in DMEM high glucose medium. One hundred µL of 7 mg/mL Geltrex was pipetted to cover the top chamber of the 8.0-µm FluoroBlok transwell insert (BD, Franklin Lakes, NJ, USA). The coated inserts were then placed in an incubator at 37℃ for 30 min for the Geltrex to solidify. Briefly, 2.0 x 10^5 cells/mL HCT-15 cells were seeded onto the coated chamber which was subsequently transferred to a 24-well plate containing 700µL

DMEM medium supplemented with 10% FBS. The cells were incubated overnight at 37 ℃. The medium was aspirated from the top chamber after 24 h and the cells were washed twice with 500 μL of 1X PBS, followed by fixing the cells in ice-cold methanol for 1 h at room temperature. The cells were then washed once with 1X PBS before stained using 50 μg/mL of propidium iodide for 1 h at room temperature in the dark. The number of cells that had invaded was visualised under inverted fluorescence microscope (Olympus IX71, Taiwan). Five images of randomly selected fields were captured on each filter using cellSens software for microscopy image analysis. Invaded cells were counted with the image J software.

3.10. Statistical Analysis

Data were analysed using Microsoft Excel and presented in means ± SEM of at least two to three independent experiments in triplicates. The differences between treated and control groups were analysed by paired Student's t-test (two-tailed distribution). *P*-value ≤ 0.05 was considered as statistically significant.

CHAPTER 4

RESULTS

2.2 Study Design of Part I

This study was divided into two main parts: Part I was on miRNA profiling and bioinformatics prediction and Part II on functional analysis. In Part I, the study focused mainly on genome-wide miRNA profiling and identification of a set of differentially expressed miRNAs in CRC-iPCs relative to the parental CRCs. Subsequently, bioinformatics analysis was used to predict functional roles and potential pathways in relation to the EMT and MET processes. A flow chart of the study design of Part I is shown in Figure 4.1.

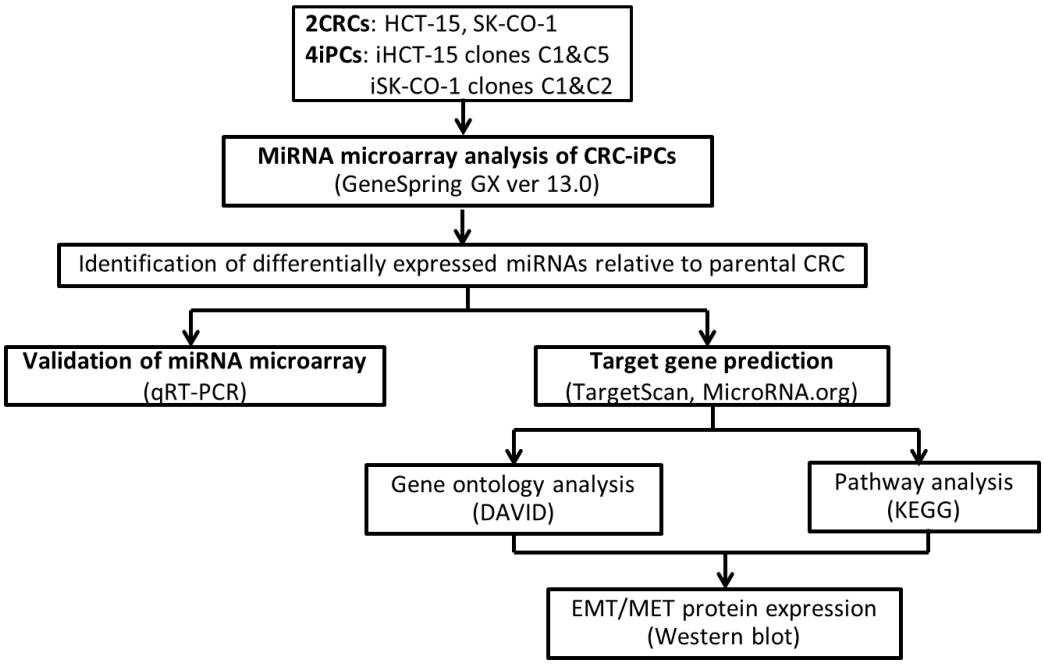

Figure 4.1 Study design of Part I of the study. Genome-wide miRNA profiling using bioinformatics databases and the elucidation of EMT/MET protein expression in CRC-iPCs. The experimental approaches performed are shown in round brackets.

4.2 Genome-wide miRNA Profiling of Colorectal Cancer Induced-Pluripotent Cancer Cells (CRC-iPCs) Showed Similarities of Both Cancer and Pluripotent Embryonic Stem Cell (ESC)

Previous studies have reported that reprogramming induces changes in miRNA expression profiles of both reprogrammed somatic and cancer cells. Besides that, miRNAs have been used to mediate cellular reprogramming which suggests the involvement of miRNAs in the regulation of stem-cell pluripotency and induction of cell fate. However, there are few studies on the miRNA expression profile in reprogrammed cancer cells when compared to somatic cells. Hence, the four CRC-iPC clones, two parental CRC cell lines and an ESC cell line were subjected to miRNA microarray analysis using the Agilent SurePrint Human MiRNA Microarray Release 21.0 to establish the genome-wide miRNA expression profile. The data obtained have been deposited at NCBI, GEO accession number: GSE87280.

Using a stringent selection criteria of $\log_2$ Fold change ≥ 2.0 or < -2.0, and a *p*-value < 0.05, 102 statistically significant miRNAs were identified by volcano plot analysis to be differentially expressed in CRC-iPCs (Figure 4.2). Among the 102 miRNAs, 50 were identified to be down-regulated and 52 were up-regulated, as indicated by light blue cubes above the green line. A full list of the 102 miRNAs is shown in Appendices A & B.

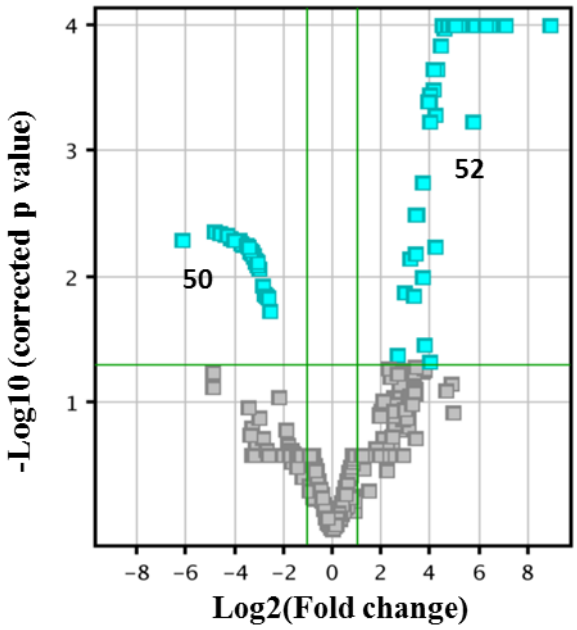

Figure 4.2 Volcano plot of differentially expressed miRNAs of parental CRC and CRC-iPC clones. The analysis was performed and generated by GeneSpring GX software version 13.0. The number of miRNAs that were significantly and differentially expressed with $\log_2$ (fold change) > 2.0 or < -2, and *p*-value <0.05 (light blue-colored cubes), are shown.

Hierarchical clustering analysis of the 102 miRNAs in the iPC clones, the parental CRCs and an ESC cell lines showed differential expression pattern of miRNAs, which could be grouped into three distinctive clusters (Figure 4.3). Cluster I miRNAs was specifically up-regulated in ESC cells and included miRNAs such as miR-130 (Pfaff et al., 2011), the mir-302 family (miR-302a, −302b, −302c & -302d) (Anokye-Danso et al., 2012; S.Lin et al., 2008), and the chromosome 19 miRNA cluster (C19MC) miRNAs (Nguyen et al., 2017), which have been shown to facilitate the reprogramming process. While cluster I miRNAs were expressed in the pluripotent ESC cells, the miRNAs were not expressed in the parental CRCs and remained unexpressed in the iPC clones, which suggests the possibility of incomplete reprogramming in the CRC-iPC cells (Figure 4.3 & Appendix C). Cluster II miRNAs, which were expressed in ESC cells, were expressed at low levels in CRC cells, but were up-regulated in the iPC cells to levels comparable to that of ESC, indicating the CRC-iPC model generated have acquired a higher pluripotent state when compared to the parental CRCs (Figure 4.3 & Appendix D). However, some of the cluster II miRNAs, such as miR-642a and miR-3162-5p, were already highly expressed in CRCs, and remained highly expressed on reprogramming in iPC cells, which highlights similarities between the processes of tumourigenesis and reprogramming (Figure 4.3). The notion is supported by the observation that cluster III miRNAs were highly expressed in the parental CRC cells, and the expression levels remained high on reprograming in the iPC cells (Figure 4.3 & Appendix D). Thus, the data suggest that the reprogrammed CRC-iPCs have retained some of the cancer molecular signatures as the parental CRCs. Cluster

III was also observed to include the let-7 and miR-200 (miR-200a,-200b,-200c) families.

A previous study has shown that the let-7 family suppresses pluripotency and induces differentiation by targeting expression of several pluripotency genes, including those encoding c-MYC and Lin28 (Li et al., 2012), whereas the miR-200 cluster is important in the early stage of somatic cell reprogramming by activating MET through blocking the E-cadherin repressor genes, ZEB1/ZEB2 (G.Wang et al., 2013).

The top ten differentially expressed up- and down-regulated miRNAs are shown in Table 4.1, arranged in a descending order of the $\log_2$ (fold change). Among the up-regulated group, five miRNAs, miR-125a-3p, miR-150-3p, miR-199a-3p, miR-1181 and miR-6789-5p, were mapped on chromosome 19 (see Table 4.1), particularly in the 19q13.2 – 19q13.4 region, whereas three miRNAs in the down-regulated group, miR-338-3p, miR-6782-5p, miR-4725-5p, were found on chromosome 17. The data indicate that reprogramming may have resulted in major expression changes of miRNAs mapping in chromosomes 17 and 19. In addition, miR-362-5p in the down-regulated group is mapped on Xp11.23 which is associated with the Xp11.22-Xp11.23 duplication syndrome (Giorda et al., 2009).

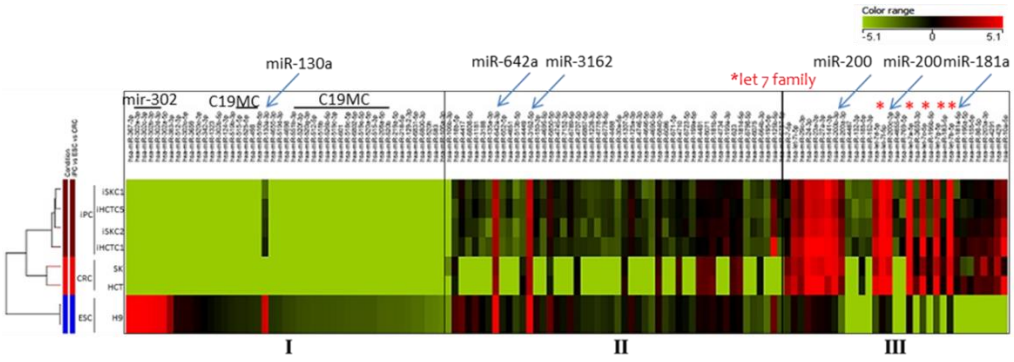

Figure 4.3 Hierarchical clustering analysis of differentially expressed miRNAs of the parental CRC, CRC-derived iPC clones and embryonic stem cells (ESCs). The relative expression levels of miRNA across samples are shown in colour-coded bar in which high expression levels is shown in red, low expression in green and black colour indicates average or weak expression. Analysis was performed using GeneSpring GX software version 13.0. The miRNAs are categorised into clusters I to III according to the cellular processes affected as described in the text; miRNAs relevant to the cellular processes described in the text are shown at the top.

Table 4.1 Top ten differentially up- or down-regulated miRNAs in reprogrammed CRC-iPCs

miRNA	Chromosome	miRNA family[a]	Log_2FC [b]
A. Up-regulated			
miR-125b-5p	11q24.1	mir-10	8.88
miR-199a-3p	19p13.2	mir-199	7.04
miR-125a-3p	19q13.41	mir-10	6.89
miR-4734	17	NA	6.36
miR-6789-5p	19	NA	6.24
miR-4417	1	NA	6.21
miR-150-3p	19q13.33	mir-150	5.86
miR-6723-5p	1	NA	5.77
miR-3934-5p	6	mir-3934	5.71
miR-1181	19	mir-1181	5.67
B. Down-regulated			
miR-192-5p	11q13.1	mir-192	-6.17
miR-338-3p	17q25.3	mir-338	-4.84
miR-455-3p	9q32	mir-455	-4.63
miR-362-5p	Xp11.23	mir-362	-4.42
miR-6741-3p	1	NA	-4.37
miR-6743-3p	11	NA	-4.34
miR-552-3p	1p34.3	mir-552	-4.15
miR-6782-5p	17	NA	-4.05
miR-4254	1	NA	-4.02
miR-4725-5p	17	NA	-3.99

[a]Based on miRBase database ver. 21; Log_2 Fold Change (Log_2FC) is relative to the respective parental CRC cells. Only $\log_2 FC > 2.0$ or < -2.0 and $p < 0.05$ are shown. NA not annotated.

4.3 Validation of microRNA Expression in CRC-iPCs

To validate the microarray data, three miRNAs each, were randomly selected, from the up- and down-regulated miRNA groups for validation by real-time RT-PCR (Figure 4.4). The mean of the $\log_2$ fold change (FC) of the two iHCT-15 and iSK-CO-1 clones relative to their respective parental CRC cell lines was calculated from three independent experiments. In all the three up-regulated miRNAs examined (miR-125b-5p, miR-199a-3p and miR-150-3p), all the mean values of the up-regulated miRNA levels obtained were statistically significant in the reprogrammed CRC-iPCs, thus confirming the microarray data (Figure 4.4). In the down-regulated group, results showed that miR-500a-3p, miR-362-5p and miR-532-3p were all down-regulated, as in the microarray data, with the exception of miR-500a-3p being slightly up-regulated in the iHCT-15 clones (Figure 4.4). Despite the minor discrepancy observed, the trend of expression of the miRNAs tested was generally consistent with that of the microarray results. Hence, the microarray data were confirmed.

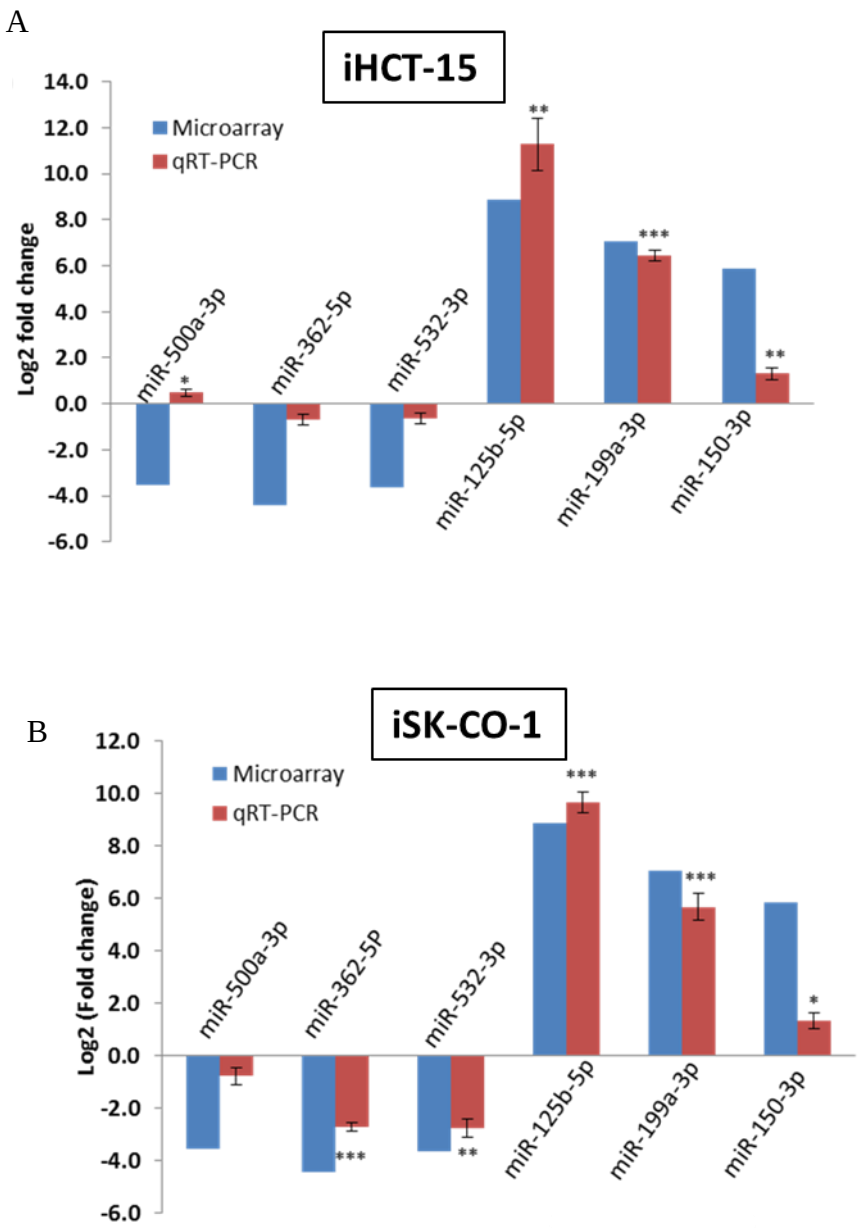

Figure 4.4 Validation of differentially-expressed miRNAs by quantitative real-time PCR. Expression validation of six randomly-selected miRNAs in four CRC-iPC clones by real-time RT-PCR. The data shown were means of data obtained from two iHCT15 (A) and iSK-CO-1 clones (B), respectively. Real-time RT-PCR data presented were from three independent experiments performed in triplicates. Expression levels of miRNAs were normalised to the respective parental CRC level. *p<0.05, **p<0.01, and ***p<0.001.

4.4 Up- and Down-regulated miRNAs Predicted to Suppress Apoptosis and Modulate Cell Migration

The putative target genes of up- and down-regulated differentially expressed miRNAs were obtained by interrogation of TargetScan and MicroRNA.org databases. To elucidate the biological roles, the predicted gene transcripts targeted by the both up- and down-regulated miRNAs, were analysed using Gene Ontology (GO) analysis and categorised based on biological processes and molecular functions.

The top 10 molecular functions of the predicted target genes of the up-regulated miRNAs are involved in activities of MAP kinase activity, tumour necrosis factor-activated receptor, glutamate dehydrogenase and scavenger receptor (Figures 4.5A & 4.5B). The tumour necrosis factor was reported to mediate cell migration in breast cancer (Wolczyk et al., 2016) and colon cancer (Zhao and Zhang, 2018) by mediating the NF-κB/Snail pathway (Wu and Zhou, 2010). Glutamate dehydrogenase is an enzyme previously reported to be involved in CRC metabolism and metastasis (Liu et al., 2015).

Furthermore, the GO analysis revealed that the putative genes targeted by the up-regulated miRNAs are enriched in biological processes related to pathways such as JNK signalling, tumour necrosis factor-mediated signalling, regulation of cell proliferation, positive regulation of apoptosis and negative

regulation of cell migration (Figures 4.5C & 4.5D). A recent study has shown that modulation of the JNK pathway is essential for reprogramming of human fibroblast cells through regulation of cell proliferation and initiation of the mesenchymal-to-epithelial (MET) process (Neganova et al., 2016). In short, the up-regulated miRNAs are predicted to target genes functions in regulating cellular apoptosis and proliferation, thus facilitating the self-renewal phenotype in reprogrammed cancer cells.

On the other hands, predicted target transcripts of the fifty down-regulated miRNAs indicated involvement in the binding of cation, metal and transmembrane receptor protein kinase activity, which is also important in signal transduction (Figures 4.6A & 4.6B). GO analysis of the top 10 biological processes showed that the down-regulated miRNAs lead to up-regulation of target genes predicted to be involved in regulation of cell adhesion, cell migration, chemotaxis and regulation of phosphatidylinositol-3-kinase (PI3K) signalling (Figure 4.6C & 4.6D). Notably, PI3K signalling has been shown to modulate cell migration by a previous report (Xu et al., 2015a). Six of the ten assigned GO terms are involved in cell migration and adhesion. Since the data were derived from the analysis of CRC-iPCs, suggesting possible involvement of the EMT/MET processes in cancer cell reprogramming. In fact, MET is required for the initiation of early phase of somatic cell reprogramming (Li et al., 2010). Taken together, the gene ontology analysis suggests that both the up- and down-regulated miRNAs may suppress apoptosis and modulate cell migration in CRC-iPCs.

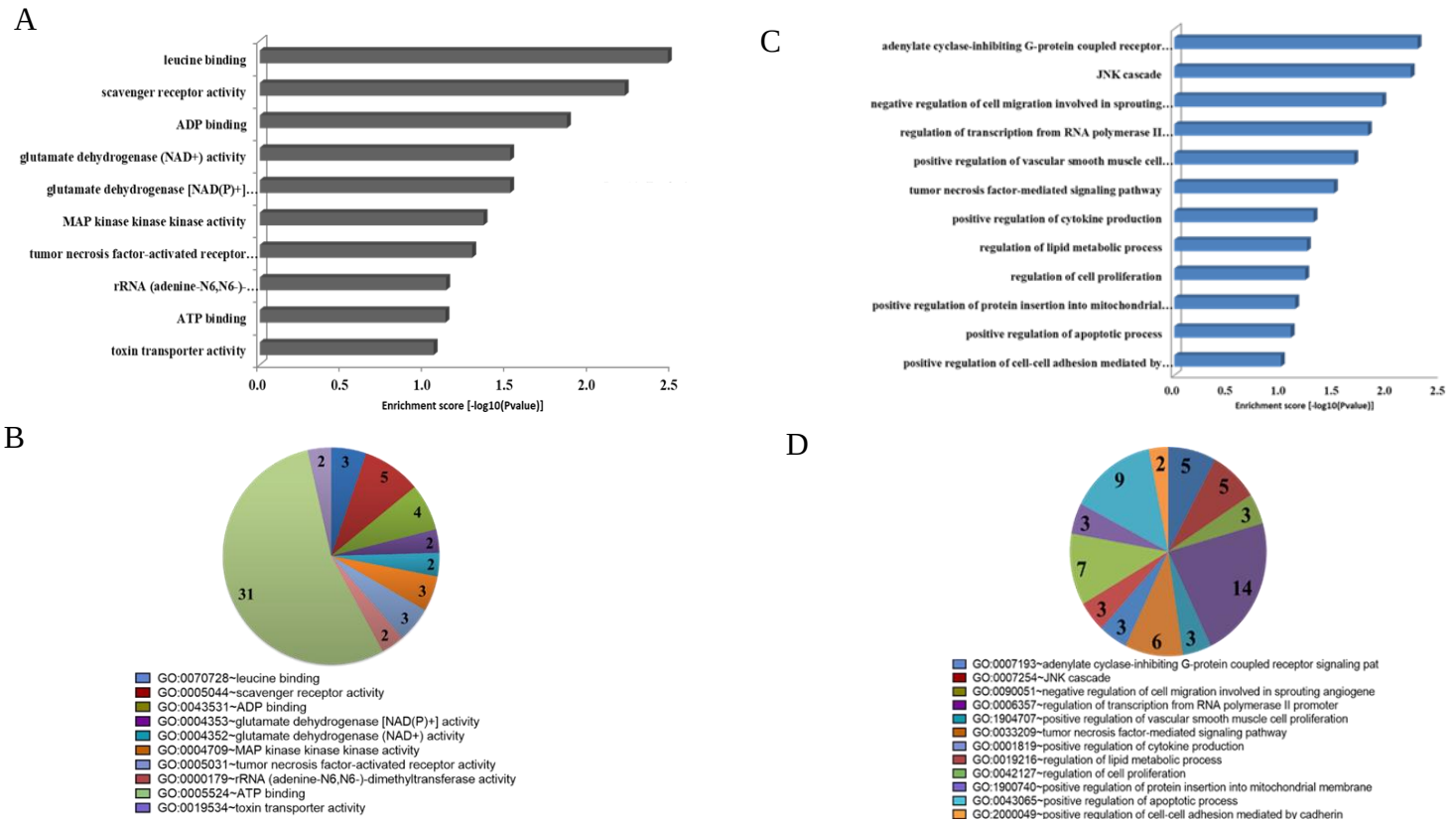

Figure 4.5 Gene Ontology (GO) analyses of the predicted genes targeted by the 52 up-regulated miRNAs. The top 10 most significantly enriched GO terms in molecular functions (A and B) and biological processes (C and D) according to respective (A and C) gene enrichment score and (B and D) gene number.

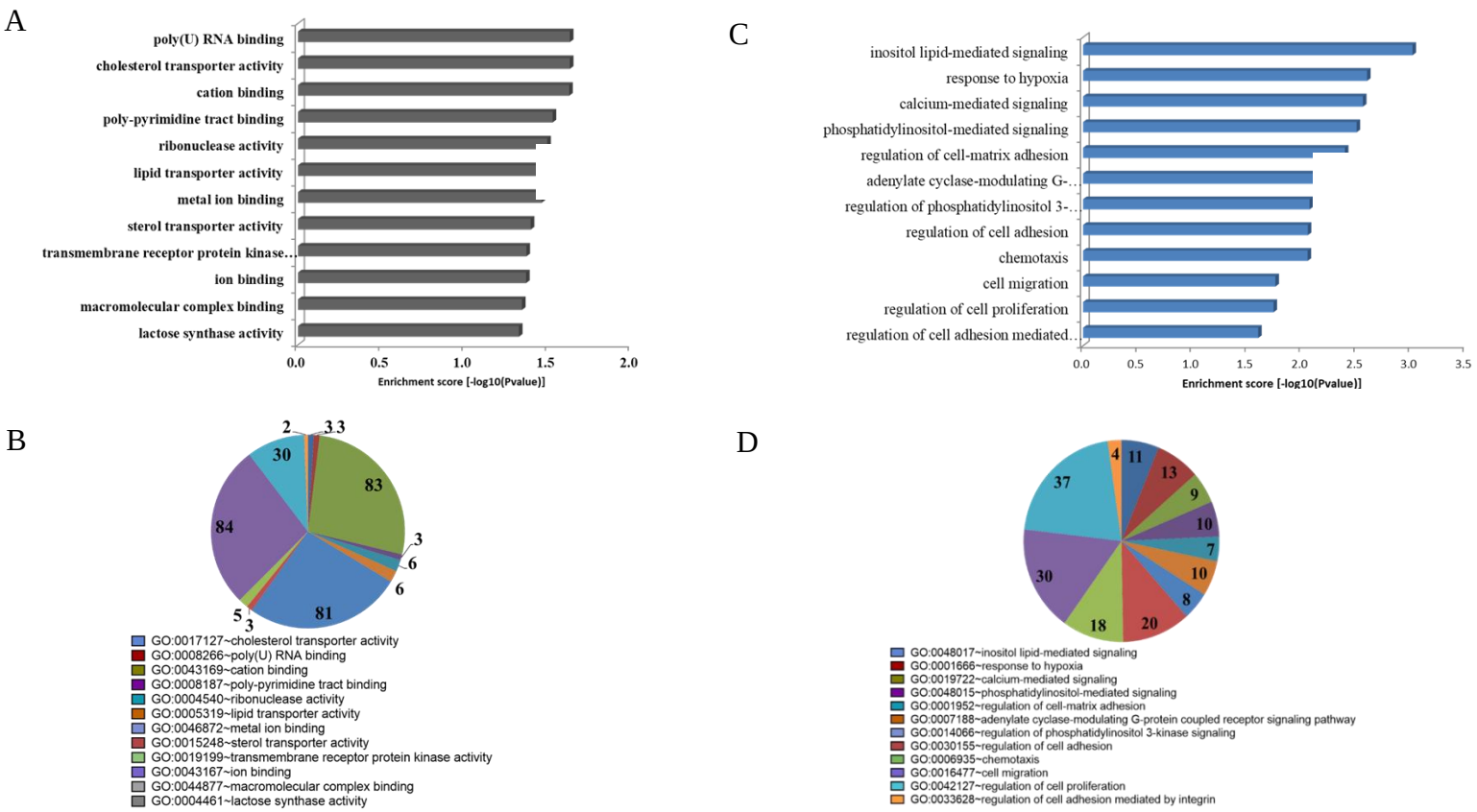

Figure 4.6 Gene Ontology (GO) analyses of the predicted genes targeted by the 50 down-regulated miRNAs. The top 10 most significantly enriched GO terms in molecular functions (A and B) and biological processes (C and D) according to respective (A and C) gene enrichment score and (B and D) gene number.

4.5 Differentially expressed MiRNAs are Predicted to Target EMT/MET-related Pathways in Reprogrammed CRC

The top ten KEGG pathway analysis of the CRC-iPC-derived data, showed four EMT/MET-associated pathways are affected by the reprogramming process, including the PI3K-AKT, TGF-β, VEGF and ERBb signalling pathways (Hardy et al., 2010; Li et al., 2010; Lu et al., 2012; Xu et al., 2015). MET conversion is required for the initial stage of somatic reprogramming which results in down-regulation of mesenchymal genes and up-regulation of epithelial genes encoding for cell junction proteins. Thus, inhibition of the EMT-inducing TGF-β signalling pathway by pluripotency factors has been reported to increase the efficiency of iPSC formation (David and Polo, 2014; Li et al., 2010). Activation of the PI3K-AKT pathway is crucial in regulating cell proliferation and in promoting EMT through phosphorylation of the AKT protein. Phosphorylated AKT protein triggers the downstream signalling cascade, which leads to changes in different biological processes, including cell cycle, survival, apoptosis and migration (Xu et al., 2015).

Blockage of VEGF signalling inhibits EMT-transcription factor TWIST to reduce the CRC migration and invasion (Lu et al., 2014). Activation of the ErbB signalling pathway also results in up-regulation of EMT-associated transcriptional repressors, such as Snail, ZEB and Twist, which in turns, inhibit the transcription of MET genes in breast cancer cells (Hardy et al., 2010). In cancer cells, EMT has been associated with the acquisition of stemness

properties. Induction of EMT has also been reported to facilitate the generation and maintenance of cancer stem cells (CSCs). Thus, the KEGG pathway analysis has highlighted involvement of the EMT/MET processes in the reprogrammed CRC-iPCs, in line with the gene ontology analysis.

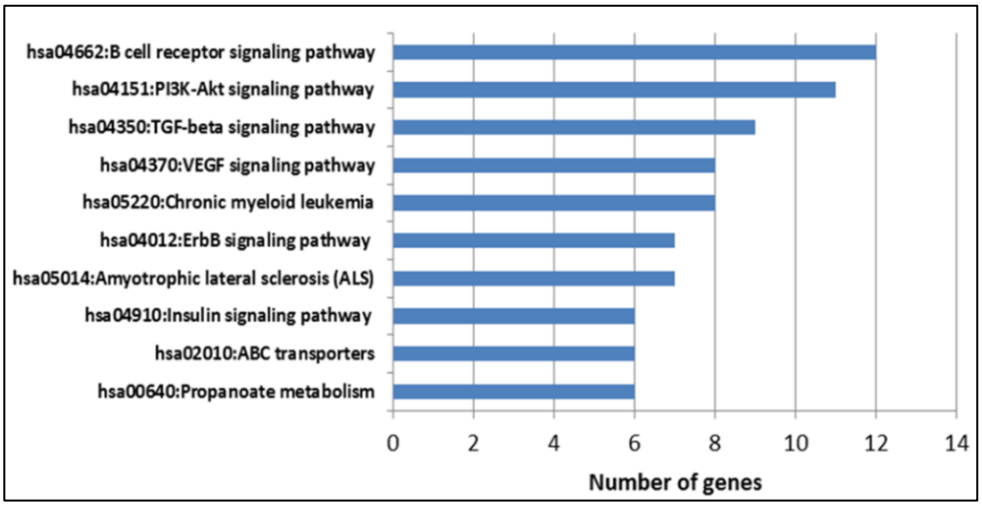

Figure 4.7 Top 10 KEGG pathways of predicted genes targeted by differentially expressed miRNAs. The predicted target genes in the KEGG pathways are also shown in Table 4.2.

Table 4.2 Top 10 predicted KEGG pathways and genes targeted by the differentially expressed miRNAs in CRC-iPC[1]

KEGG ID	KEGG pathway	Fold Enrichment	Predicted target genes	*p* value
hsa04662	B cell receptor signaling pathway	3.1	CARD11, IFITM1, MAP2K1, LYN, CD22, RAF1, AKT3, MALT1, CD79A, CD72, VAV2, VAV1	0.002
hsa04012	ErbB signaling pathway	3.3	AP2A2, MAP2K1, YWHAB, RAF1, CSK, UBA52, PXN	0.018
hsa00640	Propanoate metabolism	3.6	LDHC, LDHA, MLYCD, ACACB, SUCLA2, ALDH3A2	0.023
hsa04151	PI3K-Akt signaling pathway	2.0	FOXD4L3, YWHAG, NOS1, FOXD4L1, YWHAB, IGF2, RPS6KB1, GRAP2, FOXD4L6, AKT3, FOXD4	0.043
hsa05014	Amyotrophic lateral sclerosis (ALS)	2.5	GPX1, TNFRSF1B, NOS1, MAPK12, TP53, CCS, NEFM	0.056
hsa04910	Insulin signaling pathway	2.7	PLAC4, MAP2K1, RAF1, IGF2, RPS6KB1, GRAP2	0.068
hsa04370	VEGF signaling pathway	2.2	PRKCZ, NOS1, MAPK12, ARHGAP1, RAF1, AKT3, KDR PXN	0.073
hsa02010	ABC transporters	2.6	ABCB9, ABCG5, ABCC3, ABCB7, ABCG1, ABCA13	0.077
hsa04350	TGF-beta signaling pathway	2.0	INHBB, ACVR2A, NOG, ACVRL1, SMAD4, RPS6KB1, BMP8B, BMP8A, TGFB2	0.082
hsa05220	Chronic myeloid leukemia	2.0	CDKN1A, GAB2, MAP2K1, SMAD4, TP53, RAF1, AKT3, TGFB2	0.094

[1]Arranged in increasing *p* values.

4.6 Predicted Activation of miRNAs Targeting the TGF-β and PI3K-AKT Signalling Pathways to Regulate the EMT/MET Processes in CRC-iPCs

Based on bioinformatics analysis, TGF-β and PI3K-AKT signalling pathways were predicted to be activated in CRC-iPC models (Figures 4.8 & 4.9). In the TGF-β pathway, TGFβ2, which is a ligand of the TGFβ family, was predicted to be targeted by ten differentially expressed miRNAs, seven of which were down-regulated whereas three miRNAs were up-regulated (Figure 4.8). On the other hand, SMAD4, which forms a complex with phosphorylated R-SMAD, was predicted to be targeted by seven miRNAs, among which miR-362-5p, miR-421, miR-4259 and miR-552-3p were down-regulated (Figure 4.8). The down-regulation of these miRNAs results in up-regulation of TGFβ2 and SMAD4, thus triggering the downstream signaling cascade which enhances the transcription of EMT-associated genes such as SNAI1, Slug and ZEB1. The expression of EMT transcription factors causes repression of MET genes such as E-cadherin, leading to transition of cells towards a mesenchymal-like state.

The PI3K/AKT signalling pathway has been reported to regulate numerous cellular processes including cell survival, proliferation, motility, cell invasion and other malignant transformation associated with tumourigenesis (Yu andCui, 2016; Xu et al., 2015; Engelman, 2009). Phosphatidylinositol 3-kinase (PI3K) is activated upon stimulation of IGF-I receptor (IGF-IR) by

insulin growth factor. Four miRNAs, miR-192-3p, miR-362-3p, miR-552-3p and miR-4254, predicted to target IGF are down-regulated. On the other hands, 10 out of 12 of the up-regulated IGF-targeting miRNAs are unannotated (Figure 4.9 dash box), which may be further explored in their role in EMT. Activated PI3K is involved in the conversion of plasma lipid PIP2 to PIP3, which subsequently activates AKT by phosphorylating it to pAKT (Martini et al., 2014). AKT is predicted to be regulated by eight miRNAs, five of which, miR-149-5p, miR-181c-5p, miR-362-3p, miR-455-3p, and miR-4254, are down-regulated, whereas the remaining three AKT-targeting miRNAs, miR-195-5p, miR-671-5p and miR-769-5p, were up-regulated (Figure 4.9). Phosphorylated AKT activates IκB kinase (IKK), which causes the degradation of IκBα, an inhibitor of NF-κB (Kalimuthu et al., 2013; Downward, 2004), thus resulting in the activation of the NF-kB signaling pathway and subsequent up-regulation of SNAI1 expression. Inhibition of glycogen synthase kinase beta 3 (GSKß3) by pAKT also leads to accumulation of β-catenin (Xu et al., 2016) and activation of the Wnt signalling pathway, which in turns promotes EMT. Previous studies have also shown that the degradation of GSK beta 3 may lead to overexpression of SNAI1 (Lee et al., 2010). Overall, SNAI1 nuclear translocation increases the expression of the mesenchymal marker vimentin and represses the epithelial marker E-cadherin, to facilitate induction of the EMT process (Miyazono et al., 2009).

Taken together, bioinformatics prediction of miRNA-regulated TGF-β and PI3K-AKT pathways may work individually or synergistically to promote an EMT state in CRC-iPCs.

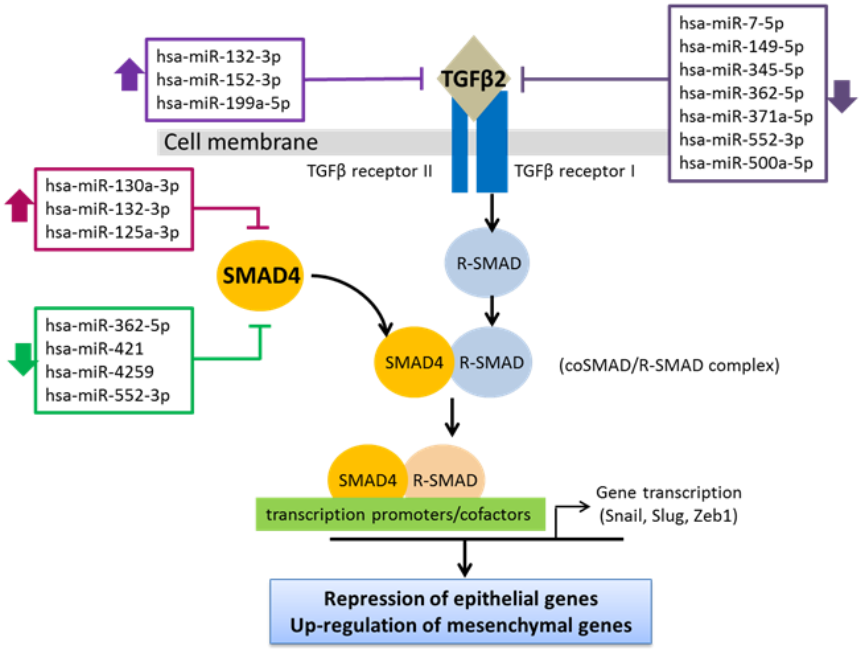

Figure 4.8 Predicted miRNA-mRNA interactions in the TGF-β signalling pathway. Predicted transcripts targeted by miRNAs are shown in boxes; up- and downward arrows indicate miRNAs that are up- and down-regulated, respectively. The TGF-β pathway scheme was adapted from Miyazono et al., 2009

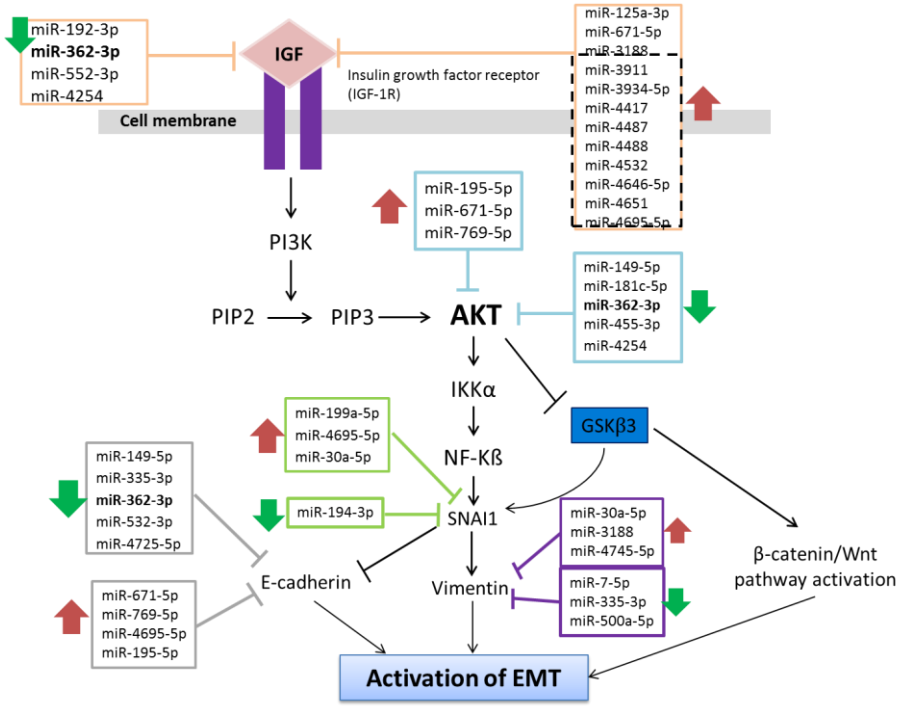

Figure 4.9 Predicted miRNA-mRNA interactions in the PI3K-AKT signaling pathway. Predicted transcripts targeted by miRNAs are shown in boxes; up- and downward arrows indicate miRNAs that are up- and down-regulated, respectively. The PI3K-AKT pathway scheme was adapted from Li et al., 2017.

4.7 Differentially-expressed miRNAs Validated Targeting at EMT/MET Genes in CRC-iPCs

To further investigate if the differentially expressed miRNAs are also associated with the MET and EMT processes, predictive targeting miRNAs of two MET genes, E-cadherin (CDH1) and occludin (OCLN), and two representative EMT genes, Snail (SNAI1) and vimentin (VIM), were used to interrogate the online databases TargetScan 7.0, miRWalk 2.0 and Diana tools (microT-CDS) (Table 4.3). Results showed that CDH1 was putatively targeted by 9 miRNAs whereas OCLN was regulated by 10 miRNAs. Similarly, the EMT genes, SNAI1 and VIM, were predicted to be targeted by 4 and 6 miRNAs respectively (Table 4.3). Hence, data showed that all four selected MET/EMT genes are targeted by one or more of the 102 differentially expressed miRNAs, indicating miRNAs modulation of MET/EMT gene expression in iPC cells.

To validate the expression of EMT/MET-targeting miRNAs, two of each miRNAs targeting SNAI1 and CDH1 were randomly chosen for qRT-PCR analysis (Figure 4.10). The expression trend was generally consistent with the microarray data with the exception of miR-194-3p which was slightly up-regulated in the iHCT-15 clones (Figure 4.10). This minor difference could be partly explained by the fact that in the miRNA microarray analysis (Table 4.3), the mean values were derived from data of the four iPC clones whereas individual iPC clones were subjected to qRT-PCR analysis.

Table 4.3 Differentially expressed miRNAs in the CRC-iPC clones target selected mesenchymal and epithelial genes

Gene	miRNA	Chromosome	miRNA family	$Log_2(FC)^1$
		EMT genes		
VIM	miR-4745-5p	19	NA	5.61
	miR-3188	19	mir-3188	4.55
	miR-30a-5p	6q13	mir-30	3.94
	miR-500a-5p	Xp11.23	mir-500	-2.85
	miR-7-5p	15q26.1	mir-7	-2.61
	miR-335-3p	7q32.2	mir-335	-2.61
SNAI1	miR-199a-5p	19p13.2	mir-199	5.06
	miR-4695-5p	1	NA	4.44
	miR-30a-5p	6q13	mir-30	3.94
	miR-194-3p	11q13.1	mir-194	-3.03
		MET genes		
CDH1	miR-671-5p	7q36.1	mir-671	5.20
	miR-769-5p	19q13.32	mir-769	5.02
	miR-4695-5p	1	NA	4.44
	miR-195-5p	17p13.1	mir-15	3.96
	miR-4725-5p	17	NA	-3.99
	miR-532-3p	Xp11.23	mir-188	-3.64
	miR-362-3p	Xp11.23	mir-362	-3.60
	miR-149-5p	2q37.3	mir-149	-3.36
	miR-335-3p	7q32.2	mir-335	-2.61
OCLN	miR-1228-3p	12	mir-1228	4.75
	miR-132-3p	17p13.3	mir-132	4.20
	miR-4463	6	NA	3.40
	miR-513b-5p	Xq27.3	mir-506	3.38
	miR-362-5p	Xp11.23	mir-362	-4.42
	miR-3591-3p	18	mir-122	-3.97
	miR-362-3p	Xp11.23	mir-362	-3.60
	miR-449b-3p	5q11.2	mir-449	-3.39
	miR-500a-5p	Xp11.23	mir-500	-2.80
	miR-335-3p	7q32.2	mir-335	-2.61

Target genes were predicted by TargetScan 7.0, miRWalk2.0 and Diana tools (microT-CDS). [1]Log_2 (fold change) data are presented in decreasing values; down-regulated miRNAs are shown as negative values. All values are statistically significant with p <0.01 compared with the respective parental CRCs. NA, not available.

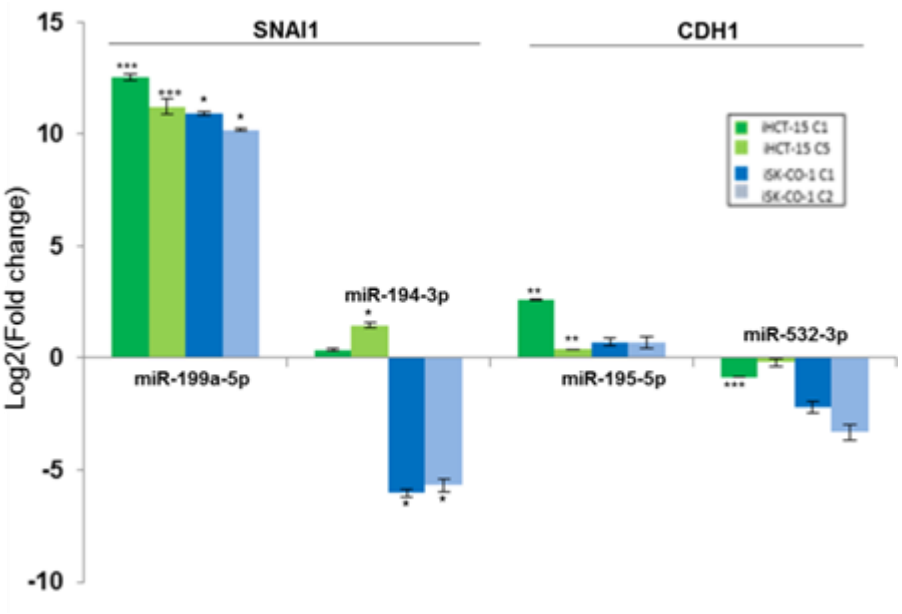

Figure 4.10 Expression of the predicted miRNAs targeting SNAI1 and CDH1 genes in the CRC-iPC clones. MiRNA expression was determined by real-time RT-PCR; the microarray-predicted up- or down-regulated miRNAs (see Table 4.3) are indicated. Expression levels were relative to the parental cells; *$p< 0.05$, **$p< 0.01$, ***$p< 0.001$.

4.8 Epithelial/Mesenchymal (E/M) Hybrid Phenotype

MET is a critical step in setting up the initial phase of somatic cell reprogramming (Li et al., 2010; Samavarchi-Tehrani et al., 2010). Hence, the expression status of MET and EMT genes is an important indicator of the cell state. To elucidate the effects of reprogramming on EMT/MET gene expression in CRC-iPCs, and the effects of re-differentiation in Post-iPCs, western blot analysis was performed. The expression of two EMT proteins, vimentin (VIM) and SNAI1, and two MET proteins, CDH1 and OCLN, were examined as they are the predicted miRNA targets (Table 4.3). Representative western blots are presented in figure 4.11A whereas quantification of the data derived from three independent experiments is shown in figure 4.11B.

Western blot results revealed that VIM was expressed at low levels in the parental HCT-15 and SK-CO-1 cells. On reprogramming, the protein levels were up-regulated to approximately 2.5- to 8-fold in the different iPC clones of both cell lines. However, the VIM levels were generally reverted back to the parental levels on re-differentiation into post-iPC cells. The SNAI1 level was high in HCT-15 but was very low in SK-CO-1. Reprogramming was observed to suppress the SNAI1 expression level in iHCT-15, but up-regulated the protein in iSK-CO-1. On differentiation, the SNAI1 levels were restored to levels similar to those of the parental cells in post-iHCT-15 clones, but up-regulated SNAI1 level was maintained in the post-iSK-CO-1 cells.

In the MET CDH1 protein western blots, a 120-kD band was detected in all cell types (Figure 4.11A, CDH1 lane, arrowhead); A second band of a lower molecular weight, 86-kD, was detected selectively only in the iPC cells. The 86-kD band was most likely the E-cadherin soluble ectodomain, a cleavage product of matrix metalloproteinases derived from the 120-kD protein (Matos et al., 2017). CDH1 was consistently up-regulated in all four iPC clones from the two CRC cell lines. However, the CDH1 levels all reverted back to approximately the parental levels on re-differentiation. The OCLN level was detected in the HCT-15 cells, but the protein was barely detectable in SK-CO-1. OCLN levels were down-regulated in the reprogrammed iHCT-15 clones but were restored to approximately the parental levels on re-differentiation into the post-iHCT-15 clones. On the other hand, OCLN levels were up-regulated in the iSK-CO-1 cells, and differentiation process further up-regulated the protein expression.

EMT and MET are functionally opposing processes in which up-regulation of one process is followed by down-regulation of the other process (Thiery et al., 2009). The western blot analysis of the iPC clones revealed that on reprogramming, both the EMT and MET proteins were generally up-regulated, with the exception of SNAI1 and OCLN, in the iHCT-15 cells. Hence, the contradictory EMT and MET expression patterns suggested the possibility that CRC reprogramming has elicited an epithelial/mesenchymal (E/M) hybrid phenotype in CRC-iPCs (Jolly, 2015; Garg, 2015). However, on re-differentiation to post-iPC cells, the expression of EMT/MET proteins was

generally reversed, indicating epigenetic regulation involvement. Different clones of the same cell line and different CRC cell lines also showed different EMT/MET expression profiles, which could be explained by the heterogeneous nature of cancer cells and cancer stage-dependent expression modes of the EMT/MET genes (Loboda et al., 2011; Heerboth et al., 2015).

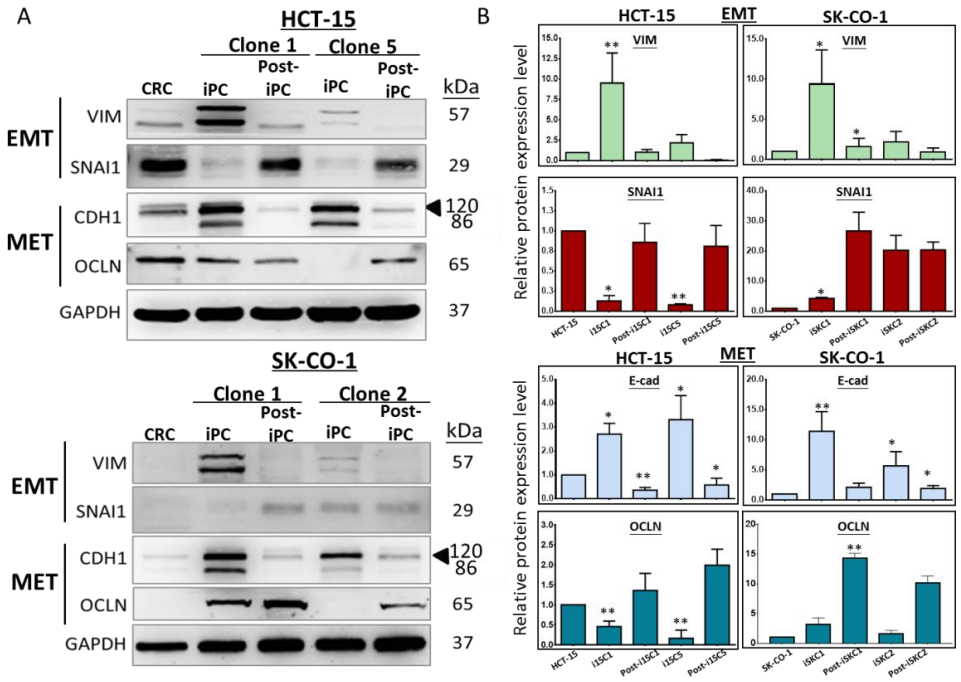

Figure 4.11 Quantification of changes of EMT and MET protein levels from three independent experiments. Data presented as mean ± SEM. P values were derived by comparing iPC vs parental cells and post-iPC vs iPC cells; *p < 0.05; **p < 0.01.

4.9 Bioinformatics Prediction of miR-362 Involvement in Cell Migration and Invasion

Five miRNAs, namely miR-188, miR-501, miR-362, miR-532, and miR-660 are located on chromosome Xp11.23 (Table 4.4). Aberrant expression of miR-532-502 was previously reported in triple-negative breast cancer (Chang et al., 2015), suggesting that dysregulation of this miRNA cluster is associated with tumourigenesis process.

MiR-188-5p was previously reported to inhibit the tumour growth and metastasis in prostate cancer (Zhang et al., 2015). On the other hand, ectopic expression of miR-660 was shown to suppress migration and invasion as well as promote apoptosis in lung cancer cells through targeting MDM2, a mediator of the p53 expression and functions (Fortunato et al., 2014).

MiR-532 was shown to increase cell migration and invasion in human gastric cancer cells (Xu et al., 2016). Besides that, miR-500a-3p was found to promote cancer stem cell properties and tumour growth in hepatocellular carcinoma by targeting negative regulators of JAK/STAT signaling (Jiang et al., 2017). Similarly, miR-362-5p expression was found to enhance the proliferation, migration and invasion in breast cancer MCF7 (Ni et al., 2016), HCC cells (Ni et al., 2015) and non-small-cell lung carcinoma (NSCLC) (Luo et al., 2018).

Notably, miR-362-3p/-5p, miR-500a-3p/-5p and miR-532-3p were down-regulated in CRC-iPCs (Table 4.4), echoing that down-regulation of these miRNAs may lead to decreased cancer phenotype such as decreased migration and invasion activities which involve the regulation of the EMT/MET processes.

Table 4.4 Down-regulated miRNAs mapping at the XP11.23 chromosomal locus were differentially expressed in CRC-iPCs

No.	Systematic name[a]	mirBase accession no[b]	Chromosome[c]	FC[d] ([iPC] vs [CRC])	P (Corr)[e]
1	hsa-miR-362-5p	MIMAT0000705	Xp11.23	-21.331	0.005
2	hsa-miR-532-3p	MIMAT0004780	Xp11.23	-12.441	0.006
3	hsa-miR-362-3p	MIMAT0004683	Xp11.23	-12.097	0.006
4	hsa-miR-500a-3p	MIMAT0002871	Xp11.23	-11.588	0.006
5	hsa-miR-500a-5p	MIMAT0004773	Xp11.23	-7.206	0.012

[a]Systematic names were taken from mirBase database; [b]mirBase accession no were taken from mirBase database; [c]Chromosome were taken from HUGO Gene Nomenclature Committee (HGNC); [d]FC, Fold change; [e]P (Corr), corrected p value, cut off at 0.05.

4.10 Study design of Part II

In Part I of the study, miR-362-5p and -3p were predicted to target the four selected EMT and MET genes, and these miRNAs have not been previously reported in relation to EMT/MET in reprogrammed cancer cells. Hence, in Part II of this study, miR-362-5p and -3p were selected for functional analysis on their effects on EMT/MET by demonstrating interactions between miR-362-5p/-3p and selected EMT/MET-related target genes, and ~~to~~ elucidating possible contribution of miR-362-5p/-3p in regulating the EMT and MET processes in colorectal cancer reprogramming and mobility. The study design of Part II is shown in Figure 4.12.

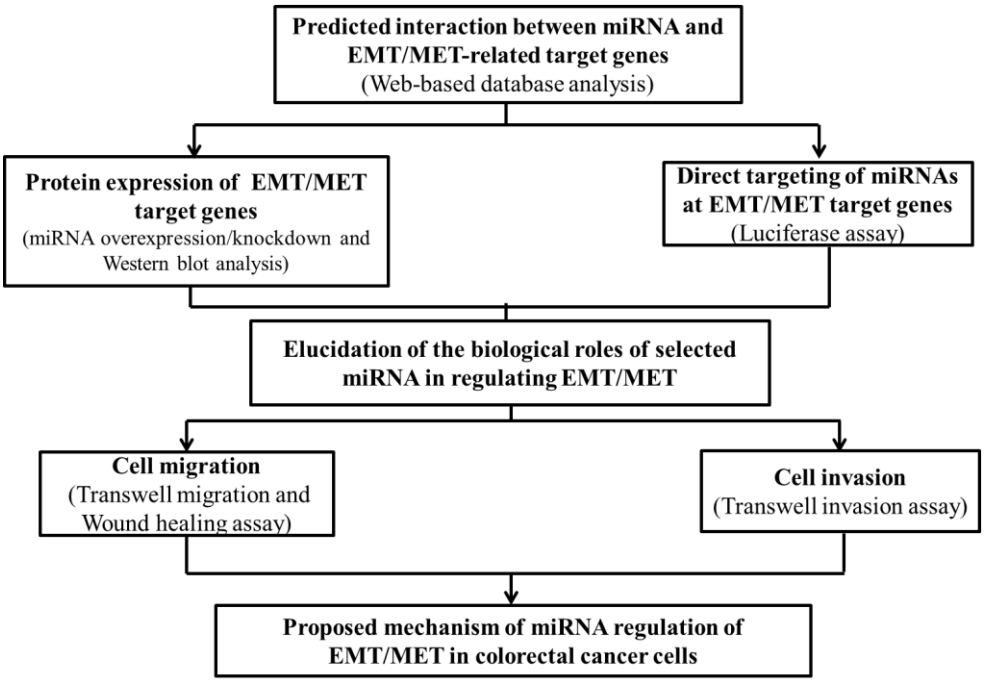

Figure 4.12. Study design of Part II of this work. Elucidation of the biological roles of miR-362-5p/-3p in regulating the EMT and MET processes in colorectal cancer cells. The experimental assays carried out are described in round brackets.

4.11 Down-regulated miR-362 Expression on Cancer and Somatic Cell Reprogramming

The function and mechanism of miR-362 in regulating EMT/MET-related genes in reprogrammed cancer cells have not been previously reported. Hence, miR-362 was selected for subsequent downstream analysis. MiR-362-5p/-3p was mapped on all the four EMT/MET-related genes.

The endogenous expression of miR-362 in different cell types was assessed including the SK-CO-1 group, an iPSC derived from somatic cells, mesenchymal stem cells (MSC), and cancer cell lines (Figure 4.11). On reprogramming, miR-362-5p/-3p expression levels were down-regulated in both the iSK-CO-1 clones and expression was restored back to approximately the levels of the parental SK-CO-1 cells (Figure 4.11). Moreover, miR-362 expression was also found to be low in MH#1, which is an iPSC cell line established from human adipose-derived stem cells, suggesting that down-regulation of miR-362 levels is associated with the reprogramming process (Figure 4.11). MiR-362-3p expression was also found to be up-regulated in umbilical cord derived-MSC (Figure 4.11), which is consistent with previous studies (Chi et al., 2016). The role and mechanism underlying miR-362-3p up-regulation in MSC has not been studied.

Varied expression levels of miR-362-5p/-3p were observed in different cancer cell lines and the expression of which may be correlated with metastatic potential of the cancer cells (Figure 4.11). MCF-7 is a non-invasive human breast cancer cell line with low metastatic potential (Gest et al., 2013) whereas JEG is a highly metastatic human placenta choriocarcinoma cell line derived from metastatic site of brain tissues, and was reported to demonstrate the strongest adhesion and invasion into the underlying endometrial stroma (Wang et al., 2017). Besides that, HCT-15 is a primary colon adenocarcinoma characterized by Duke's stage C, which shows lymph node invasion (Ehrig et al., 2013). The expression levels of miR-362-5p/-3p were very low in MCF-7 but were up-regulated in HCT15 cells and further up-regulated in JEG-3.

Taken together, the results showed that down-regulated miR-362-5p/-3p expression is associated with reprogramming process, whereas the increasing trend of miR-362-5p/3p is correlated with migration and invasion properties of the cancer cells, indicating that miR-362 may be involved in the regulation of EMT/MET processes in cancer cell reprogramming and cancer mobility. MCF-7 was chosen for overexpression of miR-362 analysis due to the presence of lower endogenous miR-362-5p/-3p levels whereas HCT-15 was used to study the effect of knockdown of miR-362.

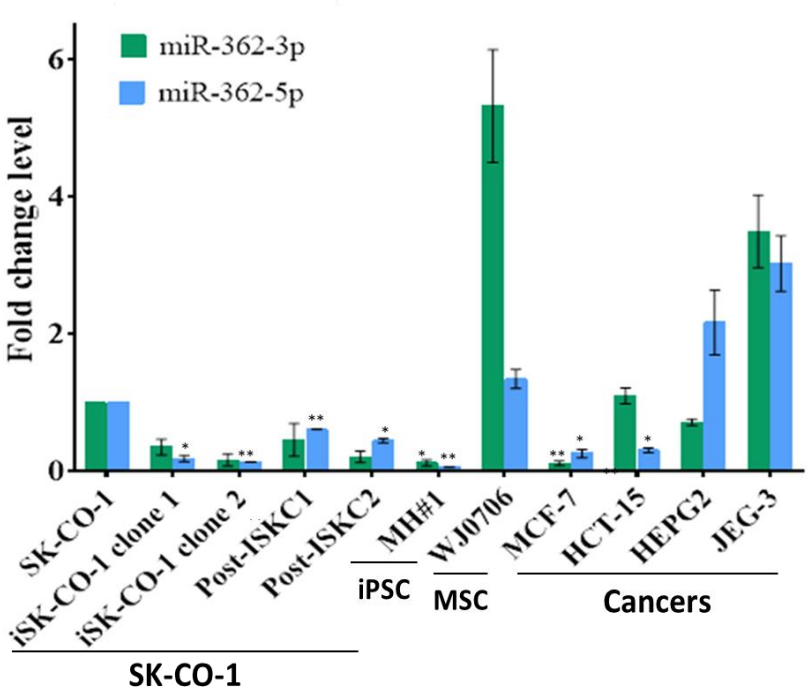

Figure 4.13 Endogenous expressions of miR-362-5p/-3p in various cell lines. The cell lines used were: SK-CO-1, colorectal cancer cells; iSK-CO-1 clones 1 and 2, iPCs derived from SK-CO-1; post-iSKCO-1 clones 1 and 2, cells differentiated from iSK-CO-1; WJ0706, mesenchymal stem cells derived from umbilical cord Wharton's Jelly; MH#1, iPSC established from human adipose derived stem cells; MCF7, breast cancer cells; HepG2, hepatocellular carcinoma cells; JEG3, choriocarcinoma cells. Real-time RT-PCR data presented were from two independent experiments performed in triplicates.
$p < 0.05$, $^{**}p < 0.01$ were relative to SK-CO-1colorectal cancer cells.

4.12 miR-362-5p/-3p Overexpression Promotes Epithelial/Mesenchymal (E/M) Hybrid State

Transfection of miR-362-5p/-3p mimics resulted in approximately 15-fold up-regulation of the miR-362-5p/-3p level 48 h post-transfection in MCF7 cells (Figure 4.14) when compared to negative control mimic (NC)-transfected cells. The effects of miR-362 overexpression on the two EMT-related genes, SMAD4 and SNAI1, and two MET-related genes, CDH1 and OCLN, were evaluated using western blot analysis (Figures 4.15A & 4.15B). Compared to untransfected MCF7 or cells transfected with the negative control mimic, miR-362-5p/-3p overexpression reduced the SMAD4 protein levels (Figure 4.15B). Upon stimulation of TGF-β signalling as mentioned above (Figure 4.8), SMAD4 acts as mediator to form a SMAD3/SMAD4 complex, which can further enhance the transcription of EMT-associated transcription factors such as SNAI1 and ZEB1. Hence, the down-regulated SMAD4 expression was previously reported to inhibit EMT in renal cell carcinoma (Mao et al., 2017), consistent with our finding.

Similarly, overexpression of miR-362-3p/5p also diminished the protein levels of both the MET genes, CDH1 and OCLN, by approximately 70% and 90%, respectively, thereby promoting EMT (Figure 4.15B).

Overall, miR-362-5p/-3p reduced both the EMT and MET protein expression levels with the exception of SNAI1, which showed no significant reduction in protein levels despite the down-regulation of SMAD4 protein, suggesting the expression of SNAI1 may be regulated by other SMAD4-independent pathways. MET and EMT, in general, are opposing processes with one process up-regulated counterbalanced by down-regulation of the other process (Thiery et al., 2009). The conflicting EMT/MET expression profiles following the transfection of miR-362-5p/-3p shows that miR-362-5p/-3p may have promoted an epithelial/mesenchymal hybrid phenotype in MCF7.

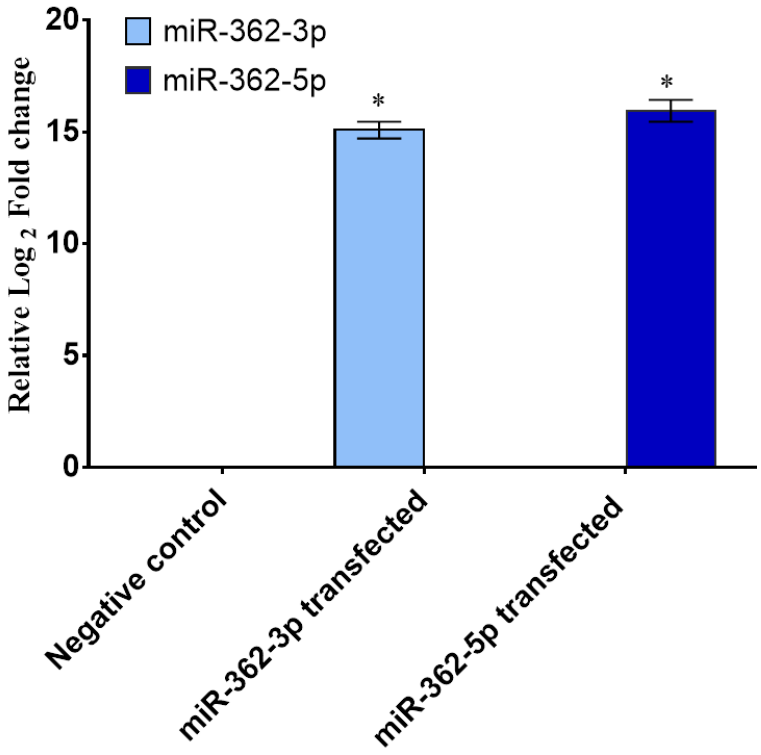

Figure 4.14 Overexpression of miR-362-5p/-3p in MCF-7 cells. MiR-362-5p/-3p mimics or a negative control mimic (NC) were transfected to MCF-7 cells for 48 h before the cells were harvested to prepare RNA for real-time PCR analysis. Data are presented in $\log_2$ fold change compared to negative control group and were derived from two independent experiments in triplicates. *p<0.05 and **p<0.01 relative to negative control mimic-transfected MCF-7 cells.

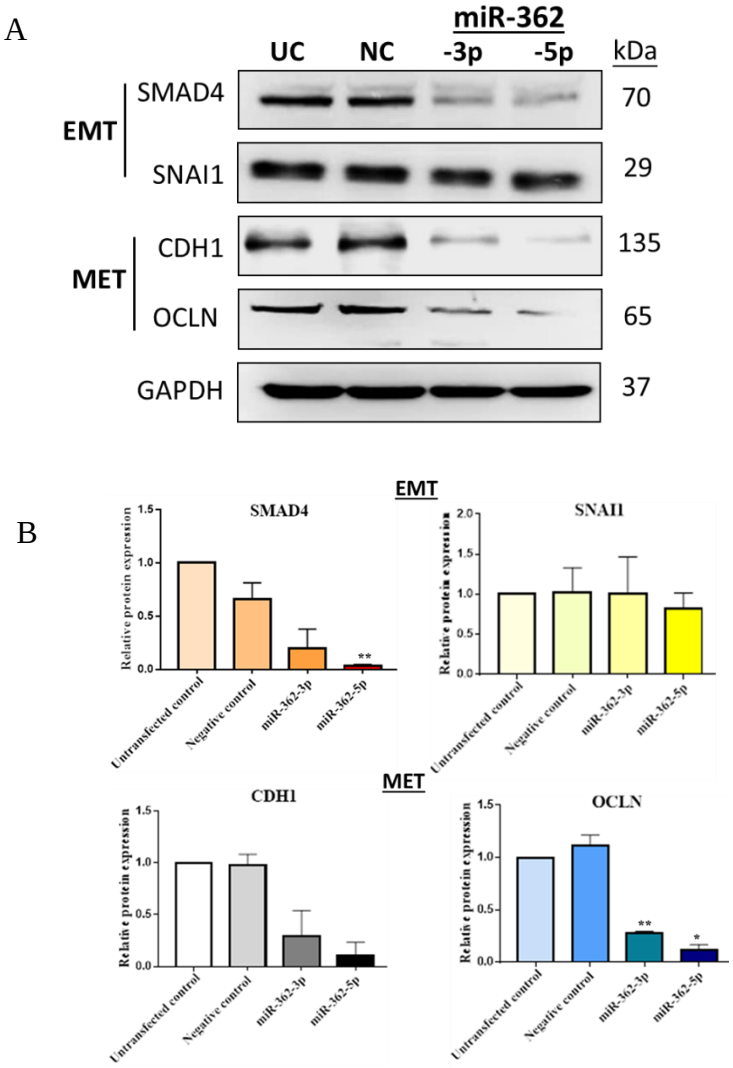

Figure 4.15 Effects of miR-362-5p/-3p overexpression on EMT/MET-related target genes at protein level. A. Representative western blots showing protein expression levels of the MET proteins (CDH1 and OCLN) and EMT proteins (SMAD4 and SNAI1) after transfection with miR-362 mimics or a validated negative control (NC). B. Quantification of EMT and MET protein expression levels derived from two independent experiments and normalised to GAPDH. Data are presented as the mean ± SEM compared to untransfected control. UC: Untransfected control ; NC: Negative control mimic; **p*<0.05 and ***p*<0.01.

4.13 miR-362-5p/-3p Knockdown Promotes MET Activation

Stable cell lines with miR-362-5p/-3p knockdown was established using miRNA sponges. The efficiency of miR-362 knockdown was assessed using qRT-PCR after two weeks of puromycin selection. Results showed that miR-362-3p and -5p were down-regulated by approximately 76% and 50%, respectively, in HCT-15 cells when compared to the negative control group (Figure 4.16).

The effects of miR-362 knockdown on the four EMT/MET genes were evaluated using western blot analysis (Fgure 4.17). miR-362-5p/-3p knockdown significantly up-regulated the protein expression of both the MET genes, CDH1 and OCLN, by 12- and 2-fold change respectively (Figure 4.17). However, the two EMT genes were observed to show different expression patterns. SNAI1 expression was decreased by 2.5- to 3-fold whereas SMAD4 was increased upon the knockdown of miR-362-5p/-3p (Figure 4.17). The inhibition of miR-362-5p/-3p showed a reversed EMT/MET expression patterns when compared to miR-362-5p/-3p overexpression with the exception of SNAI1 (Figure 4.15). Therefore, miR-362 negative regulation of endogenous expression of CDH1, OCLN and SMAD4 was confirmed. Overall, due to significant increase of the MET proteins and down-regulation of EMT-associated transcriptional repressor, SNAI1, inhibition of miR-362-5p/-3p expression promotes a MET transition.

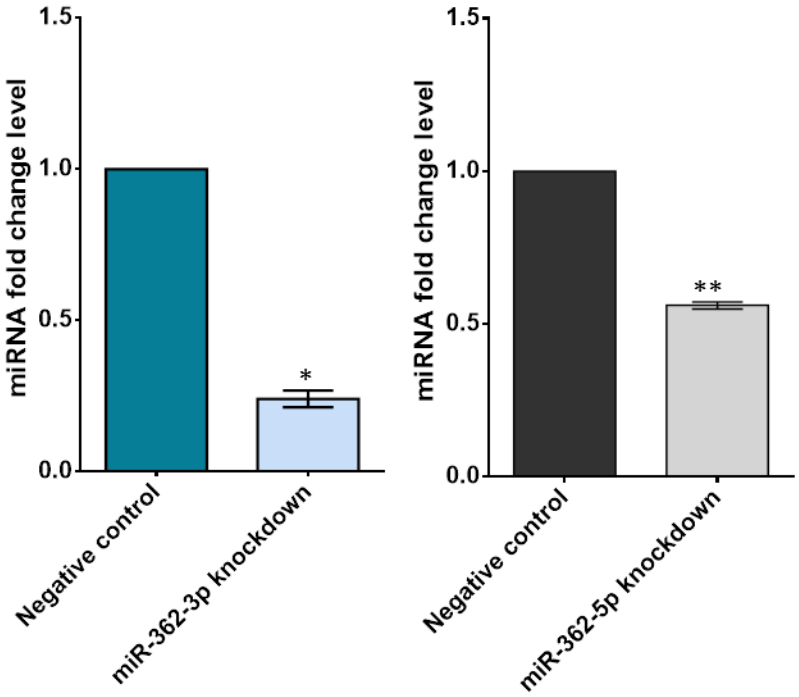

Figure 4.16 Stable knockdown of miR-362-5p/-3p in HCT-15 cells. Expression of miRNAs was quantitated by qRT-PCR and normalised to small nuclear RNA U6 (snU6). Data are presented as mean ± SEM when compared to the negative control group and were derived from three independent experiments in triplicates. *p<0.05 and **p<0.01.

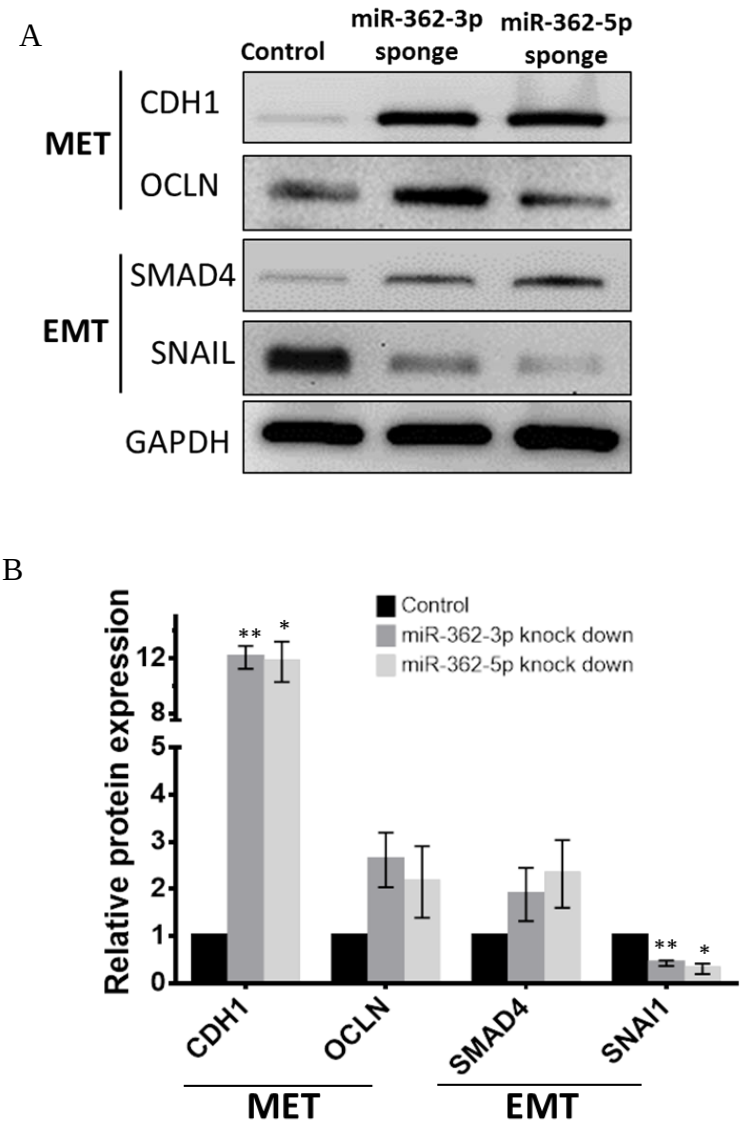

Figure 4.17 Effects of miR-362-5p/-3p knockdown on protein levels of EMT/MET-related target genes. A. Representative western blots showing protein expression of the MET (CDH1 and OCLN) and EMT proteins (SMAD4 and SNAI1) after transduction with virus supernatant containing miR-362-5p/-3p sponges, or a negative control plasmid (NC). B. Quantification of EMT and MET proteins expression derived from three independent experiments and normalised to GAPDH. Data are presented as the mean ± SEM compared to negative control group.*$p<0.05$ and **$p<0.01$.

4.14 Direct miR-362 Targeting of EMT/MET Genes

The 3'UTR luciferase construct of each EMT/MET gene was generated and cloned into the pmiRGLO luciferase plasmid. OCLN carried two clusters of miR-362-5p/-3p predicted target sites designated as OC1 and OC2, while the CDH1 construct carried a group of two miR-362-3p putative target sites, CD1 (Figure 4.18). On the other hand, the long 8,789 bp 3'UTR construct of SMAD4 encompassed four putative miR-362-3p-targeted sites and one miR-362-5p-targeted site, namely SM1,SM2 and SM3 (Figure 4.18). The 3'UTR of SNAI1 consisted of only one predicted binding site of miR-362-5p in SN1 (Figure 4.18).

The two OCLN 3'UTR constructs, OC1 and OC2, when transfected along with the miR-362-5p/-3p mimics resulted in a decrease to approximately 26% of luciferase activity relative to the control group transfected with the empty vector, or a negative control mimic (Figure 4.19). CDH1 3'UTR construct, CD1 was shown to result in 40% decrease of luciferase activity in cells co-transfected with miR-362-3p (Figure 4.20). Similarly, the cotransfection of the SNAI1 construct SN1 with miR-362-5p mimic was also observed to down-regulate the luciferase activity by 33% (Figure 4.20). SMAD4 constructs, SM1, SM2 and SM3, were separately transfected into MCF7 cells alone, or co-transfected with miR-362-5p/-3p mimic or a negative control mimic. Results showed there was around 40% and 35% reduction of luciferase activity, respectively, when miR-362-5p/-3p were co-transfected with the SMAD4 constructs (Figure 4.21).

Taken together, the results verified that miR-362-5p/-3p targeted and negatively regulated the expression of all the four selected EMT/MET-associated genes.

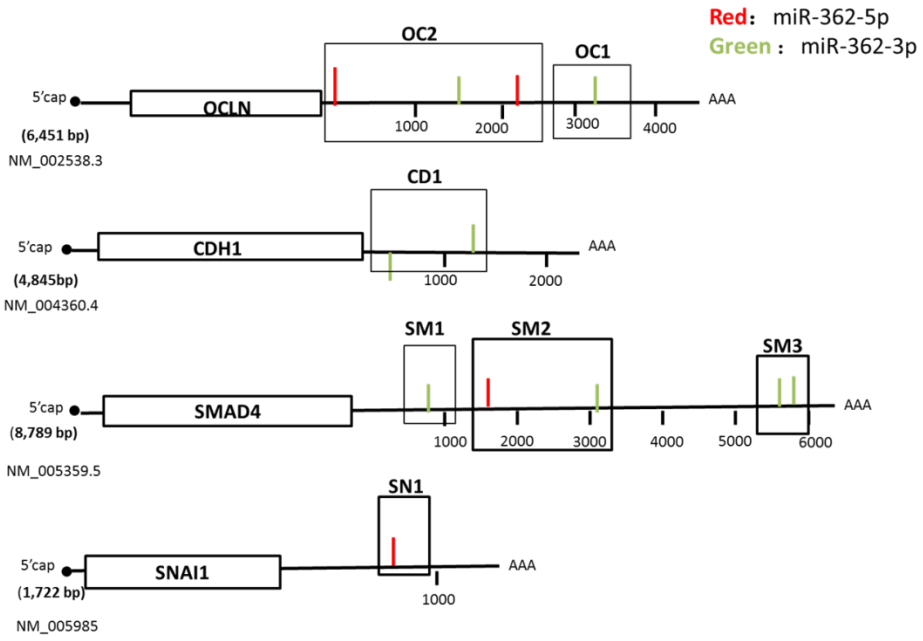

Figure 4.18 Construction of luciferase plasmids containing miR-362-3p/5p binding sites in the 3'UTR of MET/EMT target genes based on prediction logarithms. 3'-UTR luciferase construct of the OCLN, CDH1, SMAD4 and SNAI1 genes were generated (boxed) based on the prediction of miR-362-3p/5p binding sites. Red and green vertical bars indicate miR-362-5p and miR-362-3p binding sites, respectively, in each gene.

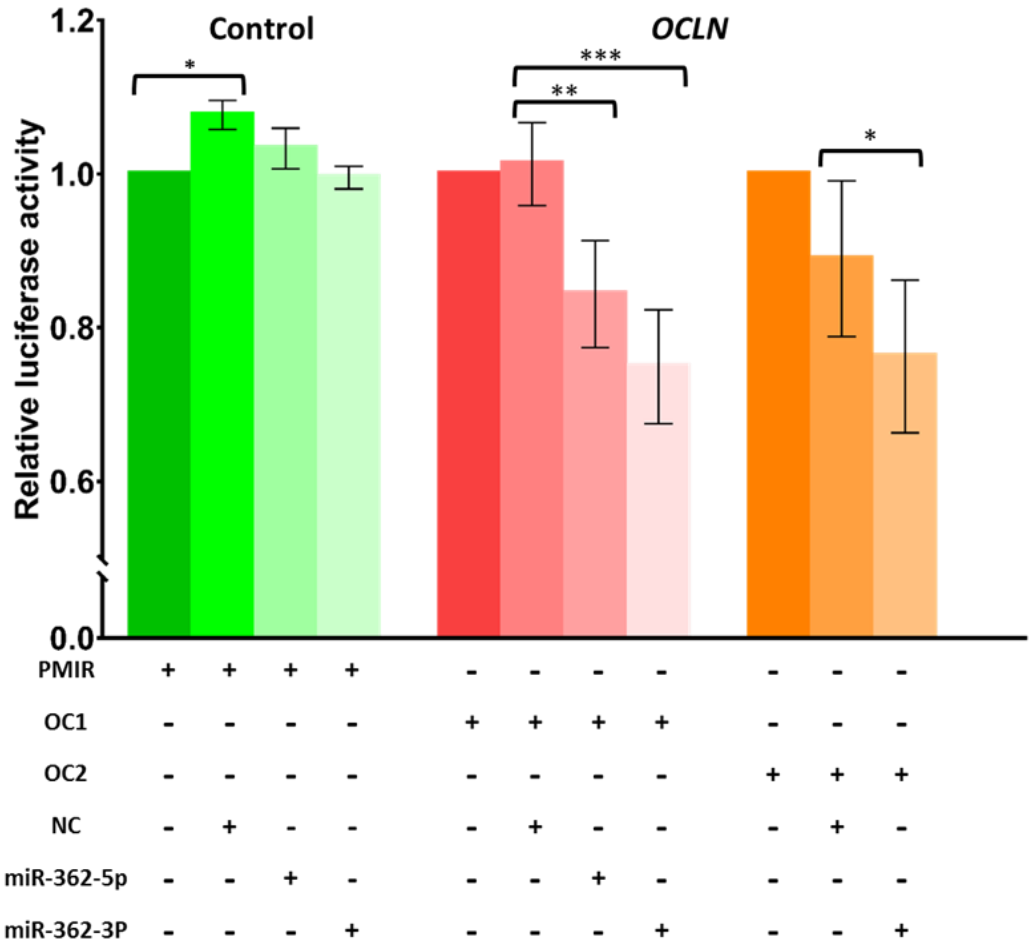

Figure 4.19 Validation of miR-362-5p/-3p direct targeting of *OCLN* in luciferase assays. The blank pmiRGlo and 3'-UTR luciferase constructs, coded OC1 and OC2 (see Figure 4.14) were each transfected alone, or co-transfected with the miR-362 mimic, or a validated negative control (NC) in MCF-7 cells prior to dual luciferase assays.*p <0.05, **p <0.01, and ***p <0.001.

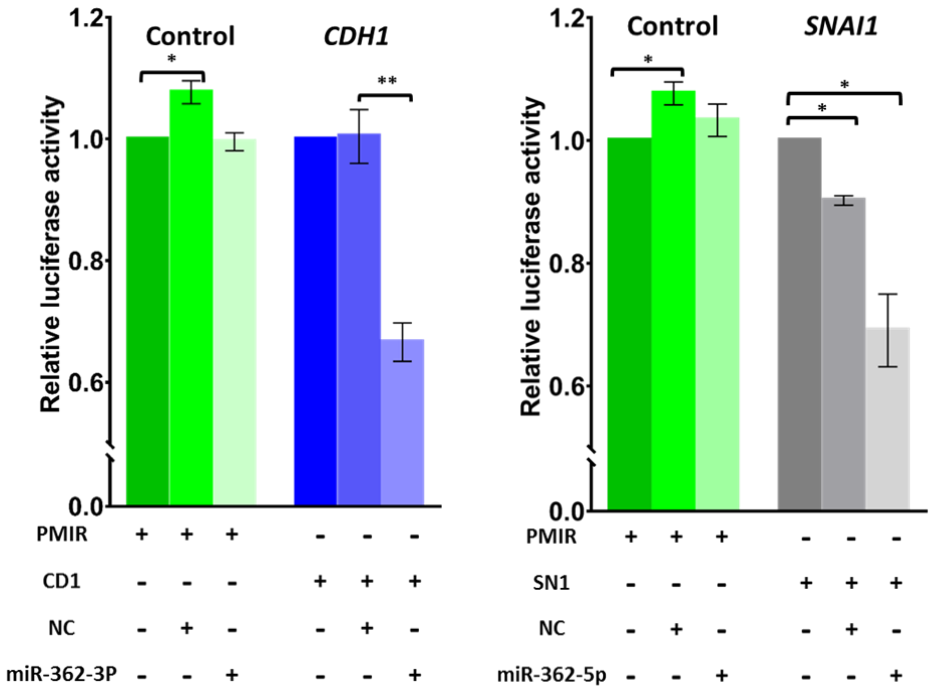

Figure 4.20 Validations of miR-362-5p/-3p direct targeting *CDH1* and *SNAI1*, respectively, in luciferase assays. The blank pmiRGlo and 3'-UTR luciferase constructs designated, CD1 and SN1 (Figure 4.14) were transfected alone, or co-transfected with the miR-362-5p/-3p mimic or a validated negative control (NC), in MCF-7 prior to dual luciferase assays. *p<0.05 and **p<0.01.

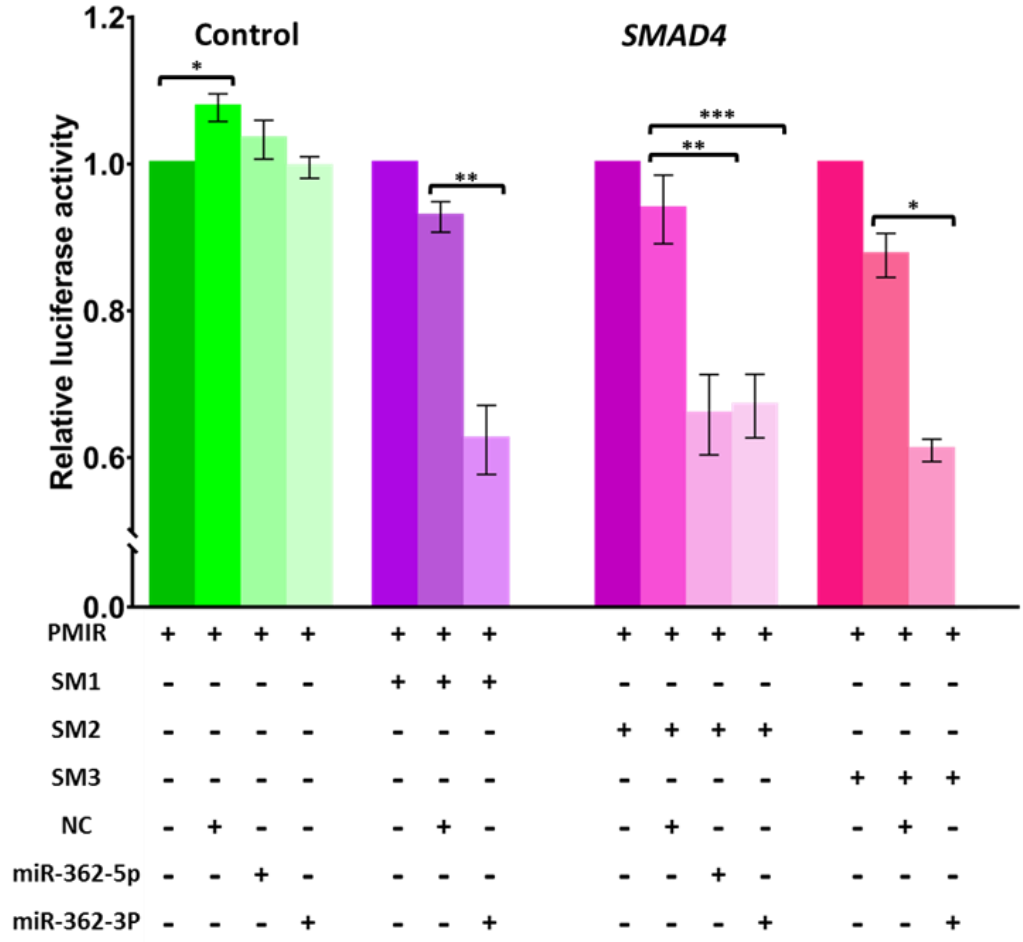

Figure 4.21 Validation of miR-362-5p/-3p direct targeting SMAD4 in luciferase assays. The blank pmiRGlo and 3'-UTR luciferase constructs coded SM1, SM2 and SM3 (Figure 4.14) were transfected alone, or co-transfected with the miR-362-5p/-3p mimic, or a validated negative control (NC), in MCF-7 prior to dual luciferase assays. *p<0.05,**p<0.01,and***p<0.001.

4.15miR-362-3p/5p Promotes Cell Migration and Invasion *in vitro*

Metastasis involves migration of cancer cells from a primary tumour site to secondary organs and invasion of extracellular matrix (ECM) of the secondary sites to establish secondary tumours.

To investigate the biological function of miR-362-5p/-3p in influencing cell migration, wound-healing and transwell migration assays were performed with the MCF7 cells. MCF7 cells were left untreated, or transfected with either the NC, the miR-362-3p or miR-362-5p mimics respectively before wound-healing assays. Wound closure of each group was determined at 0 h and after 24 h (Figure 4.22). Transfection with the miR-362-5p/-3p mimics significantly enhanced the ability of MCF7 cells to migrate from one end of the 'wound' to the other, as indicated by a 1.5-fold reduction of the wound area relative to the NC-transfected or un-transfected groups (Figure 4.22B). The transwell migration assay also demonstrated that miR-362-5p/-3p overexpression resulted in significant 2- and 1.7-fold increases in the number of migrated cells, respectively, compared with the negative-control cells (Figure 4.23B). These results suggest that miR-362-5p/-3p significantly promote cellular migratory ability.

Furthermore, the effects of miR-362-5p/-3p overexpression on the invasive ability of HCT-15 cells were assayed in transwell invasion chambers

coated with Geltrex. The number of HCT-15 cells invaded through the transwell chamber was significantly increased by at least 3-fold following transfection of the miR-362-5p/-3p mimics when compared to NC-transfected or untreated cells (Figure 4.24B).

Collectively, the data showed that miR-362-5p/-3p may function in promoting cell migration and invasion *in vitro*.

.

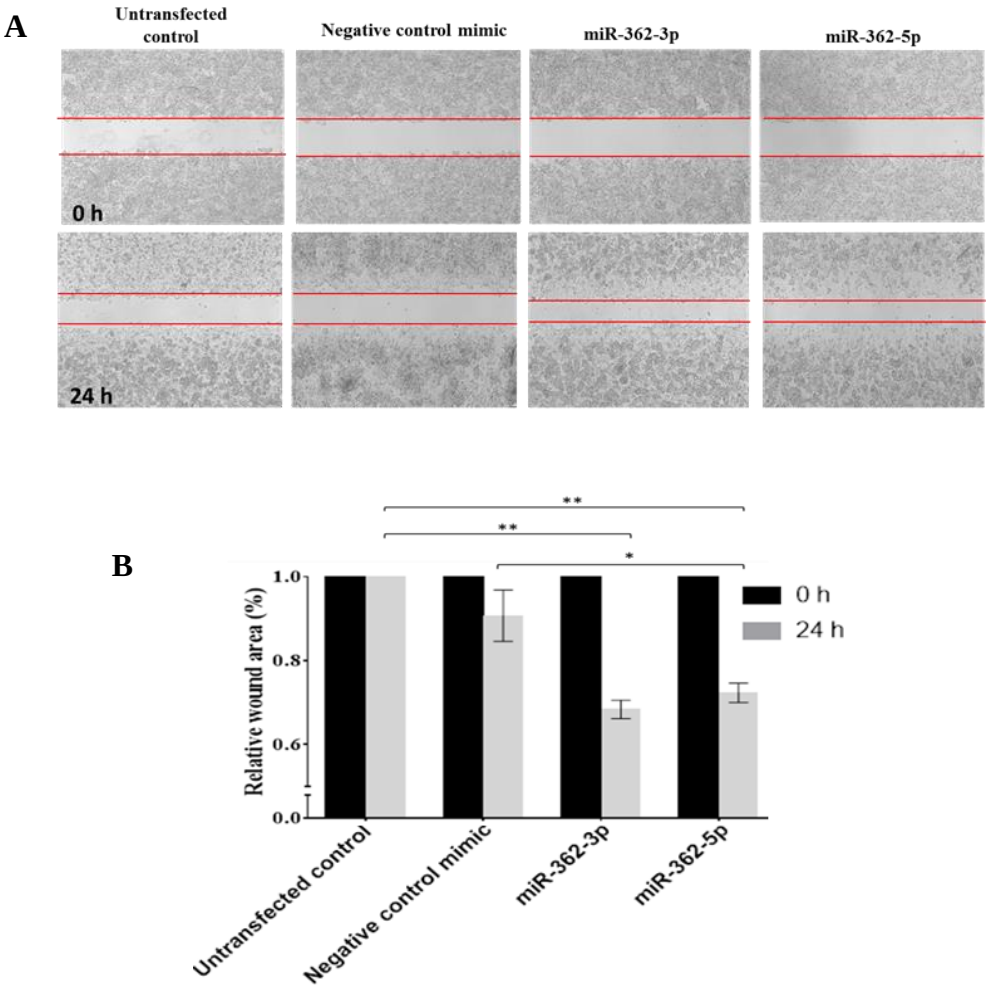

Figure 4.22 Effects of miR-362-5p/3p overexpression on cellular migration. Wound healing assay of MCF-7 cells untransfected or transfected with miR 362-5p/-3p mimics, or a negative control mimic (NC). A. Wound closure of each group was captured at 0 h and after 24 h. B. Quantitative analysis of the gap between the migrating cells expressed as percentage relative to the the initial wound area. Data are presented as mean ± SEM from three independent experiments relative to untransfected or negative control groups. *p< 0.05, **p< 0.01.

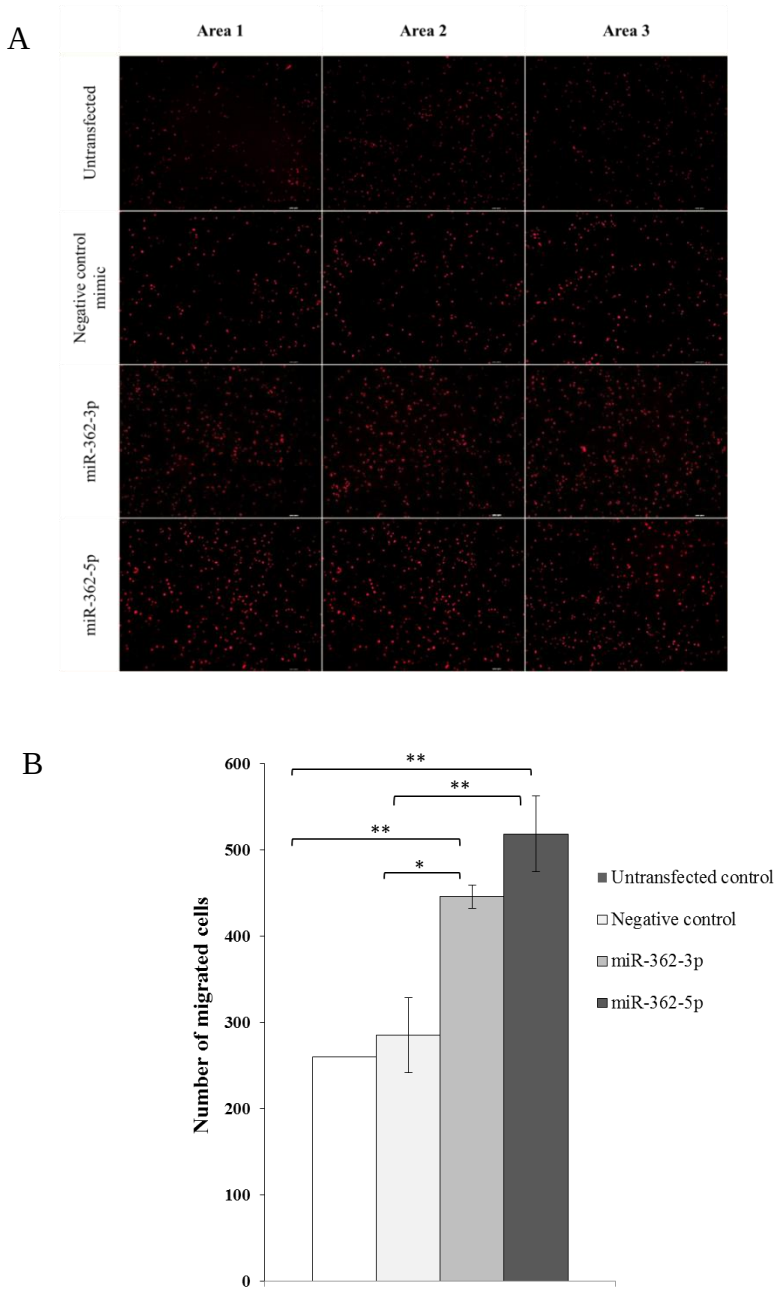

Figure 4.23 Ectopic expression of miR-362-5p/-3p increases cellular migration ability. Migration of MCF-7 cells untransfected or transfected with a negative control (NC), or miR-362-5p/3p for 48 h was analysed using transwell migration assay. A. Representative images were selected for each group. B. Quantitative analysis of cell migration in each treatment group. The average counts of the migrated cells were derived from five random microscopic fields. Data are presented as mean ± SD from three independent experiments compared to untransfected or negative control groups. *p< 0.05, **p< 0.01.

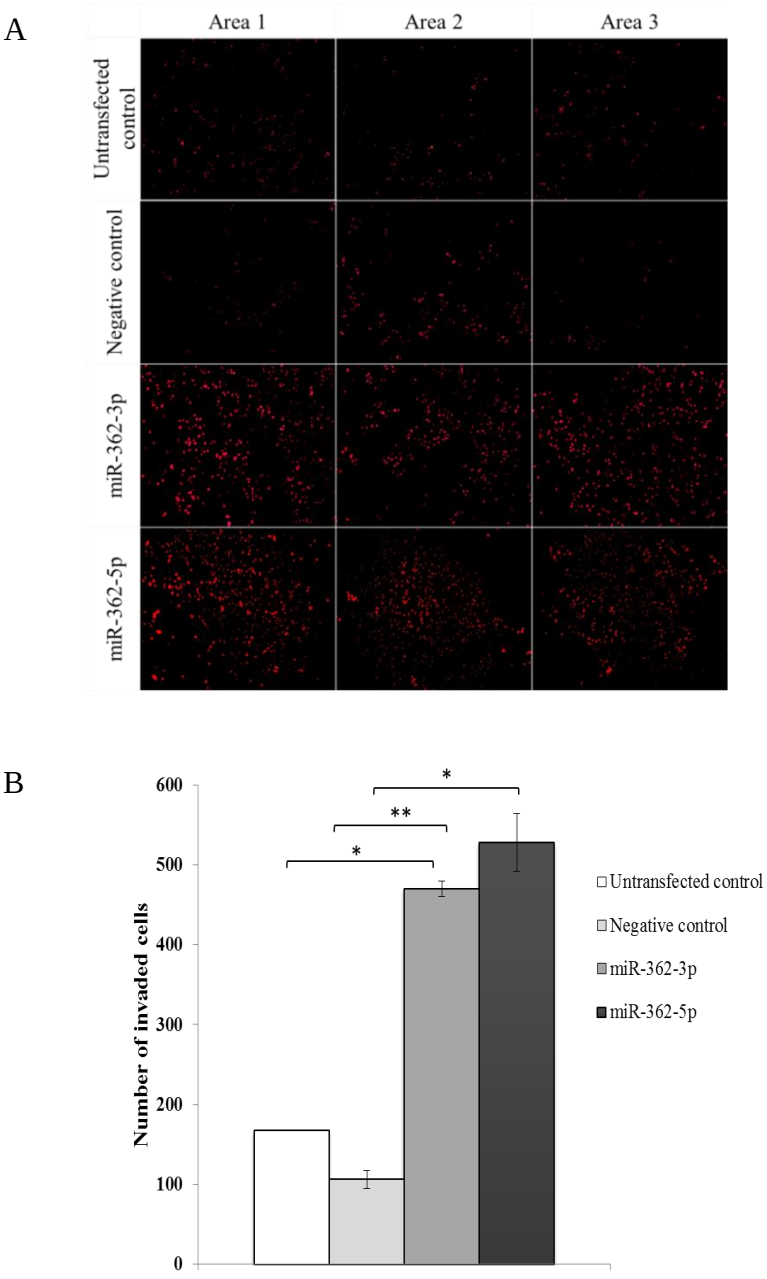

Figure 4.24 miR-362-5p/-3p overexpression enhances cellular invasion. The effects of miR-362-5p/-3p transfection on HCT-15 cells were evaluated using invasion assay after 24 h. The number of invaded cells adhering to the lower surface of the chamber was counted and analysed statistically. A. Representative images were selected for each group. B. Bar chart represents quantitative analysis of each treatment group. The average counts of invaded cells were derived from five random microscopic fields. Data are presented as mean ± SD from three independent experiments compared to untransfected or negative control groups. *$p< 0.05$, **$p< 0.01$.

CHAPTER 5

DISCUSSION

5.1 Partial Reprogramming Status of CRC-iPCs

The CRC-iPCs that were used in this study have acquired partial reprogramming status based on several lines of evidence: (i) the iPC colonies lacked clearly defined borders when compared to the ESC cells (Hiew et al., 2018).

(ii) Expression of pluripotency genes was generally down-regulated in reprogrammed CRC-iPC cells and restored back to approximately parental levels on re-differentiation (Hiew et al., 2018). In other reports, partially reprogrammed somatic and cancer cells often showed down-regulation of endogenous pluripotency genes (Wei Wang et al., 2011; Câmara et al., 2017).

(iii) The CRC-iPC cells also showed distinct differences in the miRNA profiles compared with the pluripotent H9 ESC cells, while retaining some cancerous molecular signature (Figure 4.3).

(iv) The absence of ESC-specific miRNAs, such as miR-302/367 cluster in the CRC-iPCs, which have been demonstrated to reprogramme both somatic and cancer cells (Kuo and Ying, 2012).

(v) The CRC-iPC cells failed to form teratoma *in vivo* when inoculated in nude mice (Choo et al., unpublished data;), which is a gold standard for assessing the pluripotency of fully reprogrammed human cells (Nelakanti et al., 2015). Based on previous findings, partially reprogrammed cancer cells often failed to generate teratoma, suggesting that restricted pluripotency may be commonly observed in iPCs (Oshima et al., 2014; Islam et al., 2015; Câmara et al., 2017).

(vi) Western blot analysis also showed contradictory EMT/MET gene expression profiles in the reprogrammed CRC-iPC cells (Figure 4.11). MET is crucial for early phase of somatic cell reprogramming (Samavarchi-Tehrani et al., 2010) whereas inhibition of EMT enhances reprogramming efficiency (Maherali and Hochedlinger, 2009). Western blot data of this work revealed that the four EMT and MET proteins analysed were not consistently down-regulated or upregulated in the reprogrammed CRC-iPC clones (Figure 4.11), indicating that the four CRC-iPC clones posed an intermediate state of epithelial/mesenchymal (E/M) hybrid phenotype (Jolly, 2015). Moreover, expression of the EMT/MET proteins was also generally reversed on re-

differentiation in post-iPCs, suggesting that the E/M hybrid state acquired is not permanent and is reversible, possibly via epigenetic regulation.

In somatic cells, the reprogramming process complies with a continuous stochastic model, in which all cells are transduced at equal probability into a pluripotent state (Yamanaka, 2009). In the context of cancer reprogramming, intrinsic cellular heterogeneity and the presence of oncogenic mutations, chromosomal aberrations and accumulation of DNA damages may have prevented complete successful reprogramming, to all the cancer cells, in resetting the cancer-epigenome to that resembling an embryonic stem cell-like state (Ramos-Mejia et al., 2012; Izgi et al., 2017). Therefore, multiple reports (Oshima et al., 2014; Islam et al., 2015; Câmara et al., 2017), and including data in this thesis, have shown that complete cancer-cell reprogramming is limited to certain cancer cell types, or in the same cancer type, may also be limited to some and not all clones under the same reprogramming treatment. Hence, limited acquired pluripotency may be a common feature in reprogramming cancer cells.

The status of partial reprogramming and the E/M hybrid phenotype of the CRC-iPCs observed in the study highlighted challenges in obtaining fully reprogrammed human cancer cells. Taken together, in line with other previous studies, the CRC-iPC model supports the elite model of cancer reprogramming in which only a small population of cancer cells can be fully reprogrammed (Lai et al., 2013).

5.2 CRC Reprogramming in Modelling Colorectal Cancer Development

CRC, as in all cancers, is a multistage cancer. the CRC-iPCs generated may be differentiated to generate cells of early stages of tumorigenesis, which are still associated with the acquired early-stage genetic mutations. To date, a few studies have reported elucidation of disease progression using the iPC derived from malignant cancers (Carette et al., 2010; Kumano et al., 2012; Kim et al., 2013). For example, CML-derived iPCs was found to be imatinib-resistant (Carette et al., 2010). However, re-differentiation of CML-derived iPCs to haematopoetic cells recapitulated the disease phenotype and the differentiated cells reverted to being susceptible to imatinib, exemplifying the acquisition of cancer phenotype during hematopoietic differentiation (Kumano et al., 2012). Besides, enhanced drug sensitivity and reduced tumour growth were reported in reprogrammed hepatocellular carcinoma (Koga et al., 2014) and colorectal cancer cells (Miyazaki et al., 2015) when compared to the respective parental cancer cells. These findings of diminished cancer malignancy support the hypothesis that cancer reprogramming, at least in some cases, reverses an advanced cancer stage to a less aggressive early disease stage (Kim et al., 2013; Papapetrou, 2016).

Furthermore, given that cancer-cell population is heterogeneous, cancer-cell reprogramming is a process of clonal selection in which distinct clones at different stages of cancer development can be generated and identified on the basis of their distribution in the original tumour (Papapetrou,

2016). As reflected in our CRC-iPC model, the two distinct clones generated from each of the respective CRC cell line that were included in this study also showed different patterns of EMT/MET gene regulation (Figure 4.11). Hence, the effects of dysregulation of specific oncogenes or tumour suppressor genes, and other cancer-associated factors, in the CRC tumorigenicity process can be elucidated via cancer-cell reprogramming followed by appropriate iPC differentiation.

5.3 Role of EMT/MET in Regulation of the Reprogramming Process

The process of reprogramming involves multiple steps controlled by the core pluripotency factors which gradually induce an ESC-like gene expression while suppressing the developmental programme. MET is activated during the initial phase of reprogramming of somatic cells (David and Polo, 2014), which is exemplified by up-regulation of MET markers such as E-cadherin (CDH1) and occludin (OCLN), leading to an epithelial-like morphology with the gain of cell polarity and the formation of tightly packed cell clusters (Li et al., 2014). Besides, the epithelial gene, CDH1 was reported to be able to functionally replace OCT4 in somatic-cell reprogramming (Redmer et al., 2011). In addition, transcription of members of the miR-200 family, activated by promoter binding of OCT4 and SOX2, was shown to promote MET via targeting and suppressing the EMT-related gene ZEB1 to facilitate iPSC formation (G.Wang et al., 2013). These reports show that triggering MET is favourable for the reprogramming process. On the other hand, the reversed

EMT process counteracts the de-differentiation process. Suppression of the EMT-inducing TGF-β pathway was demonstrated to improve reprogramming efficiency (Maherali and Hochedlinger, 2009), as shown by promoted reprogramming by the miR-302/-367 cluster by reducing the TGF-β–induced phosphorylation of SMAD2 and SMAD3 (Subramanyam et al., 2011; Balzano et al., 2018).

However, EMT activation has also been associated with the acquisition of stem-cell properties in cancer stem cells (CSCs), likely playing a compensatory role to MET in reprogramming towards cellular pluripotency (Liu and Fan, 2015). As examples, the EMT-associated genes, SNAI1 and VIM have been demonstrated to successfully reprogramme both mouse and human somatic cells by targeting the well-known reprogramming barriers, p53 and let-7 respectively, indicating that EMT may serve as alternative route in cellular reprogramming (Unternaehrer et al., 2014; Kong et al., 2014). In line with this notion, sequential introduction of the OSKM reprogramming factors was also observed to increase iPSC efficiency by inducing a temporary EMT response followed by MET in somatic-cell reprogramming (Liu et al., 2013).

In summary, the association of stemness and the regulation of both the EMT and MET processes in a context-dependent manner have been reported by different studies; the data show that dynamic transition between EMT and MET is critical for cellular reprogramming.

5.4 Association of Stemness with Epithelial/Mesenchymal (E/M) Hybrid Phenotype

Current models suggest the existence of a dynamic balance between both EMT and MET in the regulation of stemness and cellular plasticity (Jolly, 2015). Due to the dynamic plasticity, besides having cells with fixed mesenchymal (M) or epithelial (E) phenotypes, cells in a hybrid EMT/MET (E/M) state, or also referred to as partial EMT, can be encountered when transition occurs in both directions simultaneously. Such E/M hybrid states have been associated with higher stemness (Nieto et al., 2016; Forte et al., 2017).

Cells in the hybrid E/M state retain both epithelial (cell–cell adhesion) and mesenchymal (migration) characteristics, therefore allowing collective cell migration (Jolly et al., 2015). Recent studies showed that co-expression of both epithelial and mesenchymal markers promotes multiple stemness characteristics such as spheroid formation and tumour-initiating abilities in breast, ovarian and prostate cancer stem cells (Strauss et al., 2011; Grosse-Wilde et al., 2015; Ruscetti et al., 2015) . In another study the E/M hybrid state was induced in trophoblast stem (TS) cells comparable to that of invasive breast cancer cells, and the results indicated increased stemness traits, such as self-renewal, multi-lineage potential and cell motility in the hybrid state (Jordan et al., 2011).

Beside tumour progression, the E/M hybrid phenotype has seen observed under normal physiological condition. In skin injury, basal epithelial cells undergo partial EMT to temporarily suppress the adherent immotile phenotype and confer the cells migratory, invasive and proliferative traits , which subsequently contribute to wound healing (Shaw and Martin, 2016). Similar phenomena are also observed in adult hepatic and renal stem cells, which acquire hybrid E/M state upon tissue injury to facilitate repair and regeneration (G. et al., 2011; Conigliaro et al., 2013).

The EMT and MET processes are co-regulated by numerous epigenetic and transcription factors as well as miRNAs to result in changes in gene and protein expression patterns corresponding to a particular cell fate. For instances, Let7/Lin28 and miR-200/ZEB are proposed to control the core EMT transcriptional network (Ye et al., 2015; Forte et al., 2017). The E/M hybrid state exists in cells showing high expression of Let7/miR-200 and low expression of Lin28/ZEB (Jolly et al., 2015). In this study, up-regulated expression of miR-200 in CRC-iPCs may modulate an epithelial transition by suppressing ZEB whereas a higher Let7 expression may in turn inhibit Lin28, hence causing cells to transit towards mesenchymal-like state (see Appendix D). Therefore, along with the interplay with other mediators, the equilibrium between miRNAs and the EMT/MET-related target genes plays a fundamental role in determining the balance between epithelial and mesenchymal transitions.

In brief, the concept of a dynamic "intermediate state" between EMT and MET may reconcile contradictory results reported in different studies and highlighting the likelihood that intermediate states are more likely to be associated with stemness features in both normal and transformed cells.

5.5 MiR-362-5p/-3p Promotes an E/M Hybrid Phenotype and Cellular Migration and Invasion

EMT is activated in the early step of cancer metastasis where cancer cells lose their cell–cell adhesion and gain the motility to migrate and invade across the endothelial lamina in a process called intravasation. The cancer cells are then distributed in the bloodstream as circulating tumour cells (CTCs), until they reach secondary metastatic sites. In the new stromal environment, MET is re-activated for cell-to-cell attachment to facilitate the formation of secondary tumours, completing the cascade of "metastasis-invasion" (Tsai and Yang, 2013).

The sequential EMT-MET cascade, or the relationship between EMT, MET and cancer cell plasticity, was reported in breast cancer stem cells (CSCs), in which the CSCs isolated were categorised into mesenchymal–like ($CD44^{+}/CD24^{-}$) or epithelia-like ($ALDH^{+}$ $CD44^{high}$ $EPCAM^{high}$) based on modulation of cell surface markers (Biddle et al., 2011; Liu et al., 2014). Previous studies showed that epithelial-like CSC were capable of giving rise to

two distinct cell populations with either epithelial or mesenchymal-like phenotypes *in vitro* (Biddle et al., 2011; Liu et al., 2014) as well as showing increased self-renewal and stem-cell properties such as the formation of mammospheres (Celià-Terrassa et al., 2012). However, the plasticity to switch between two lineages was not observed in the mesenchymal-like CSC population (Biddle et al., 2011; Liu et al., 2014). These findings support the notion that not all CSCs display the same extent of EMT properties.

MiR-362-5p/-3p overexpression identified in the CRC-iPCs down-regulated expression of both the MET genes (CDH1 and OCLN) as well as SMAD4, which is a central mediator of TGF-β-induced EMT (Figure 5.1). The inconsistent EMT/MET gene expression may result in inclination of cancer cells towards an E/M hybrid phenotype. As mentioned in the previous paragraph, an E/M hybrid phenotype has also been observed in cancer stem cells as well as in circulating tumour cell clusters (CTCs), which may lead to tumour relapse and metastasis (Barriere et al., 2015).

The intermediate E/M state allows cells to retain both the epithelial (cell attachment) and mesenchymal (motility) phenotypes, to facilitate cluster migration (Jolly, 2015). The collective sheets of cells show higher plasticity to switch between a proliferative mode for colonisation while retaining the invasive mode for subsequent metastasis (Bednarz-Knoll et al., 2012). Moreover, the cells are resistant to anoikis as the hybrid cells move in clusters

(Aceto et al., 2014; Joosse et al., 2015). Another advantage is that extravasation into distant site is more favourable as cell clusters are more likely to be trapped in narrow blood vessels (Joosse et al., 2015). Cells in E/M hybrid state have also been reported to have higher tumour-initiating and metastatic potentials than complete EMT phenotype (Hou et al., 2012).

Collectively, this work presents evidence that partially reprogrammed CRC-iPCs may have elicited a hybrid E/M phenotype. In addition, miR-362-5p/-3p overexpression also produced results consistent with an E/M hybrid phenotype as well as enhanced cell migration and invasion. The higher plasticity in tumour cells to convert between the epithelial and mesenchymal states may provide the cells better adaptive strategies in response to stress conditions.

Besides, our results also showed that miR-362 regulation is differentially altered by the reprogramming process and that miR-362 are regulators of the EMT/MET genes, thus clinical variations of miR-362 expression in different cancers (Figure 4.11) may be used as a diagnostic and/or prognostic biomarker tool to predict disease outcome or recurrence. Likewise, miR-362 may serve as a cancer therapeutic target as it affects cancer cell migration and invasion by regulating the EMT/MET genes in CRC.

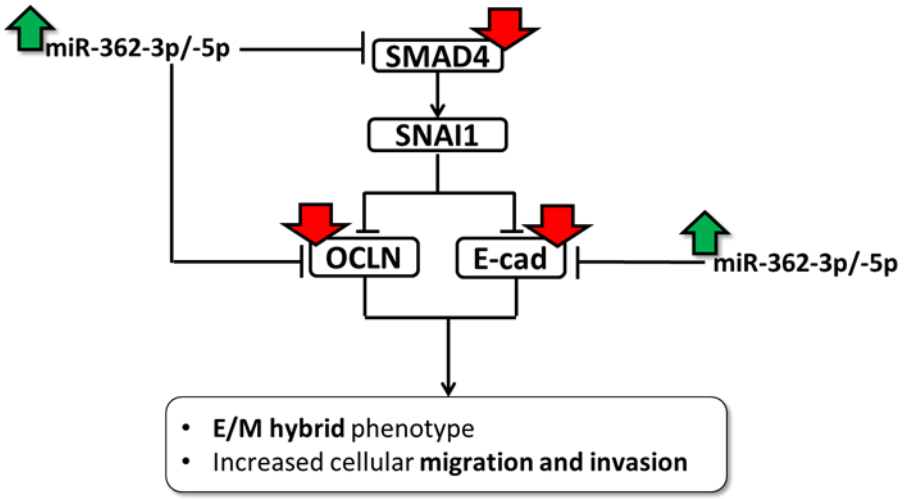

Figure 5.1 A proposed scheme of miR-362-5p/-3p overexpression in the regulation of cellular migration and invasion. Scheme was modified from Miyazono et al., 2009. MiR-362-5p/-3p promotes an E/M hybrid phenotype by down-regulating both MET-related genes (OCLN and E-cadherin) and the EMT marker SMAD4, resulting in enhanced cellular migration and invasion. See text (section 5.4) for further description of the proposed scheme.

5.6 Down-regulation of MiR-362-5p/-3p Activates MET, Which is Required For the Initial Stage of Reprogramming in CRC-iPCs

The core pluripotency factors OSKM have previously been demonstrated to inhibit various factors of the TGF-β signalling pathway (Li et al., 2010). OCT4 and SOX2 suppress the EMT transcription factor SNAI1, and c-Myc inhibits TGF-β receptors, causing the up-regulation of epithelial genes such as E-cadherin (Li et al., 2010; Samavarchi-Tehrani et al., 2010). Hence, OSKM down-regulation may have resulted in the activation TGF-β signalling pathway, which in turns up-regulates SNAI1 expression, thereby promoting EMT transition (Figure 5.2) (Hiew et al., 2018).

In this study, miR-362-5p/-3p inhibition was observed to down-regulate the EMT-inducer SNAI1 expression as well as promote MET by up-regulating the expression of both the MET-related genes, CDH1 and OCLN (Figure 5.2), to enhance the early phase of the reprogramming process in CRC-iPCs (Samavarchi-Tehrani et al., 2010; David and Polo, 2014).

Cellular reprogramming has been reported to be associated with the loss of mesenchymal signatures such as SNAIL1 marker, and the acquisition of epithelial signatures including E-cadherin marker (J.Chen et al., 2012). Based on a previous study, the SNAI1-SMAD4 complex promotes the TGFβ-regulated decline of E-cadherin expression by binding to the multiple enhancer

regulatory sequence (E-boxes) within the E-cadherin gene (Lamouille et al., 2014). On the contrary, E-cadherin and occludin are two MET endpoint markers required for establishing cell to cell adhesion and contact crucial for the establishment of the iPSC phenotype (Chen et al., 2010; Redmer et al., 2011; Faiola et al., 2017). Overexpression of E-cadherin has previously been shown to replace OCT4 and enhances reprogramming efficiency (Redmer et al., 2011) whereas knocking down of endogenous E-cadherin or blocking the E-cadherin extracellular binding domain reduces iPSC formation (Chen et al., 2010).

The success of resetting the epigenome of cancer cells to that of ESC is multifactorial. Hence, there exists a dynamic interplay between multiple targeting miRNAs and other regulatory factors to confer either an epithelial or mesenchymal phenotype to the CRC-iPCs. Transition between MET and EMT, linked by expression of pluripotency genes and miRNAs, may play a vital role in inducing pluripotency in cancer cells.

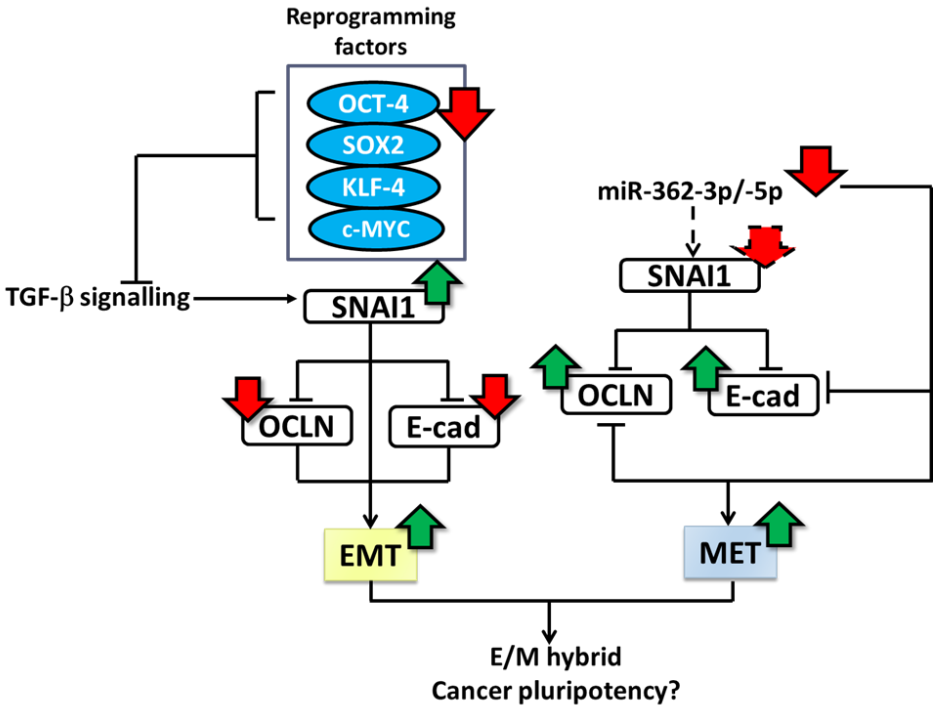

Figure 5.2. A proposed scheme of miR-362-5p/-3p involvement in the regulation of colorectal cancer cell reprogramming. Scheme was modified from Miyazono et al., 2009; Hiew et al., 2018**.** Green and red arrows indicate regulation of gene expression observed in this study. Blue oval shape indicates reprogramming factors whereas white rectangle box shows MET/EMT-related genes. In brief, down-regulation of reprogramming factors results in activation of TGF-β signalling, thus promoting EMT. Inhibition of miR-362-5p/-3p expression facilitates reprogramming by down-regulating SNAI1 and up-regulating MET-related genes (OCLN and E-cad), therefore promoting MET, a required process for initial reprogramming. See text (Section 5.5) for further description of the proposed scheme.

CHAPTER 6

CONCLUSION

6.1 Summary of Main Findings

In this study, genome-wide miRNA profiling analysis showed that 102 miRNAs were differentially expressed in the CRC-iPC cells upon reprogramming when compared with the parental CRCs. Hierarchical clustering analysis of the differentially expressed miRNAs revealed that the CRC-iPCs shared similarities with the parental cancer cells, suggesting retention of molecular signatures of the parental CRCs. Furthermore, CRC-iPC also shares miRNA profile similarities with pluripotent ESC, but with the absence of expression of numerous ESC-specific miRNAs, suggesting limited pluripotency. Based on bioinformatics analysis, the putative target genes of the differentially expressed miRNAs are predicted to be involved in suppression of apoptosis and regulation of cell migration. Moreover, reprogramming is also predicted to activate miRNAs targeting the TGF-β and PI3K-AKT signalling pathways in the CRC-iPC cells, linking with involvement of the EMT and MET processes. On western blot analysis, contradictory expression of selected EMT and MET proteins was observed in the CRC-iPC cells, suggesting an epithelial/mesenchymal (E/M) hybrid phenotype possibly elicited by partial reprogramming.

Among the differentially expressed miRNAs analysed, the EMT genes, SMAD4 and SNAI1, and the MET genes, CDH1 and OCLN, are all targeted by the down-regulated miR-362-5p and -3p in CRC-iPCs. Overexpression of miR-362-5p/-3p mimics down-regulated both EMT and MET proteins, except SNAI1, consistent with an E/M hybrid phenotype. On the contrary, inhibition of miR-362-3p/-5p, as was shown by miRNA profiling to be down-regulated in CRC-iPCs, enhanced MET, an event that facilitates the early stage of reprogramming. Direct targeting of miR-362-3p/-5p on the four EMT/MET genes was further validated by luciferase assays. The biological role of miR-362-3p/-5p was also elucidated. Overexpression of miR-362-3p/-5p significantly enhanced cell migration and invasion, supporting that miR-362-3p/-5p affects cellular migration, invasion and CRC reprogramming via targeting and regulating EMT/MET genes.

6.2 Conclusions

In conclusion, data of this study showed that CRC-iPCs cells were only partially reprogrammed, highlighting challenges faced by fully reprogramming cancer cells due to accumulated genetic and epigenetic modifications. Partial reprogramming may have elicited an E/M hybrid phenotype in the CRC-iPC cells examined. The findings that miR-362-5p/-3p, as identified to be down-regulated in CRC-iPCs, failed to regulate EMT and MET gene expression in a consistent and opposing manner, echo an E/M hybrid phenotype as found in the CRC-iPC cells. Nonetheless, miR-

362-5p/-3p over-expression led to increased cellular migration and invasion by targeting and regulating the EMT/MET genes, in line with, miR-362-5p/-3p down-regulation, in the CRC-iPCs, and possible decreased cancer phenotypes on cancer-cell reprogramming.

6.3 Limitation and Future Studies

Results in this study suggested that partial reprogramming induced an E/M hybrid phenotype in the CRC-iPCs. However, only two genes were selected for representation of each of the EMT and MET groups. To further validate and confirm the hypothesis, other EMT genes, such as N-cadherin and Fibronectin, and MET genes, such as claudins and cytokeratin, are best included.

Cancer stem cells (CSCs) play a crucial role in tumour metastasis and recurrence (Pan et al., 2017). Besides the conventional spheroidal-enrichment culture, CSC-like cells have also been generated from cancer tissues through iPSC technology, as in the work presented in this thesis. The induced pluripotent cancer cells, some of which may not have gone through complete reprogramming, show increased sphere formation ability, enhanced chemoresistance and colon CSC marker expression (Oshima et al., 2014). To further establish a study model for the early stages of CRC tumorigenesis, CRC-iPC cells may be further differentiated into intestinal lineages by lineage-specific differentiation using Activin A (Wang et al., 2015) and Wnt/β-catenin signalling activation factors (Ogaki et al., 2013) for the elucidation of

dysregulation of CSC-related genes, including EMT/MET genes, underlying CRC pathogenesis and metastasis. Other studies have also reported the lineage-directed differentiation of reprogrammed cancer cells (Carette et al., 2010; Miyoshi et al., 2010; Kim et al., 2013).

Moreover, another finding in this study that miR-362-5p/-3p overexpression enhanced cellular migration and invasion was limited to *in vitro* observation; *in vivo* experiments may further be conducted to reflect or mimic more realistically tumour growth and interactions with microenvironment. One way to achieve this is a mouse model to further assess the efficacy of miR-362-3p/-5p in modulating the cancer-cell metastasis *in vivo*. Orthotropic implantation of CRC cells, in which the miR-362-3p/-5p expression has been stably knocked-down, can be performed in immune-deficient BALB/c nude mice, followed by analysis of the effects on the metastatic ability and local tumour growth and metastatic ability *in vivo.*

REFERENCES

Aceto, N. et al., 2014. Circulating Tumour Cell Clusters Are Oligoclonal Precursors of Breast Cancer Metastasis. *Cell*, 158(5), pp.1110–1122.

Al-Sohaily, S. et al., 2012. Molecular pathways in colorectal cancer. *Journal of Gastroenterology and Hepatology*, 27(9), pp.1423–1431.

Andrés-León, E., Cases, I., Alonso, S. and Rojas, A.M., 2017. Novel miRNA-mRNA interactions conserved in essential cancer pathways. *Scientific reports*, 7(1), p.46101.

Anokye-Danso, F. et al., 2011. Highly Efficient miRNA-Mediated Reprogramming of Mouse and Human Somatic Cells to Pluripotency. *Cell Stem Cell*, 8(4), pp.376–388.

Anokye-Danso, F., Snitow, M. and Morrisey, E.E., 2012. How microRNAs facilitate reprogramming to pluripotency. *Journal of Cell Science*, 125(18), pp.4179–4787.

Balzano, F. et al., 2018. MiR200 and MiR302: Two big families influencing stem cell behavior. *Molecules*, 23(2).

Barriere, G. et al., 2015. Epithelial Mesenchymal Transition: a double-edged sword. *Clinical and translational medicine*, 4, p.14.

Bartel, D.P., 2009. MicroRNAs: Target Recognition and Regulatory Functions. *Cell*, 136(2), pp.215–233.

Baumann, V. and Winkler, J., 2014. miRNA-based therapies: strategies and delivery platforms for oligonucleotide and non-oligonucleotide agents. *Future medicinal chemistry*, 6(17), pp.1967–84.

Bednarz-Knoll, N., Alix-Panabières, C. and Pantel, K., 2012. Plasticity of disseminating cancer cells in patients with epithelial malignancies. *Cancer and Metastasis Reviews*, 31(3–4), pp.673–687.

Bellam, N. and Pasche, B., 2010. TGF-β Signaling Alterations and Colon Cancer. In: *Cancer treatment and research*. pp. 85–103.

Bernhardt, M. et al., 2017. Melanoma-Derived iPCCs Show Differential Tumourigenicity and Therapy Response. *Stem Cell Reports*, 8(5), pp.1379–1391.

Biddle, A. et al., 2011. Cancer Stem Cells in Squamous Cell Carcinoma Switch between Two Distinct Phenotypes That Are Preferentially Migratory or Proliferative. *Cancer Research*, 71(15), pp.5317–5326.

Brabletz, T., 2012. To differentiate or not — routes towards metastasis. *Nature Reviews Cancer*, 12(6), pp.425–436.

Brenner, H., Kloor, M. and Pox, C.P., 2014. Colorectal cancer. *The Lancet*, 383(9927), pp.1490–1502. Brosens, L.A.A., Offerhaus, G.J.A. andGiardiello, F.M., 2015. Hereditary Colorectal Cancer: Genetics and Screening. *The Surgical clinics of North America*, 95(5), pp.1067–80.

Calon, A. et al., 2012. Dependency of colorectal cancer on a TGF-β-driven program in stromal cells for metastasis initiation. *Cancer cell*, 22(5), pp.571–84.

Câmara, D.A.D. et al., 2017. Murine melanoma cells incomplete reprogramming using non-viral vector. *Cell Proliferation*, 50(4), pp.1–10.

Câmara, D.A.D., Mambelli, L.I., Porcacchia, A.S. and Kerkis, I., 2016. Advances and challenges on cancer cells reprogramming using induced pluripotent stem cells technologies. *Journal of Cancer*, 7(15), pp.2296–2303.

Cao, H. et al., 2015. Epithelial-mesenchymal transition in colorectal cancer metastasis: A system review. *Pathology Research and Practice*, 211(8), pp.557–569.

Carette, J.E. et al., 2010. Brief report Generation of iPSCs from cultured human malignant cells. *Blood*, 115(20), pp.4039–4042.

Celià-Terrassa, T. et al., 2012. Epithelial-mesenchymal transition can suppress major attributes of human epithelial tumour-initiating cells. *The Journal of clinical investigation*, 122(5), pp.1849–68.

Chang, Y.Y. et al., 2015. Deregulated microRNAs in triple-negative breast cancer revealed by deep sequencing. *Molecular Cancer*, 14(1), pp.1–13.

Chapman, H.A., 2011. Epithelial-Mesenchymal Interactions in Pulmonary Fibrosis. *Annual Review of Physiology*, 73(1), pp.413–435.

Chen, J. et al., 2011. BMPs functionally replace Klf4 and support efficient reprogramming of mouse fibroblasts by Oct4 alone. *Cell research*, 21(1), pp.205–12.

Chen, J., Han, Q. and Pei, D., 2012. EMT and MET as paradigms for cell fate switching. *Journal of Molecular Cell Biology*, 4(2), pp.66–69.

Chen, M.L., Liang, L.Sen and Wang, X.K., 2012. miR-200c inhibits invasion and migration in human colon cancer cells SW480/620 by targeting ZEB1. *Clinical & experimental metastasis*, 29(5), pp.457–69.

Chen, T. et al., 2010. E-cadherin-mediated cell-cell contact is critical for induced pluripotent stem cell generation. *Stem cells (Dayton, Ohio)*, 28(8), pp.1315–25.

Chi, Y. et al., 2016. Interferon alters the microRNA profile of umbilical cord derived mesenchymal stem cells. *Molecular Medicine Reports*, 14(5), pp.4187–4197.

Chi, Y. and Zhou, D., 2016. MicroRNAs in colorectal carcinoma - from

pathogenesis to therapy. *Journal of Experimental & Clinical Cancer Research*, 35(1), p.43.

Choi, Y.J. et al., 2011. miR-34 miRNAs provide a barrier for somatic cell reprogramming. *Nature cell biology*, 13(11), pp.1353–60.

Choo, K.B. et al., 2014. MicroRNA-5p and -3p co-expression and cross-targeting in colon cancer cells. *Journal of biomedical science*, 21(1), p.95.

Choong, P.F. et al., 2014. Heterogeneity of osteosarcoma cell lines led to variable responses in reprogramming. *International journal of medical sciences*, 11(11), pp.1154–60.

Colussi, D., Brandi, G., Bazzoli, F. andRicciardiello, L., 2013. Molecular pathways involved in colorectal cancer: implications for disease behavior and prevention. *International journal of molecular sciences*, 14(8), pp.16365–85.

Conigliaro, A. et al., 2013. Evidence for a common progenitor of epithelial and mesenchymal components of the liver. *Cell death and differentiation*, 20(8), pp.1116–23.

Craene, B.De and Berx, G., 2013. Regulatory networks defining EMT during cancer initiation and progression. *Nature Reviews Cancer*, 13(2), pp.97–110.

David, L. and Polo, J.M., 2014. Phases of reprogramming. *Stem Cell Research*, 12(3), pp.754–761.

Dong, Y. et al., 2011. MicroRNA dysregulation in colorectal cancer: a clinical perspective. *British Journal of Cancer*, 104(6), pp.893–898.

Downward, J., 2004. PI 3-kinase, Akt and cell survival. *Seminars in Cell and Developmental Biology*, 15(2), pp.177–182.

Ehrig, K. et al., 2013. Growth inhibition of different human colorectal cancer xenografts after a single intravenous injection of oncolytic vaccinia virus GLV-1h68. *Journal of Translational Medicine*, 11(1), p.1.

Engelman, J.A., 2009. Targeting PI3K signalling in cancer: Opportunities, challenges and limitations. *Nature Reviews Cancer*, 9(8), pp.550–562.

Evans, J.P. et al., 2016. From mice to men: Murine models of colorectal cancer for use in translational research. *Critical Reviews in Oncology/Hematology*, 98, pp.94–105.

Faiola, F. et al., 2017. NAC1 Regulates Somatic Cell Reprogramming by Controlling Zeb1 and E-cadherin Expression. *Stem cell reports*, 9(3), pp.913–926.

Fan, F. et al., 2012. Overexpression of Snail induces epithelial-mesenchymal transition and a cancer stem cell-like phenotype in human colorectal cancer cells. *Cancer Medicine*, 1(1), pp.5–16.

Feng, Y.-H. and Tsao, C.-J., 2016. Emerging role of microRNA-21 in cancer.

Biomedical reports, 5(4), pp.395–402.

Ferlay, J. et al., 2010. Estimates of worldwide burden of cancer in 2008: GLOBOCAN 2008. *International Journal of Cancer*, 127(12), pp.2893–2917.

Forte, E. et al., 2017. EMT/MET at the crossroad of stemness, regeneration and oncogenesis: The Ying-Yang equilibrium recapitulated in cell spheroids. *Cancers*, 9(8), pp.1–15.

Fortunato, O. et al., 2014. Mir-660 is downregulated in lung cancer patients and its replacement inhibits lung tumourigenesis by targeting MDM2-p53 interaction. *Cell Death and Disease*, 5(12), pp.e1564-9.

Freeman, T.J. et al., 2012. Smad4-mediated signaling inhibits intestinal neoplasia by inhibiting expression of β-catenin. *Gastroenterology*, 142(3), p.562–571.e2.

G., S., Chandra, V., Phadnis, S. andBhonde, R., 2011. Glomerular parietal epithelial cells of adult murine kidney undergo EMT to generate cells with traits of renal progenitors. *Journal of Cellular and Molecular Medicine*, 15(2), pp.396–413.

Garg, M., 2015. Urothelial cancer stem cells and epithelial plasticity: current concepts and therapeutic implications in bladder cancer. *Cancer and Metastasis Reviews*, 34(4), pp.691–701.

Garnett, M.J. and McDermott, U., 2014. The evolving role of cancer cell line-based screens to define the impact of cancer genomes on drug response. *Current opinion in genetics & development*, 24, pp.114–9.

Geng, L. et al., 2014. MicroRNA-192 suppresses liver metastasis of colon cancer. *Oncogene*, 33(46), pp.5332–40.

Gest, C. et al., 2013. Rac3 induces a molecular pathway triggering breast cancer cell aggressiveness: Differences in MDA-MB-231 and MCF-7 breast cancer cell lines. *BMC Cancer*, 13.

Giorda, R. et al., 2009. Complex Segmental Duplications Mediate a Recurrent dup(X)(p11.22-p11.23) Associated with Mental Retardation, Speech Delay, and EEG Anomalies in Males and Females. *American Journal of Human Genetics*, 85(3), pp.394–400.

Golovko, D., Kedrin, D., Yilmaz, Ö.H. andRoper, J., 2015. Colorectal cancer models for novel drug discovery. *Expert Opinion on Drug Discovery*, 10(11), pp.1217–1229.

Granados-Romero, J.J. et al., 2017. Colorectal cancer: a review. *International Journal of Research in Medical Sciences*, 5(11), p.4667.

Gregory, R.I. et al., 2004. The Microprocessor complex mediates the genesis of microRNAs. *Nature*, 432(7014), pp.235–40.

Griffiths-Jones, S. et al., 2006. miRBase: microRNA sequences, targets and

gene nomenclature. *Nucleic acids research*, 34(Database issue), pp.D140-4.

Grosse-Wilde, A. et al., 2015. Stemness of the hybrid Epithelial/Mesenchymal State in Breast Cancer and Its Association with Poor Survival Ben-Jacob, E., (ed.). *PLOS ONE*, 10(5), p.e0126522.

Gulhati, P. et al., 2011. mTORC1 and mTORC2 regulate EMT, motility, and metastasis of colorectal cancer via RhoA and Rac1 signaling pathways. *Cancer research*, 71(9), pp.3246–56.

Haggar, F.A. and Boushey, R.P., 2009. Colorectal cancer epidemiology: incidence, mortality, survival, and risk factors. *Clinics in colon and rectal surgery*, 22(4), pp.191–7.

Hardy, K.M., Booth, B.W. and Hendrix, M.J.C., 2010. Erb/EFG Signaling and EMT in mammary development and breast cancer. *Journal of Mammary Gland Biology and Neoplasia*, 15(2), pp.191–199.

Hawkins, K., Joy, S. and McKay, T., 2014. Cell signalling pathways underlying induced pluripotent stem cell reprogramming. *World Journal of Stem Cells*, 6(5), p.620.

Heerboth, S. et al., 2015. EMT and tumour metastasis. *Clinical and Translational Medicine*, 4(1), p.6.

Hiew, M.S.Y. et al., 2018. Incomplete cellular reprogramming of colorectal cancer cells elicits an epithelial/mesenchymal hybrid phenotype. *Journal of Biomedical Science*, 25(1), pp.1–13.

Hill, L., Browne, G. and Tulchinsky, E., 2013. ZEB/miR-200 feedback loop: at the crossroads of signal transduction in cancer. *International journal of cancer*, 132(4), pp.745–54.

Hou, J.-M. et al., 2012. Clinical Significance and Molecular Characteristics of Circulating Tumour Cells and Circulating Tumour Microemboli in Patients With Small-Cell Lung Cancer. *Journal of Clinical Oncology*, 30(5), pp.525–532.

Hu, K., 2014. All roads lead to induced pluripotent stem cells: the technologies of iPSC generation. *Stem cells and development*, 23(12), pp.1285–300.

Hutvágner, G. et al., 2001. A cellular function for the RNA-interference enzyme Dicer in the maturation of the let-7 small temporal RNA. *Science (New York, N.Y.)*, 293(5531), pp.834–8.

Islam, S.M.R. et al., 2015. Sendai virus-mediated expression of reprogramming factors promotes plasticity of human neuroblastoma cells. *Cancer science*, 106(10), pp.1351–61.

Izgi, K., Canatan, H. and Iskender, B., 2017. Current status in cancer cell reprogramming and its clinical implications. *Journal of Cancer Research and Clinical Oncology*, 143(3), pp.371–383.

Jansson, M.D. andLund, A.H., 2012. MicroRNA and cancer. *Molecular Oncology*, 6(6), pp.590–610.

Jiang, C. et al., 2017. miR-500a-3p promotes cancer stem cells properties via STAT3 pathway in human hepatocellular carcinoma. *Journal of Experimental & Clinical Cancer Research*, 36(1), p.99.

Jolly, M.K. et al., 2015. Coupling the modules of EMT and stemness: A tunable "stemness window" model. *Oncotarget*, 6(28), pp.25161–74.

Jolly, M.K., 2015. Implications of the Hybrid Epithelial/Mesenchymal Phenotype in Metastasis. *Frontiers in Oncology*, 5(July), pp.1–19.

Joosse, S.A., Gorges, T.M. and Pantel, K., 2015. Biology, detection, and clinical implications of circulating tumour cells. *EMBO molecular medicine*, 7(1), pp.1–11

Jordan, N.V., Johnson, G.L. and Abell, A.N., 2011. Tracking the intermediate stages of epithelial-mesenchymal transition in epithelial stem cells and cancer. *Cell Cycle*, 10(17), pp.2865–2873.

Judson, R.L., Babiarz, J.E., Venere, M. andBlelloch, R., 2009. Embryonic stem cell-specific microRNAs promote induced pluripotency. *Nature biotechnology*, 27(5), pp.459–61.

Kalimuthu, S. and Se-Kwon, K., 2013. Cell survival and apoptosis signaling as therapeutic target for cancer: Marine bioactive compounds. *International Journal of Molecular Sciences*, 14(2), pp.2334–2354.

Kalluri, R. and Weinberg, R. a, 2009. Review series The basics of epithelial-mesenchymal transition. *Journal of Clinical Investigation*, 119(6), pp.1420–1428.

Katsiampoura, A. et al., 2017. Modeling of Patient-Derived Xenografts in Colorectal Cancer. *Molecular Cancer Therapeutics*, 16(7), pp.1435–1442.

Kim, J. et al., 2013. An iPSC Line from Human Pancreatic Ductal Adenocarcinoma Undergoes Early to Invasive Stages of Pancreatic Cancer Progression. *Cell Reports*, 3(6), pp.2088–2099.

Kim, Y.-K. and Kim, V.N., 2007. Processing of intronic microRNAs. *The EMBO Journal*, 26(3), pp.775–783.

Koga, C. et al., 2014. Reprogramming using microRNA-302 improves drug sensitivity in hepatocellular carcinoma cells. *Annals of surgical oncology*, 21 Suppl 4(S4), pp.S591-600.

Kola, I. and Landis, J., 2004. Can the pharmaceutical industry reduce attrition rates? *Nature Reviews Drug Discovery*, 3(8), pp.711–716.

Kong, Q. et al., 2014. Identification and characterization of an oocyte factor required for porcine nuclear reprogramming. *Journal of Biological Chemistry*, 289(10), pp.6960–6968.

Korpal, M., Lee, E.S., Hu, G. and Kang, Y., 2008. The miR-200 Family Inhibits Epithelial-Mesenchymal Transition and Cancer Cell Migration by Direct Targeting of E-cadherin Transcriptional Repressors *ZEB1* and *ZEB2*. *Journal of Biological Chemistry*, 283(22), pp.14910–14914.

Kumano, K. et al., 2012. Generation of induced pluripotent stem cells from primary chronic myelogenous leukemia patient samples. *Blood*, 119(26), pp.6234–6242.

Kuo, C.-H. andYing, S.-Y., 2012. Advances in microRNA-mediated reprogramming technology. *Stem cells international*, 2012, p.823709.

Lai, J. et al., 2013. Elite model for the generation of induced pluripotent cancer cells (iPCs). Johnson, R., (ed.). *PloS one*, 8(2), p.e56702.

Lamouille, S., Xu, J. andDerynck, R., 2014. Molecular mechanisms of epithelial–mesenchymal transition. *Nature Reviews Molecular Cell Biology*, 15(3), pp.178–196.

Lee, Y. et al., 2004. MicroRNA genes are transcribed by RNA polymerase II. *The EMBO Journal*, 23(20), pp.4051–4060.

Lee, Y. et al., 2003. The nuclear RNase III Drosha initiates microRNA processing. *Nature*, 425(6956), pp.415–9.

Lee, Y.J. andHan, H.J., 2010. Troglitazone ameliorates high glucose-induced EMT and dysfunction of SGLTs through PI3K/Akt, GSK-3β, Snail1, and β-catenin in renal proximal tubule cells. *American Journal of Physiology-Renal Physiology*, 298(5), pp.F1263–F1275.

Li, H. et al., 2017. IGF-IR signaling in epithelial to mesenchymal transition and targeting IGF-IR therapy: Overview and new insights. *Molecular Cancer*, 16(1), pp.1–15.

Li, J.-M. et al., 2012. Down-regulation of fecal miR-143 and miR-145 as potential markers for colorectal cancer. *Saudi medical journal*, 33(1), pp.24–9.

Li, M. andHe, L., 2012. microRNAs as novel regulators of stem cell pluripotency and somatic cell reprogramming. *Bioessays*, 34(8), pp.670–680.

Li, R. et al., 2010. A mesenchymal-to-Epithelial transition initiates and is required for the nuclear reprogramming of mouse fibroblasts. *Cell Stem Cell*, 7(1), pp.51–63.

Li, X.-L., Zhou, J., Chen, Z.-R. andChng, W.-J., 2015. P53 mutations in colorectal cancer - molecular pathogenesis and pharmacological reactivation. *World journal of gastroenterology*, 21(1), pp.84–93.

Li, X., Pei, D. andZheng, H., 2014. Transitions between epithelial and mesenchymal states during cell fate conversions. *Protein and Cell*, 5(8), pp.580–591.

Lin, C.-P., Choi, Y.J., Hicks, G.G. andHe, L., 2012. The emerging functions of

the p53-miRNA network in stem cell biology. *Cell cycle (Georgetown, Tex.)*, 11(11), pp.2063–72.

Lin, S.-L. et al., 2011. Regulation of somatic cell reprogramming through inducible mir-302 expression. *Nucleic acids research*, 39(3), pp.1054–65.

Lin, S. et al., 2008. Mir-302 reprograms human skin cancer cells into a pluripotent ES-cell-like state Mir-302 reprograms human skin cancer cells into a pluripotent ES-cell-like state. , pp.2115–2124.

Lin, S.L. et al., 2008. Mir-302 reprograms human skin cancer cells into a pluripotent ES-cell-like state. *Rna*, 14(10), pp.2115–2124.

Lipchina, I. et al., 2011. Genome-wide identification of microRNA targets in human ES cells reveals a role for miR-302 in modulating BMP response. *Genes & development*, 25(20), pp.2173–86.

Liu, G. et al., 2015. Glutamate dehydrogenase is a novel prognostic marker and predicts metastases in colorectal cancer patients. *Journal of Translational Medicine*, 13(1), pp.1–10.

Liu, S. et al., 2014. Breast cancer stem cells transition between epithelial and mesenchymal states reflective of their normal counterparts. *Stem Cell Reports*, 2(1), pp.78–91.

Liu, X. et al., 2013. Sequential introduction of reprogramming factors reveals a time-sensitive requirement for individual factors and a sequential EMT-MET mechanism for optimal reprogramming. *Nature Cell Biology*, 15(7), pp.829–838.

Liu, X. andFan, D., 2015. The epithelial-mesenchymal transition and cancer stem cells: functional and mechanistic links. *Current pharmaceutical design*, 21(10), pp.1279–91.

Loboda, A. et al., 2011. EMT is the dominant program in human colon cancer. *BMC Medical Genomics*, 4(1), p.9.

Lu, K.V. et al., 2012. VEGF Inhibits Tumour Cell Invasion and Mesenchymal Transition through a MET/VEGFR2 Complex. Cancer Cell, 22(1), pp.21–35.

Lu, M. et al., 2013. MicroRNA-based regulation of epithelial-hybrid-mesenchymal fate determination. *Proceedings of the National Academy of Sciences of the United States of America*, 110(45), pp.18144–9.

Lund, E. et al., 2004. Nuclear Export of MicroRNA Precursors. *Science*, 303(5654), pp.95–98.

Lüningschrör, P., Hauser, S., Kaltschmidt, B. andKaltschmidt, C., 2013. MicroRNAs in pluripotency, reprogramming and cell fate induction. *Biochimica et Biophysica Acta (BBA) - Molecular Cell Research*, 1833(8), pp.1894–1903.

Luo, D. et al., 2018. Aberrant Expression of miR-362 Promotes Lung Cancer

Metastasis through Down-regulation of Sema3A. *Journal of Immunology Research*, 2018, pp.1–10.

MacDonald, B.T., Tamai, K. and He, X., 2009. Wnt/β-Catenin Signaling: Components, Mechanisms, and Diseases. *Developmental Cell*, 17(1), pp.9–26.

MacFarlane, L.-A. andR. Murphy, P., 2010. MicroRNA: Biogenesis, Function and Role in Cancer. *Current Genomics*, 11(7), pp.537–561.

Maherali, N. and Hochedlinger, K., 2009. Tgfbeta signal inhibition cooperates in the induction of iPSCs and replaces Sox2 and cMyc. *Current biology : CB*, 19(20), pp.1718–23.

Mallanna, S.K. and Rizzino, A., 2010. Emerging roles of microRNAs in the control of embryonic stem cells and the generation of induced pluripotent stem cells. *Developmental biology*, 344(1), pp.16–25.

Maniataki, E. and Mourelatos, Z., 2005. A human, ATP-independent, RISC assembly machine fueled by pre-miRNA. *Genes & development*, 19(24), pp.2979–90.

Marson, A. et al., 2008. Connecting microRNA Genes to the Core Transcriptional Regulatory Circuitry of Embryonic Stem Cells. *Cell*, 134(3), pp.521–533.

Mathieu, J. et al., 2011. HIF induces human embryonic stem cell markers in cancer cells. *Cancer research*, 71(13), pp.4640–52.

Matos, M.L. et al., 2017. Identification of a Novel Human E-Cadherin Splice Variant and Assessment of Its Effects Upon EMT-Related Events. *Journal of Cellular Physiology*, 232(6), pp.1368–1386.

McIntyre, R.E., Buczacki, S.J.A., Arends, M.J. andAdams, D.J., 2015. Mouse models of colorectal cancer as preclinical models. *BioEssays*, 37(8), pp.909–920.

Mejlvang, J. et al., 2007. Direct repression of cyclin D1 by SIP1 attenuates cell cycle progression in cells undergoing an epithelial mesenchymal transition. Margolis, B., (ed.). *Molecular biology of the cell*, 18(11), pp.4615–24.

Melton, C., Judson, R.L. andBlelloch, R., 2010. Opposing microRNA families regulate self-renewal in mouse embryonic stem cells. *Nature*, 463(7281), pp.621–626.

Mendell, J.T. andOlson, E.N., 2012. MicroRNAs in Stress Signaling and Human Disease. *Cell*, 148(6), pp.1172–1187.

Miyazaki, S. et al., 2015. A Cancer Reprogramming Method Using MicroRNAs as a Novel Therapeutic Approach against Colon Cancer: Research for Reprogramming of Cancer Cells by MicroRNAs. *Annals of surgical oncology*, 22 Suppl 3(S3), pp.S1394-401.

Miyazono, K., 2009. Transforming growth factor-β signaling in epithelial-

mesenchymal transition and progression of cancer. *Proceedings of the Japan Academy, Series B*, 85(8), pp.314–323.

Miyoshi, N. et al., 2010. Defined factors induce reprogramming of gastrointestinal cancer cells. *Proceedings of the National Academy of Sciences*, 107(1), pp.40–45.

Miyoshi, N. et al., 2011. Reprogramming of mouse and human cells to pluripotency using mature microRNAs. *Cell Stem Cell*, 8(6), pp.633–638.

Mohyeldin, A., Garzón-Muvdi, T. andQuiñones-Hinojosa, A., 2010. Oxygen in Stem Cell Biology: A Critical Component of the Stem Cell Niche. *Cell Stem Cell*, 7(2), pp.150–161.

Molinari, F. andFrattini, M., 2014. Functions and Regulation of the PTEN Gene in Colorectal Cancer. *Frontiers in Oncology*, 3, p.326.

Najdi, R., Holcombe, R. andWaterman, M., 2011. Wnt signaling and colon carcinogenesis: Beyond APC. *Journal of Carcinogenesis*, 10(1), p.5.

Neganova, I. et al., 2016. JNK/SAPK Signaling Is Essential for Efficient Reprogramming of Human Fibroblasts to Induced Pluripotent Stem Cells. *Stem cells (Dayton, Ohio)*, 34(5), pp.1198–212.

Nelakanti, R.V, Kooreman, N.G. andWu, J.C., 2015. Teratoma formation: a tool for monitoring pluripotency in stem cell research. *Current protocols in stem cell biology*, 32, p.4A.8.1-17.

Neureiter, D., 2012. Epigenetic control of epithelial-mesenchymal-transition in human cancer (Review). *Molecular and Clinical Oncology*, pp.3–11.

Nguyen, P.N.N. et al., 2017. MIR-524-5p of the primate-specific C19MC miRNA cluster targets TP53IPN1-and EMT-Associated genes to regulate cellular reprogramming. *Stem Cell Research and Therapy*, 8(1), pp.1–15.

Ni, F. et al., 2016. Down-regulation of miR-362-5p inhibits proliferation, migration and invasion of human breast cancer MCF7 cells. *Oncology Letters*, 11(2), pp.1155–1160.

Ni, F. et al., 2015. MicroRNA-362-5p promotes tumour growth and metastasis by targeting CYLD in hepatocellular carcinoma. *Cancer Letters*, 356(2), pp.809–818.

Nieto, M.A., Huang, R.Y.-J., Jackson, R.A. andThiery, J.P., 2016. EMT: 2016. *Cell*, 166(1), pp.21–45.

Ocaña, O.H. et al., 2012. Metastatic Colonization Requires the Repression of the Epithelial-Mesenchymal Transition Inducer Prrx1. *Cancer Cell*, 22(6), pp.709–724.

Ogaki, S., Shiraki, N., Kume, K. andKume, S., 2013. Wnt and Notch Signals Guide Embryonic Stem Cell Differentiation into the Intestinal Lineages. *STEM CELLS*, 31(6), pp.1086–1096.

Oshima, N. et al., 2014. Induction of Cancer Stem Cell Properties in Colon Cancer Cells by Defined Factors Singh, S.R., (ed.). *PLoS ONE*, 9(7), p.e101735.

Park, S.-M., Gaur, A.B., Lengyel, E. andPeter, M.E., 2008. The miR-200 family determines the epithelial phenotype of cancer cells by targeting the E-cadherin repressors ZEB1 and ZEB2. *Genes & development*, 22(7), pp.894–907.

Pfaff, N. et al., 2011. MiRNA screening reveals a new miRNA family stimulating iPS cell generation via regulation of Meox2. *EMBO Reports*, 12(11), pp.1153–1159.

Pourhoseingholi, M.A., 2012. Increased burden of colorectal cancer in Asia. *World journal of gastrointestinal oncology*, 4(4), pp.68–70.

Ramalingam, P. et al., 2014. Biogenesis of intronic miRNAs located in clusters by independent transcription and alternative splicing. *RNA (New York, N.Y.)*, 20(1), pp.76–87.

Ramos-Mejia, V., Fraga, M.F. andMenendez, P., 2012. IPSCs from cancer cells: Challenges and opportunities. *Trends in Molecular Medicine*, 18(5), pp.245–247.

Raskov, H., Pommergaard, H.-C., Burcharth, J. andRosenberg, J., 2014. Colorectal carcinogenesis--update and perspectives. *World journal of gastroenterology*, 20(48), pp.18151–64.

Redmer, T. et al., 2011. E-cadherin is crucial for embryonic stem cell pluripotency and can replace OCT4 during somatic cell reprogramming. *EMBO reports*, 12(7), pp.720–726.

Ren, A., Dong, Y., Tsoi, H. andYu, J., 2015. Detection of miRNA as Non-Invasive Biomarkers of Colorectal Cancer. *International Journal of Molecular Sciences*, 16(2), pp.2810–2823.

Rokavec, M. et al., 2014. IL-6R/STAT3/miR-34a feedback loop promotes EMT-mediated colorectal cancer invasion and metastasis. *Journal of Clinical Investigation*, 124(4), pp.1853–1867.

DeRosa, M. et al., 2015. Genetics, diagnosis and management of colorectal cancer (Review). *Oncology Reports*, 34(3), pp.1087–1096.

Ruscetti, M. et al., 2015. Tracking and Functional Characterization of Epithelial-Mesenchymal Transition and Mesenchymal Tumour Cells during Prostate Cancer Metastasis. *Cancer Research*, 75(13), pp.2749–2759.

Saitoh, M. (2018). Involvement of partial EMT in cancer progression. *The Journal of Biochemistry*, 164(4), pp.257-264.

Samavarchi-Tehrani, P. et al., 2010. Functional genomics reveals a BMP-driven mesenchymal-to-epithelial transition in the initiation of somatic cell reprogramming. *Cell stem cell*, 7(1), pp.64–77.

Shaw, T.J. and Martin, P., 2016. Wound repair: a showcase for cell plasticity and migration. *Current opinion in cell biology*, 42, pp.29–37.

Shyh-Chang, N. and Daley, G.Q., 2013. Lin28: primal regulator of growth and metabolism in stem cells. *Cell stem cell*, 12(4), pp.395–406.

Škovierovï¿½, H. et al., 2017. Molecular regulation of epithelial-to-mesenchymal transition in tumourigenesis (Review). *International Journal of Molecular Medicine*, 41(3), pp.1187–1200.

Spike, B.T. and Wahl, G.M., 2011. p53, Stem Cells, and Reprogramming: Tumour Suppression beyond Guarding the Genome. *Genes & cancer*, 2(4), pp.404–19.

Strauss, R. et al., 2011. Analysis of epithelial and mesenchymal markers in ovarian cancer reveals phenotypic heterogeneity and plasticity. Gullberg, D., (ed.). *PloS one*, 6(1), p.e16186.

Stricker, S. andPollard, S., 2014. Reprogramming cancer cells to pluripotency: an experimental tool for exploring cancer epigenetics. *Epigenetics*, 9(6), pp.798–802.

Subramanyam, D. et al., 2011. Multiple targets of miR-302 and miR-372 promote reprogramming of human fibroblasts to induced pluripotent stem cells. *Nature biotechnology*, 29(5), pp.443–448.

Suman, S. et al., 2014. Activation of AKT signaling promotes epithelial-mesenchymal transition and tumour growth in colorectal cancer cells. *Molecular Carcinogenesis*, 53(S1), pp.E151–E160.

Sun, C. andLiu, Y.K., 2011. Induced pluripotent cancer cells: Progress and application. *Journal of Cancer Research and Clinical Oncology*, 137(1), pp.1–8.

Sun, Y. et al., 2014. miR-429 inhibits cells growth and invasion and regulates EMT-related marker genes by targeting Onecut2 in colorectal carcinoma. *Molecular and Cellular Biochemistry*, 390(1–2), pp.19–30.

Sun, Z. et al., 2014. MicroRNA-335 inhibits invasion and metastasis of colorectal cancer by targeting ZEB2. *Medical oncology (Northwood, London, England)*, 31(6), p.982.

Szabo, V. et al., 2015. Mechanism of tumour vascularization in experimental lung metastases. *The Journal of Pathology*, 235(3), pp.384–396.

Takahashi, K., Okita, K., Nakagawa, M. andYamanaka, S., 2007. Induction of pluripotent stem cells from fibroblast cultures. *Nature Protocols*, 2(12), pp.3081–3089.

Takahashi, K. andYamanaka, S., 2006. Induction of Pluripotent Stem Cells from Mouse Embryonic and Adult Fibroblast Cultures by Defined Factors. *Cell*, 126(4), pp.663–676.

Takaishi, M., Tarutani, M., Takeda, J. andSano, S., 2016. Mesenchymal to Epithelial Transition Induced by Reprogramming Factors Attenuates the Malignancy of Cancer Cells. Coleman, W.B., (ed.). *PloS one*, 11(6), p.e0156904.

Tang, W. et al., 2014. MicroRNA-29a promotes colorectal cancer metastasis by regulating matrix metalloproteinase 2 and E-cadherin via KLF4. *British journal of cancer*, 110(2), pp.450–8.

Tariq, K. andGhias, K., 2016. Colorectal cancer carcinogenesis: a review of mechanisms. *Cancer biology & medicine*, 13(1), pp.120–35.

Tay, Y. et al., 2008. MicroRNAs to Nanog, Oct4 and Sox2 coding regions modulate embryonic stem cell differentiation. *Nature*, 455(7216), pp.1124–8.

Tay, Y.M.-S. et al., 2008. MicroRNA-134 modulates the differentiation of mouse embryonic stem cells, where it causes post-transcriptional attenuation of Nanog and LRH1. *Stem cells (Dayton, Ohio)*, 26(1), pp.17–29.

Tétreault, N. andDeGuire, V., 2013. MiRNAs: Their discovery, biogenesis and mechanism of action. *Clinical Biochemistry*, 46(10–11), pp.842–845.

Thiery, J.P., 2002. Epithelial–mesenchymal transitions in tumour progression. *Nature Reviews Cancer*, 2(6), pp.442–454.

Thiery, J.P., Acloque, H., Huang, R.Y.J. andNieto, M.A., 2009. Epithelial-Mesenchymal Transitions in Development and Disease. *Cell*, 139(5), pp.871–890.

Thornton, J.E. andGregory, R.I., 2012. How does Lin28 let-7 control development and disease? *Trends in Cell Biology*, 22(9), pp.474–482.

Tian, Y. et al., 2011. Regulation of lung endoderm progenitor cell behavior by miR302/367. *Development (Cambridge, England)*, 138(7), pp.1235–45.

Tsai, J.H. et al., 2012. Spatiotemporal Regulation of Epithelial-Mesenchymal Transition Is Essential for Squamous Cell Carcinoma Metastasis. *Cancer Cell*, 22(6), pp.725–736.

Tsai, J.H. andYang, J., 2013. Epithelial-mesenchymal plasticity in carcinoma metastasis. *Genes & development*, 27(20), pp.2192–206.

Unternaehrer, J.J. et al., 2014. The epithelial-mesenchymal transition factor SNAIL paradoxically enhances reprogramming. *Stem Cell Reports*, 3(5), pp.691–698.

Veettil, S.K. et al., 2017. Colorectal cancer in Malaysia: Its burden and implications for a multiethnic country. *Asian Journal of Surgery*, 40(6), pp.481–489.

Vu, T. and Datta, P.K., 2017. Regulation of EMT in colorectal cancer: A culprit in metastasis. *Cancers*, 9(12), pp.1–22.

Wang, B. et al., 2014. miR-29b suppresses tumour growth and metastasis in colorectal cancer via downregulating Tiam1 expression and inhibiting epithelial-mesenchymal transition. *Cell death & disease*, 5(7), p.e1335.

Wang, G. et al., 2013. Critical regulation of miR-200 / ZEB2 pathway in Oct4 / Sox2-induced mesenchymal-to-epithelial transition and induced pluripotent stem cell generation. *Proceedings of the National Academy of Sciences of the United States of America*, 110(8), pp.2858–63.

Wang, R. et al., 2013. Functional role of miR-34 family in human cancer. *Current drug targets*, 14(10), pp.1185–91.].

Wang, W. et al., 2011. Rapid and efficient reprogramming of somatic cells to induced pluripotent stem cells by retinoic acid receptor gamma and liver receptor homolog 1. *Proceedings of the National Academy of Sciences of the United States of America*, 108(45), pp.18283–8.

Wang, W. et al., 2011. Rapid and efficient reprogramming of somatic cells to induced pluripotent stem cells by retinoic acid receptor gamma and liver receptor homolog 1. *Proceedings of the National Academy of Sciences*, 108(45), pp.18283–18288.

Wang, X.H. et al., 2017. IL-33 restricts invasion and adhesion of trophoblast cell line JEG3 by down-regulation of integrin α4β1 and CD62L. *Molecular Medicine Reports*, 16(4), pp.3887–3893.

Wang, Y. et al., 2008. Embryonic stem cell-specific microRNAs regulate the G1-S transition and promote rapid proliferation. *Nature genetics*, 40(12), pp.1478–83.

Wang, Y. et al., 2013. miR-294/miR-302 promotes proliferation, suppresses G1-S restriction point, and inhibits ESC differentiation through separable mechanisms. *Cell reports*, 4(1), pp.99–109.

Wang, Y., Luo, J., Zhang, H. andLu, J., 2016. microRNAs in the Same Clusters Evolve to Coordinately Regulate Functionally Related Genes. *Molecular biology and evolution*, 33(9), pp.2232–47.

Wang, Y. andZhou, B.P., 2013. Epithelial-mesenchymal Transition---A Hallmark of Breast Cancer Metastasis. *Cancer hallmarks*, 1(1), pp.38–49.

Wang, Z. et al., 2015. Activin A can induce definitive endoderm differentiation from human parthenogenetic embryonic stem cells. *Biotechnology Letters*, 37(8), pp.1711–1717.

Winter, J. et al., 2009. Many roads to maturity: microRNA biogenesis pathways and their regulation. *Nature cell biology*, 11(3), pp.228–34.

Wolczyk, D. et al., 2016. TNF-α promotes breast cancer cell migration and enhances the concentration of membrane-associated proteases in lipid rafts. *Cellular Oncology*, 39(4), pp.353–363.

Wu, Y. andZhou, B.P., 2010. TNF-α/NFκ-B/Snail pathway in cancer cell

migration and invasion. *British Journal of Cancer*, 102(4), pp.639–644.

Xiong, H. et al., 2012. Roles of STAT3 and ZEB1 Proteins in E-cadherin Down-regulation and Human Colorectal Cancer Epithelial-Mesenchymal Transition. *Journal of Biological Chemistry*, 287(8), pp.5819–5832.

Xu, W., Yang, Z. andLu, N., 2015. A new role for the PI3K/Akt signaling pathway in the epithelial-mesenchymal transition. *Cell adhesion & migration*, 9(4), pp.317–24.

Xu, X. et al., 2016. miRNA-532-5p functions as an oncogenic microRNA in human gastric cancer by directly targeting RUNX3. *Journal of Cellular and Molecular Medicine*, 20(1), pp.95–103.

Yamanaka, S., 2009. Elite and stochastic models for induced pluripotent stem cell generation. *Nature*, 460(7251), pp.49–52.

Ye, D. et al., 2012. MiR-138 Promotes Induced Pluripotent Stem Cell Generation Through the Regulation of the p53 Signaling. *STEM CELLS*, 30(8), pp.1645–1654.

Ye, X. et al., 2015. Distinct EMT programs control normal mammary stem cells and tumour-initiating cells. *Nature*, 525(7568), pp.256–260.

Yilmaz, M. andChristofori, G., 2009. EMT, the cytoskeleton, and cancer cell invasion. *Cancer and Metastasis Reviews*, 28(1–2), pp.15–33.

Yu, J.S.L. andCui, W., 2016. Proliferation, survival and metabolism: the role of PI3K/AKT/mTOR signalling in pluripotency and cell fate determination. *Development*, 143(17), pp.3050–3060.

Zhang, H. et al., 2015. miR-188-5p inhibits tumour growth and metastasis in prostate cancer by repressing LAPTM4B expression. *Oncotarget*, 6(8), pp.6092–6104. A

Zhang, J., Tian, X.-J. and Xing, J., 2016. Signal Transduction Pathways of EMT Induced by TGF-β, SHH, and WNT and Their Crosstalks. *Journal of Clinical Medicine*, 5(4), p.41.

Zhang, J.X. et al., 2014. MiR-29c mediates epithelial-to-mesenchymal transition in human colorectal carcinoma metastasis via PTP4A and GNA13 regulation of β-catenin signaling. *Annals of Oncology*, 25(11), pp.2196–2204.

Zhang, X. et al., 2013. Terminal differentiation and loss of tumourigenicity of human cancers via pluripotency-based reprogramming. *Oncogene*, 32(18), pp.2249–60, 2260.e1–21.

Zhao, P. andZhang, Z., 2018. TNF-α promotes colon cancer cell migration and invasion by upregulating TROP-2. *Oncology Letters*, 15(3), pp.3820–3827.

Zhao, S. et al., 2008. Inhibition of STAT3 Tyr705 phosphorylation by Smad4 suppresses transforming growth factor beta-mediated invasion and metastasis in pancreatic cancer cells. *Cancer research*, 68(11), pp.4221–8.

Zheng, H. and Kang, Y., 2014. Multilayer control of the EMT master regulators. *Oncogene*, 33(14), pp.1755–63.

Zheng, Y.-B. et al., 2014. miR-132 inhibits colorectal cancer invasion and metastasis via directly targeting ZEB2. *World journal of gastroenterology*, 20(21), pp.6515–22.

Zhu, D. et al., 2018. Induced Pluripotent Stem Cells and Induced Pluripotent Cancer Cells in Cancer Disease Modeling. , pp.1–15.

APPENDICES

APPENDIX A

Supplementary Table 1: Fifty two up-regulated miRNAs in CRC-iPCs

miRNA	miRNA accession number[a]	miRNA family[b]	Chromosomal site[c]	Log2(FC)[d]
hsa-miR-30a-5p	MIMAT0000087	mir-30	6q13	3.942
hsa-miR-125a-3p	MIMAT0004602	mir-10	19q13.41	6.889
hsa-miR-125b-5p	MIMAT0000423	mir-10	11q24.1	8.881
hsa-miR-130a-3p	MIMAT0000425	mir-130	11q12.1	4.646
hsa-miR-132-3p	MIMAT0000426	mir-132	17p13.3	4.199
hsa-miR-135a-3p	MIMAT0004595	mir-135	3p21.1	3.963
hsa-miR-150-3p	MIMAT0004610	mir-150	19q13.33	5.856
hsa-miR-152-3p	MIMAT0000438	mir-148	17q21.32	4.246
hsa-miR-195-5p	MIMAT0000461	mir-15	17p13.1	3.956
hsa-miR-199a-3p	MIMAT0000232	mir-199	19p13.2	7.041
hsa-miR-199a-5p	MIMAT0000231	mir-199	19p13.2	5.062
hsa-miR-210-3p	MIMAT0000267	mir-210	11p15.5	3.647
hsa-miR-371a-5p	MIMAT0004687	mir-290	19q13.42	4.177
hsa-miR-513b-5p	MIMAT0005788	mir-506	Xq27.3	3.38
hsa-miR-652-5p	MIMAT0022709	mir-652	Xq23	4.148
hsa-miR-671-5p	MIMAT0003880	mir-671	7q36.1	5.202
hsa-miR-769-5p	MIMAT0003886	mir-769	19q13.32	5.019
hsa-miR-1181	MIMAT0005826	mir-1181	19	5.67
hsa-miR-1185-1-3p	MIMAT0022838	mir-154	14	3.144
hsa-miR-1228-3p	MIMAT0005583	mir-1228	12	4.745
hsa-miR-1249-3p	MIMAT0005901	mir-1249	22q13.31	2.911
hsa-miR-3188	MIMAT0015070	mir-3188	19	4.55
hsa-miR-3911	MIMAT0018185	-	9	2.641
hsa-miR-3934-5p	MIMAT0018349	mir-3934	6	5.71
hsa-miR-4417	MIMAT0018929	-	1	6.214
hsa-miR-4463	MIMAT0018987	-	6	3.399
hsa-miR-4487	MIMAT0019021	-	11	4.106
hsa-miR-4488	MIMAT0019022	mir-4488	11	4.91
hsa-miR-4532	MIMAT0019071	-	20	3.468
hsa-miR-4646-5p	MIMAT0019707	-	6	4.723

Supplementary Table 1 (continued)

miRNA	miRNA accession number[a]	miRNA family[b]	Chromosomal site[c]	Log_2 (FC)[d]
hsa-miR-4651	MIMAT0019715	-	7	4.955
hsa-miR-4655-5p	MIMAT0019721	-	7	4.775
hsa-miR-4690-5p	MIMAT0019779	-	11	3.948
hsa-miR-4695-5p	MIMAT0019788	-	1	4.437
hsa-miR-4734	MIMAT0019859	-	17	6.36
hsa-miR-4745-5p	MIMAT0019878	-	19	5.61
hsa-miR-4746-3p	MIMAT0019881	-	19	5.522
hsa-miR-4778-5p	MIMAT0019936	-	2	4.496
hsa-miR-5194	MIMAT0021125	-	8	3.308
hsa-miR-6752-5p	MIMAT0027404	-	11	3.722
hsa-miR-6757-5p	MIMAT0027414	-	12	5.136
hsa-miR-6778-5p	MIMAT0027456	-	17	4.747
hsa-miR-6789-5p	MIMAT0027478	-	19	6.237
hsa-miR-6798-5p	MIMAT0027496	-	19	3.919
hsa-miR-6808-5p	MIMAT0027516	-	1	4.737
hsa-miR-6867-5p	MIMAT0027634	-	17	4.729
hsa-miR-7152-3p	MIMAT0028215	-	10	4.889
hsa-miR-8089	MIMAT0031016	-	5q35.3	3.654

miRNAs are arranged according to numerical order. [a]accession number derived from miRBase; [b]miRNA family are taken from miRBase database; [c]Chromosomal sites are taken from HUGO Gene Nomenclature Committee (HGNC); [d]Log_2(FC): Log_2(Fold change); miRNAs are differentially-expressed if Log_2(FC)> 2.0 or < -2.0.

APPENDIX B

Supplementary Table 2: Fifty down-regulated miRNAs in CRC-iPCs

miRNA	miRNA accession number[a]	miRNA family[b]	Chromosomal site[c]	$Log_2(FC)$[d]
hsa-miR-7-5p	MIMAT0000252	mir-7	15q26.1	-2.61
hsa-miR-126-3p	MIMAT0000445	mir-126	9q34.3	-3.515
hsa-miR-149-5p	MIMAT0000450	mir-149	2q37.3	-3.359
hsa-miR-181c-5p	MIMAT0000258	mir-181	19p13.13	-3.247
hsa-miR-183-3p	MIMAT0004560	mir-183	7q32.2	-2.77
hsa-miR-192-3p	MIMAT0004543	mir-192	11q13.1	-3.515
hsa-miR-192-5p	MIMAT0000222	mir-192	11q13.1	-6.167
hsa-miR-194-3p	MIMAT0004671	mir-194	11q13.1	-3.033
hsa-miR-200a-5p	MIMAT0001620	mir-8	1p36.33	-3.625
hsa-miR-335-3p	MIMAT0004703	mir-335	7q32.2	-2.605
hsa-miR-338-3p	MIMAT0000763	mir-338	17q25.3	-4.837
hsa-miR-345-5p	MIMAT0000772	mir-345	14q32.2	-2.745
hsa-miR-362-3p	MIMAT0004683	mir-362	Xp11.23	-3.597
hsa-miR-362-5p	MIMAT0000705	mir-362	Xp11.23	-4.415
hsa-miR-421	MIMAT0003339	mir-95	Xq13.2	-3.241
hsa-miR-449b-3p	MIMAT0009203	mir-449	5q11.2	-3.392
hsa-miR-454-3p	MIMAT0003885	mir-454	17q22	-3.216
hsa-miR-455-3p	MIMAT0004784	mir-455	9q32	-4.629
hsa-miR-455-5p	MIMAT0003150	mir-455	9q32	-3.138
hsa-miR-500a-3p	MIMAT0002871	mir-500	Xp11.23	-3.535
hsa-miR-500a-5p	MIMAT0004773	mir-500	Xp11.23	-2.849
hsa-miR-505-3p	MIMAT0002876	mir-505	Xq27.1	-3.336
hsa-miR-532-3p	MIMAT0004780	mir-188	Xp11.23	-3.637
hsa-miR-552-3p	MIMAT0003215	mir-552	1p34.3	-4.154
hsa-miR-3200-3p	MIMAT0015085	mir-3200	22	-3.294
hsa-miR-3591-3p	MIMAT0019877	mir-122	18	-3.969
hsa-miR-3935	MIMAT0018350	-	16	-3.639
hsa-miR-3940-3p	MIMAT0018356	mir-3940	19	-3.103

Supplementary Table 2 (continued)

miRNA	miRNA accession number[a]	miRNA family[b]	Chromosomal site[c]	Log2(FC)[d]
hsa-miR-3945	MIMAT0018361	-	4	-3.566
hsa-miR-4254	MIMAT0016884	-	1	-4.023
hsa-miR-4259	MIMAT0016880	-	1	-3.062
hsa-miR-4323	MIMAT0016875	-	19	-3.154
hsa-miR-4652-3p	MIMAT0019717	-	7	-3.824
hsa-miR-4687-5p	MIMAT0019774	-	11	-3.608
hsa-miR-4725-5p	MIMAT0019843	-	17	-3.989
hsa-miR-4769-3p	MIMAT0019923	-	X	-3.147
hsa-miR-6129	MIMAT0024613	mir-6129	17	-3.85
hsa-miR-6730-3p	MIMAT0027362	-	1	-3.28
hsa-miR-6730-5p	MIMAT0027361	-	1	-3.467
hsa-miR-6736-3p	MIMAT0027374	-	1	-3.116
hsa-miR-6737-3p	MIMAT0027376	-	1	-3.859
hsa-miR-6741-3p	MIMAT0027384	-	1	-4.366
hsa-miR-6743-3p	MIMAT0027388	-	11	-4.336
hsa-miR-6752-3p	MIMAT0027405	-	11	-3.742
hsa-miR-6766-3p	MIMAT0027433	-	15	-3.737
hsa-miR-6779-3p	MIMAT0027459	-	17	-2.736
hsa-miR-6782-5p	MIMAT0027464	-	17	-4.052
hsa-miR-6785-3p	MIMAT0027471	-	17	-3.54
hsa-miR-6797-3p	MIMAT0027495	-	19	-3.383
hsa-miR-6803-3p	MIMAT0027507	-	19	-3.477

miRNAs are arranged according to numerical order. [a]accession number derived from miRBase; [b]miRNA family are taken from miRBase database; [c]Chromosomal sites are taken from HUGO Gene Nomenclature Committee (HGNC); [d]Log_2(FC): Log_2(Fold change); miRNAs are differentially-expressed if Log_2(FC)> 2.0 or < -2.0.

APPENDIX C

Supplementary Table 3: Cluster I miRNAs associated with the modulation of reprogramming process

miRNA	Family	Log_2(fold change) iPC vs CRC[a]	Log_2(fold change) iPC vs ESC[b]
		Cluster I	
miR-130a-3p	mir-130	4.6461377	-5.80656
miR-302a-3p	mir-302	-0.8402815	-13.211192
miR-302a-5p		-0.8402815	-11.8833275
miR-302b-3p		-0.8402815	-12.11458
miR-302b-5p		-0.8402815	-6.5738697
miR-302c-3p		-0.8402815	-12.443087
miR-302c-5p		-0.8402815	-7.6779056
miR-302d-3p		-0.8402815	-11.94684
miR-498	C19MC	-0.8402815	-5.9553742
miR-512-3p		-0.8402815	-7.684702
miR-512-5p		-0.8402815	-5.0344677
miR-515-3p		-0.8402815	-4.8008533
miR-515-5p		-0.8402815	-6.094796
miR-516b-5p		-0.8402815	-5.8819146
miR-518b		-0.8402815	-5.0204396
miR-518c-5p		-0.8402815	-4.878671
miR-519b-3p		-0.8402815	-6.20168
miR-519c-3p		-0.8402815	-4.9577136
miR-519d-3p		-0.8402815	-5.7168207
miR-519e-5p		-0.8402815	-4.8293204
miR-520a-5p		-0.8402815	-4.816074
miR-520b		-0.8402815	-4.5597577
miR-520c-3p		-0.8402815	-7.3049417
miR-520f-3p		-0.8402815	-5.131268
miR-520g-3p		-0.8402815	-5.0725846
miR-520h		-0.8402815	-3.9666684
miR-525-5p		-0.8402815	-6.0795727
miR-526b-5p		-0.8402815	-4.980953

[a]Log_2 fold change of iPCs in relative to the parental CRC cells; [b]Log_2 fold change of iPCs in relative to the ESCs.

APPENDIX D

Supplementary Table 4: Cluster II and III miRNAs associated with the modulation of reprogramming process

miRNA	Family	Log_2(fold change) iPC vs CRC[a]	Log_2(fold change) iPC vs ESC[b]
		Cluster II	
miR-642a-3p	mir-642	0.71249723	-1.4479289
miR-3162-5p	NA	0.50024843	-1.0586226
		Cluster III	
let-7a-5p		0.316	5.9331636
let-7b-5p		0.159	6.4127464
let-7c-5p		0.465	5.9936905
let-7d-5p	let 7	-0.442	5.295085
let-7f-5p		0.0166	5.6159344
let-7g-5p		-0.269	6.2615
let-7i-5p		-0.487	2.7759283
miR-181a-5p	mir-181	-0.6985439	6.718727
miR-200a-3p		-0.6929922	4.7573786
miR-200b-3p	mir-200	-0.8206234	4.6905313
miR-200c-3p		-0.029519081	5.6546283

[a]Log_2 fold change of iPCs in relative to the parental CRC cells; [b]Log_2 fold change of iPCs in relative to the ESCs. NA, not available.